Title
Understanding the Link between Myopia and Glaucoma- Clues from Intraocular Pressure and Optic Discs

Author
El-Nimri, Nevin Wadie

Publication Date
2019

Peer reviewed|Thesis/dissertation

Understanding the Link between Myopia and Glaucoma- Clues from Intraocular Pressure and Optic Discs

by

Nevin Wadie El-Nimri

A dissertation submitted in partial satisfaction of the

the requirement for the degree of

Doctor of Philosophy

in

Vision Science

in the

Graduate Division

of the

University of California, Berkeley

Committee in charge:

Professor Christine F. Wildsoet, Chair
Professor John G. Flanagan
Professor Nicholas P. Jewell

Spring 2019

Understanding the Link between Myopia and Glaucoma-
Clues from Intraocular Pressure and Optic Discs

By
Nevin Wadie El-Nimri

University of California, Berkeley

Abstract

Understanding the Link between Myopia and Glaucoma-
Clues from Intraocular Pressure and Optic Discs

By Nevin Wadie El-Nimri

Doctor of Philosophy in Vision Science

University of California, Berkeley

Professor Christine Wildsoet, Chair

Myopia (near-sightedness) has become a significant public health concern, as its prevalence continues to increase in the United States and around the world. Further, myopia is also linked to potentially blinding ocular disease. Growing evidence from a number of studies links myopia with an increased risk of glaucoma, a leading cause of irreversible blindness. Eyes with primary open angle glaucoma typically exhibit high intraocular pressure (IOP) and altered diurnal IOP rhythms. The structural organization of the lamina cribrosa (LC) of the optic nerve head may also render eyes more vulnerable to nerve fiber damage, the origin of vision loss in glaucoma. One or more of these factors may also contribute to the increased risk of glaucoma in myopic eyes.

IOP could play a role in normal ocular “growth” (enlargement), by exerting a stretching influence on the scleral wall of the eye. During myopia development and progression, scleral remodelling is upregulated, rendering it more susceptible to the stretching influences of IOP, with eye enlargement accelerating as a consequence. The converse that ocular elongation can be slowed by decreasing IOP and so the tension experienced by the sclera was tested in a set of experiments using a topical ocular hypotensive drug, specifically latanoprost. Its effects on both normal and “myopic” ocular growth in guinea pigs undergoing monocular form deprivation were examined, and treatment-induced ultrastructural changes in the sclera were quantified.

With advances in high-resolution imaging and electron microscopy, we were able to characterize the effects of the above ocular hypotensive drug on the microarchitectural changes in the sclera and optic nerve head, including the LC.

Our results demonstrate that daily topical latanoprost is effective in both lowering IOP and slowing myopia progression in myopic guinea pig eyes. It also seems to protect the myopic scleral remodelling. These findings will open the opportunities to explore lowering IOP as a myopia control treatment option that may also reduce any future risk of glaucoma in myopic children.

To my dearest parents who have led the way:
Wadie Nimri MD. and Lama Nimri

Table of Contents

Figures

Tables

List of Abbreviations

AL	Axial length
AT	Artificial tears
CAI	Carbonic anhydrase inhibitor
FD	Form deprivation
IOP	Intraocular pressure
LC	Lamina cribrosa
MMP	Matrix metalloproteinase
NTG	Normal tension glaucoma
OAL	Optical axial length
ODD	Optic disc dimensions
ONH	Optic nerve head
PGs	Prostaglandin Analogues
POAG	Primary open-angle glaucoma
SE	Spherical equivalent refractive error
SEM	Scanning electron microscopy
TEM	Transmission electron microscopy
TIMP	Tissue inhibitor of MMPs

Acknowledgements

I would like to express the deepest appreciation to my committee chair, Dr Christine Wildsoet, who has the attitude and the substance of a genius: she continually and convincingly conveyed a spirit of adventure in regards to research and excitement in regard to teaching. Without her guidance, patience and constant enthusiasm, this dissertation would not have been possible. Thank you for always reminding me of the big picture, and always listening. You were right, it did all work out.

I wish to express my sincere thanks to Dean John Flanagan for always demanding and inspiring excellence. Your energy and kindness helped me stay motivated to get through it all.

Special thanks to Professor Nicholas Jewell for his guidance, support and endless enthusiasm. I have a new found appreciation for statistics now, and I am very grateful for your help.

In addition, I would like to thank my friends and family for their support and love. Many thanks to my parents, Lama & Wadie Nimri, my siblings, Ramzi and Lorin Nimri, my cousins, Suhair and Sawsan Nimri, and my friend Paul Cullen for their endless motivation. To all the other vision science students, thank you for all of your help and support over the last five years.

Chapter 1 Myopia and intraocular pressure

1.1 Myopia, eye growth, and refractive error

1.1.1.1 Increasing prevalence of myopia in the US and around the world

Myopia (near-sightedness) has become a significant global public health concern, as its prevalence continues to increase in the United States and around the world. Myopia's prevalence has increased from 25% to 49% for 30 years in the United States (Vitale et al., 2009). Myopia prevalence figures for Asian countries, such as Singapore, China, Japan, and South Korea, are even more dramatic; it has now reached epidemic levels of 80% to 90% in many of them (Pan et al., 2015), with a prevalence figure of 96.5% reported for young Korean males in Seoul (Jung et al., 2012).

A report published in 2008 by the World Health Organization estimated that a total of 153 million people in the age range of 5-50 years were visually impaired from uncorrected refractive errors, which was considered the second leading cause of blindness globally (Resnikoff et al., 2008). This figure is likely to be now much higher, due to the rising prevalence of myopia globally. Recent projections from the International Data Base estimated that ~50% of the world's population will be myopic by 2050, with 9.8 % being highly myopic (Holden et al., 2016).

1.1.1.2 Economic impacts of myopia in the US and around the world

Glasses, contact lenses, and/or refractive surgery are commonly used to correct myopia, which represents the focusing error created by a mismatch between the eye's optical power and its length. However, with the rising myopia prevalence, the net cost of these treatments, as well as the cost of treatments for myopia-associated complications, are also increasing. In the United States, yearly cost estimates for refractive error corrections range from 3.8 to 7.2 billion dollars for the segment of the population, 12 years and older (Vitale et al., 2006). In a now relatively old study, the cost of annual screening for uncorrected refractive errors and corrective spectacles in school children was estimated to be in the order of hundreds of millions of dollars per year for each of the African, Asian, American, and European continents (Baltussen et al., 2009). In a slightly later report, the estimated annual global cost of distance vision corrections, which largely reflect the needs of myopes, was 202 billion dollars (Fricke et al., 2012).

The global productivity loss was estimated at 244 billion dollars from uncorrected myopia in 2015 (Naidoo et al., 2019).

1.1.1.3 Myopia as a risk factor for ocular diseases

Myopia is associated with many vision-threatening complications, including myopic maculopathy, macular holes, staphylomas, retinal detachment, chorioretinal atrophy, choroidal neovascularization, cataract, and glaucoma, the risks for which increase with increasing levels of myopia in all cases (Flitcroft, 2012; Saw, 2006).

As noted earlier, due to the increase in myopia prevalence and the associated economic impacts of myopia, it has become a worldwide public health concern. Its association with potentially blinding pathologies adds to these concerns. Therefore, the development of new effective myopia control treatments to prevent and/or slow down the progression of myopia is essential.

1.1.1.4 Animal models of myopia

Chicks

Chicks remain the most commonly used model in myopia research. That manipulation of vision via form-deprivation in young chicks could induce myopia (Wallman et al., 1978) was considered a major breakthrough in the field of myopia research.

Among their greatest advantages are that they are easy to obtain and house, mature rapidly, and can be raised in large numbers, leading to faster research advancement. Chicks also respond quickly and reliably to form-deprivation (Hodos and Kuenzel, 1984) and imposed hyperopic defocus, becoming myopic in both cases. They were also found to compensate bidirectionally to optical defocus imposed by positive and negative lenses (Irving et al., 1992; Schaeffel et al., 1988; Wildsoet and Wallman, 1995).

Although chicks have many advantages as models for human myopia, they also present with a number of disadvantages. Unlike mammals and primates, chicks have a bilayered sclera, with an inner cartilage layer, which thickens with myopia induction, and an outer fibrous layer, which thins (Rada et al., 1991). Also, while chicks have ocular accommodation, like humans, the associated change of refracting power involves both corneal and lenticular mechanisms, rather than the lens alone as in humans (Glasser et al., 1995, 1994). Finally, the chick eye has a well-developed choroidal lymphatic vessel network, which contributes to observed optical defocus-induced thickness changes, by which the retina is moved forward (positive lens wear) or backward (negative lens wear) towards the altered focal plane (Wallman et al., 1995). These choroidal thickness changes, which are dramatic in chicks, has led to similar investigations in mammals and primates, which proved to have similar responses, albeit on a smaller scale (Howlett and McFadden, 2006; Hung et al., 2000).

Tree shrews

Tree shrews are small, non-rodent animals that have a cone-dominated retina and fibrous only sclera. The ocular structures of tree shrew are very similar to humans, with the exception of their relatively thicker lens (Norton and McBrien, 1992). They also respond rapidly (< 2 hours) to form-deprivation and myopia-inducing negative lenses, although they appear to have more limited capacity to respond to positive lenses than chicks (Metlapally and McBrien, 2008).

Tree shrews studies have contributed to our understanding of the myopic changes in the mammalian sclera, including but not limited to changes in scleral biomechanics (Frost and Norton, 2007; Jobling et al., 2004, 2009, McBrien et al., 2000, 2001, 2009; Moring et al., 2007; J. Siegwart and Norton, 2001; Siegwart and Norton, 2005).

As any other animal model, tree shrews have some disadvantages, including that they are not readily available and require high maintenance.

Rhesus Monkeys and Marmosets

Earliest studies involving lid suture in young rhesus macaques revealed myopic changes (Wiesel and Raviola, 1977). In effect, this procedure imposed form deprivation, which was later replaced with diffusers, by way of achieving the latter, as well as negative lenses. Studies in rhesus macaques have contributed significantly to our understanding of the respective roles of the central and peripheral retina in emmetropization (Huang et al., 2011; Smith et al., 2013b, 2007), the mechanism underlying recovery from myopia post-termination of myopia-inducing stimuli (Huang et al., 2012; Qiao-Grider et al., 2004), and the differential effects of bright light on form deprivation and lens-induced myopia progression (Smith et al., 2013a, 2012).

The main advantage of the monkey as a myopia model is their close ocular and visual similarities to humans (Edwards, 1996; Norton, 1999). However, there is a large variation in individual animals' response to form-deprivation (Tigges et al., 1990) and defocusing (positive/ negative) lenses (Hung et al., 1995). Furthermore, the high maintenance cost, as reflected in the low number of rhesus monkeys per study are among the other disadvantages of this primate model.

Marmosets, as an alternative primate myopia model, have the advantages over macaque monkeys of being much smaller in size, easier to breed, cheaper to maintain, and they develop more rapidly (Graham and Judge, 1999). Marmosets also respond to both types of myopia-inducing stimuli (Troilo et al., 2007, 2006). Among applications of this model have been studies to uncover the relationship between accommodation and the development of myopia (Troilo et al., 2009, 2007) and of scleral remodeling during the development of myopia (Rada et al., 2000; Troilo et al., 2006).

Mice

The mouse, which is the most recently introduced myopia model, has been shown to respond to both form-deprivation and imposed hyperopic defocus (Schaeffel et al., 2004; Tejedor and De la Villa, 2003). This model offers a number of advantages, including larger litter sizes. Because its genome has been completely sequenced, the mouse also allows studies of both genetic and environmental influences on myopia progression in the same animal (Pardue et al., 2013). On the other hand, mice have poor visual acuity, of approximately 0.4 cycles per degree (Prusky et al., 2004) and a rod-dominated retina. Furthermore, it is harder to measure refractive errors and axial lengths in mice, due to their extremely small eyes. Studies have mostly used infrared photorefractors to measure refractive errors. Nonetheless, there is significant variation in refractive errors reported among different research groups for mice, despite similarities in ages and strains of the mice used, suggesting significant inter-animal variability (Pardue et al., 2013). The axial elongation to diopter of myopia ratio for mice (5.4 to 6.5 μm per 1 D myopia) (Schmucker and Schaeffel, 2004), is below the tolerance of high frequency A-scan ultrasonography, which has been mainly used to measure axial lengths in studies involving other myopia animal models. Thus to measure axial length in mice, researchers have used instead advanced technologies, such as laser micrometry (Wisard et al., 2010), magnetic resonance imaging (Tkatchenko et al., 2010), and low coherence interferometry (Park et al., 2012; Schmucker and Schaeffel, 2004).

Guinea pigs

The first myopia studies involving guinea pigs began in 1995. As in chicks, they were found to compensate to hyperopic defocus imposed with negative lenses and for a lesser degree to myopic defocus imposed with positive lenses (Howlett and McFadden, 2009). The process of emmetropization in guinea pigs (Howlett and McFadden, 2007; Zhou et al., 2006), their response to form-deprivation (Howlett and McFadden, 2006), and to both positive and negative lenses (Howlett and McFadden, 2009) have all now been well characterized, making them an increasingly popular animal model for ocular growth studies.

Guinea pigs combine the advantages of fibrous-only sclera, which is comprised of extracellular matrix, including fibrillar collagens, proteoglycans, glycoproteins, and matrix secreting fibroblasts (like mammalian and primate models), a relatively smaller size and ease of housing. Guinea pigs are also easier to handle than tree shrews, which, for example, tend to be more aggressive and are susceptible to handling stress. Their eyes are also significantly larger than mice, whose eyes have a much larger depth-of-focus, rendering them less sensitive to imposed optical defocus. The visual acuity of guinea pigs is about 1.0 cycle per degree, also significantly better than that of mice (Ostrin L, Mok-Yee J, Wildsoet C, 2011). Guinea pigs also have a well-organized, collagen-based lamina cribrosa, which is absent in mice (May and Lütjen-Drecoll, 2002). Finally guinea pigs are born with their eyes open and well-developed vision (precocial) (Edwards et al., 1974), unlike tree shrews and monkeys. These various features have

also contributed to their increasing popularity as a model in myopia studies and have motivated us to use them in our studies.

1.1.1.5 Parallels between form-deprivation and lens-induced myopia changes in animals

Over the past several decades, animal studies of myopia have commonly used form-deprivation (FDM) by diffusers, or hyperopic defocus by negative lenses (LIM), both of which accelerate ocular growth. However, there remains disagreement regarding whether these two models of myopia involve the same or different underlying mechanisms, yet understanding such mechanisms is critical to understand the etiology of human myopia.

Results of two studies suggest that both myopia models involve dopaminergic mechanisms; specifically, retinal dopamine levels are reduced in eyes subjected to form-deprivation (Stone et al., 1989) as well as eyes wearing negative lenses (Guo et al., 1995). In addition, quinpirole and apomorphine (both agonists) inhibit both FDM and LIM (Schmid and Wildsoet, 2004).

Acetylcholine is another widely studied molecule in the context of eye growth regulation and myopia. Results of relevant studies here suggest different cholinergic mechanisms may be involved in the two myopia models. For example, an M4 muscarinic antagonist inhibited FDM (Mcbrien et al., 2011), but was only partially effective in inhibiting LIM (Diether et al., 2005). Also while atropine is known to be effective at inhibiting myopia in both types of myopia, the combination of atropine and apomorphine was less effective in inhibiting FDM compared to atropine alone, but more effective in inhibiting LIM (Schmid and Wildsoet, 2004).

Several studies point to the possibility of different retinal mechanisms being involved in these two models. As one example, in ERG recordings in chicks, the amplitudes of a- and b- waves were found to be similar in both models but oscillatory potential amplitudes reduced in FD eyes only (Fujikado et al., 1997). As another example, optic nerve section was shown to enhance axial elongation in response to FD by about 50% more than the effect of negative lenses (-15 D) (Choh et al., 2006).

The time course of myopia induction and recovery also appear to be different between the two models. For example, it takes about 72 hours for chick eyes wearing diffusers to show detectible dimensional differences from fellow eyes, compared to ~25 hours for negative-lens wearing eyes to differ from their fellow eyes. Interocular differences in axial elongation were approximately 5 times greater in lens- compared to diffuser-wearing chicks after only 48 hours of treatment. Scleral proteoglycan synthesis was also reported to be higher after 8 hours of negative lens exposure compared to 27 hours of FD (Kee et al., 2001).

Light manipulations seem to also have different effects on the two models. For example, constant (24 h) light is reported to strongly inhibit the FD response in chicks but had minimal effect on LIM (Bartmann et al., 1994), and likewise high diurnal light levels are reported to strongly inhibits FDM, but only slow negative lens compensation (Ashby and

Schaeffel, 2010). Disruption of the diurnal light cycle also appears to differentially affect FDM and LIM. For example, interrupting the night (darkness period) by short periods of light (e.g., light exposure for 30 min), was found to inhibit FDM, but had no effect on LIM (Kee et al., 2001), while 5 minutes of light every 20 minutes during the usual dark period inhibited LIM, but had no effect on FDM (Kee et al., 2001).

Another critical difference between the two models is that one – the form deprivation model, is open loop, while the other – the negative lens model, is closed loop. In the first case, the induced accelerated growth does not correct the imposed deprivation condition, while in the second case, the growth is compensatory, progressively attenuating the imposed defocus. In the following chapters of this dissertation, our choice of form deprivation myopia over lens-induced myopia avoids the potential problem of ocular growth returning to normal due to compensation to the imposed defocus, thereby allowing unambiguous detection of inhibitory drug treatment effects (Chapters 2 and 3).

1.1.2.1 Current myopia control treatments used in humans

The management of myopia is largely limited to optical devices and ophthalmic surgical procedures to correct the refractive errors. However, certain contact lens designs, including corneal reshaping therapy and some bifocal soft contact lenses, have more recently been employed as myopia control therapies, with promising results (Aller and Wildsoet, 2008; Cho et al., 2005; Walline et al., 2009). More recently, topical atropine has grown in popularity among clinicians after demonstration that even relatively low doses can slow myopia progression (Avetisov et al., 2018; Bedrossian, 1979; Chua et al., 2006; Fan et al., 2007; Kennedy et al., 2000; Kinoshita et al., 2018; Shih et al., 2009; Tran et al., 2018; Young, 1965).

A number of studies have now demonstrated that there is a significant slowing of axial elongation in children wearing overnight corneal reshaping contact lenses compared to other methods of optical correction of myopia. Studies from the United States, Hong Kong, and Australia all show fairly similar results: a reduction in the rate of axial elongation using these lenses (Cho et al., 2005; Swarbrick et al., 2011a; Walline et al., 2009). Two independent investigations compared axial elongation in wearers of corneal reshaping contact lens to historical control groups of single vision spectacle wearers (Cho et al., 2005) and soft contact lens wearers (Walline et al., 2009). These studies found an approximately 50 percent reduction in axial elongation with corneal reshaping lenses over a two-year period. Clinical data from another study by Swarbrick et al., reported slowed elongation with monocular corneal reshaping contact lenses compared to alignment fit gas permeable contact lenses fitted to the contralateral fellow eyes of the same subjects (Swarbrick et al., 2011). In yet another recent randomized clinical trial, subjects wearing corneal reshaping contact lenses showed a slower increase in axial length, by 43%, compared to subjects wearing single vision spectacles. In this study, it was also concluded that younger myopic children tended to have faster axial elongation and may benefit from earlier intervention with corneal reshaping contact lenses (Cho and Cheung, 2012).

Soft bifocal contact lenses have proven to be another effective myopia control treatment (Aller and Wildsoet, 2008; Lopes-Ferreira et al., 2011; Ticak and Walline, 2013). The most commonly used bifocal contact lens design in these studies includes a peripheral add (less negative power) (Aller and Wildsoet, 2008), which is assumed to impose peripheral myopic blur, which from animal studies is known to act as a "stop signal" (Benavente-Perez et al., 2014; Liu and Wildsoet, 2012, 2011). In non-randomized clinical trials, soft bifocal contact lenses have been found to slow myopia progression compared to single vision spectacles or contact lenses, by up to 51% (Anstice and Phillips, 2011; Sankaridurg et al., 2011; Aller and Wildsoet, 2008), which is comparable to the average reduction achieved with corneal reshaping contact lenses (Cho and Cheung, 2012; Walline, 2012).

Atropine, a muscarinic antagonist, applied topically, is currently considered to be the most effective myopia control treatment. Atropine 1% slows myopia progression by up to 81%, but it also causes significant mydriasis and cycloplegia, as ocular side-effects (Chua et al., 2006; Lu and Chen, 2010). In one of many clinical trials of topical atropine, the Atropine for the Myopia 1 study (ATOM1) (Chia et al., 2012), the efficacy and safety of lower atropine concentrations (0.5%, 0.1%, and 0.01%) in controlling the progression of myopia was evaluated over a period of 5 years, leading to the conclusion that 0.01% topical atropine has comparable efficacy in controlling myopia progression beyond the first 12 months of treatment, with differences in myopia progression and axial length between the three groups becoming clinically insignificant, while the 0.01% concentration also resulting in less visual side-effects compared to higher atropine concentrations (0.5%, and 0.1%; ATOM2) (Chia et al., 2016). Following the release of results from ATOM study, low-concentration atropine has seen increasing popularity as a myopia control therapy, although there remain discrepancies between results of relevant clinical trials and many unanswered questions related to the optimal concentration and dosing regimen. For example, the Low-Concentration Atropine for Myopia Progression (LAMP) study evaluated the safety and efficacy of three relatively low concentrations of atropine (0.05%, 0.025%, and 0.01%) over a one-year period. The results from this trial suggest that 0.05% atropine is the more effective than the two lower concentrations in controlling myopia progression and ocular elongation, while being as well tolerated as the other two concentrations (Yam et al. 2019). How long does the effect of atropine last when treatment is terminated? Results from the ATOM1 study hint at a rebound effect, i.e. after termination of 1% atropine treatment, eyes showed higher rates of myopia progression compared to eyes treated with placebo. However, the absolute rate of myopia progression, averaged over 3 years, was still significantly lower in this atropine group than in the placebo group (Tong et al., 2009).

1.1.2.2 The association between myopia and intraocular pressure and the use of ocular hypotensive drugs to control myopia progression

Because of the known association between myopia and glaucoma, the role of intraocular pressure (IOP) in the development of myopia has been the subject of a number of studies. Some, albeit not all, studies have linked human myopia and/or longer axial lengths with higher than average IOPs [e.g.,(Abdalla and Hamdi, 1970;

Detry-Morel, 2011; Edwards and Brown, 1993; Wong et al., 2003)]. The Beaver Dam Eye study is among those linking myopic refractions with increased IOP (Wong et al., 2003). IOP was also reported to be higher in moderately and highly myopic Hispanics compared to those with either low myopic or emmetropic refractions (del Buey et al., 2014). Most studies have involved adults. However, in one study of children, IOP was reported to be also higher in myopic compared to nonmyopic eyes (Quinn et al., 1995). However, in still other adult studies, myopic eyes were reported to have slightly higher but clinically insignificant IOP compared to emmetropic and hyperopic eyes (Detry-Morel, 2011; Xu et al., 2007). Finally, in a study involving 9-11 year-old children, IOP was found not to be associated with either refractive error or axial length (Lee et al., 2004). Whether such myopia-related differences in IOP are a cause or an effect of myopia also remains unclear (Jensen, 1992; Manny et al., 2008; Genset et al. 2012).

That diurnal IOP patterns may play a role in myopic eye growth is suggested by results from several experimental myopia studies (I. Papastergiou et al., 1998; Nickla et al., 2002; Nickla et al., 1998). However, while some human studies suggest that daytime IOP is higher in myopes compared to emmetropes (Abdalla and Hamdi, 1970; Pärssinen, 1990; Quinn et al., 1995; Tomlinson and Phillips, 1970); studies of the diurnal IOP rhythms in human myopia have been limited. In one such study by Liu et al (2002), investigated diurnal IOP changes in young adults with moderate and severe myopia, with 12 measurements of IOP and axial length taken at 2-hour intervals. These authors concluded that IOP recorded in the supine position at night is not higher in young adults with moderate to severe myopia compared with age-matched adults with emmetropia or mild myopia. Results from this study further suggested that the correlation between IOP and myopia might be limited to daytime IOP (Wilensky, 1991; Liu et al., 1999). On the other hand, IOP recorded in the sitting position during the day was higher in healthy young adults with moderate to severe myopia compared to those with emmetropia and mild myopia. These findings were confirmed in another study that examined the diurnal variations in IOP for a range of refractive errors in healthy young adults and found that daytime IOP was highest and nighttime IOP was lowest in myopic eyes. Furthermore, the myopic group showed a smaller 24-hour IOP variation than the emmetropic group, with the hyperopic group having the largest 24-hour IOP variation (Loewen et al., 2010) (Figure 1.1). One possible reason for myopes having elevated day-, but not night-time IOP could be due to accommodation, which could induce transient IOP elevation with a decrease in anterior chamber depth, narrowing of the angle and thickening of the lens in progressing myopes. However, although emmetropes show similar structural changes with accommodation, no associated elevation in IOP has observed (Yan et al., 2014).

Interestingly, Liu et al. showed that the day-to-night variation of IOP was less in untreated, newly diagnosed early glaucoma patients compared to age-matched healthy individuals (Liu et al., 2003). In yet another study of young myopic eyes with open-angle glaucoma, no significant nighttime IOP elevation was found in habitual supine position while IOP was found to be elevated in age-matched control eyes. From these observations, a negative relationship between the nighttime IOP and axial length was revealed (Jeong et al., 2014).

IOP is not the only process that shows diurnal oscillations; axial length and choroidal thickness also display diurnal rhythms, i.e. over the course of the 24 hr light/ dark cycle. Studies in chicks have also shown that changes in the daily light-dark cycle can alter such diurnal rhythms, which may be important for ocular growth and emmetropization (Lauber et al., 1961, 1966,1972). For example, when chicks are exposed to constant light or constant darkness, excessive axial elongation and corneal flattening results. Note that diurnal rhythms in axial length and choroidal thickness are not limited to chickens, but have been also documented in primates, including marmosets (Nickla et al., 2002) and humans (Chakraborty et al., 2011). Axial length diurnal rhythms are also reported to be altered in the myopic eyes of form-deprived chicks (Weiss, 2003). Thus while in normal chicks, choroidal thickness peaks around midnight when the axial length is shortest (Nickla et al. 1998, papastergiou et al. 1998), form-deprived chicks undergo rapid eye elongation during both the day and night (Weiss et al. 1993). While the mechanical contribution to ocular growth of IOP rhythms remains to be resolved, an IOP increase of 100 mmHg was reported to induce ~25 D of axial myopia in young chicks in an unrelated study (Genest et al., 2012), suggesting that exaggerated changes in IOP can play a role in myopia onset and progression.

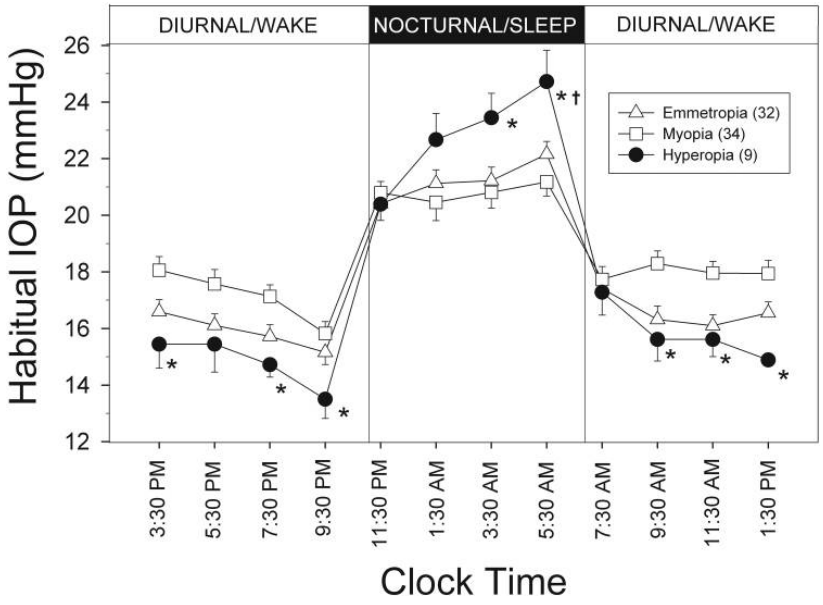

Figure 1.1: (adapted from Loewen et al., 2010). Twenty-four-hour IOP profiles recorded from hyperopic, emmetropic, and myopic groups in habitual body positions, i.e., sitting during the daytime/awake period and supine during the nighttime/sleep period. Error bars, SEM. *P < 0.05, different from the myopic group; †P < 0.05, different from the emmetropic group; one-way ANOVA and post hoc Bonferroni test.

According to Laplace's law, the tangential tension experienced by the wall of a spherical shell is directly proportional to both internal/inflationary pressure, and its radius of curvature. By applying this law to the eye, the tension experienced by the scleral wall

will be directly related to IOP and thus, at least theoretically, axial elongation can be reduced by reducing IOP.

The notion of using ocular hypotensive drugs to control myopia progression is not new. Two previous studies have tested this idea in the form-deprived myopia chick model (Jin and Stjernschantz, 2000; Schmid et al., 2000). Nonetheless, the choice of drug in one case and delivery route in the second case were arguably poor. One of these studies tested the effect of the ocular hypotensive drug, timolol, a beta-blocker, which proved to have a minimal protective effect against myopia in the chick model (Schmid et al., 2000). However, this outcome is perhaps not surprising, given more recent human studies showing little effect of this drug on IOP at night (Liu et al., 2004) when myopic growth occurs (Nickla et al., 1998). The effect of 0.25% timolol was also tested in children in a randomized clinical trial, which showed no significant difference in the progression of myopia when compared to single vision spectacles (Jensen, 1991). Other earlier studies likewise found timolol to have no significant effect on axial elongation, despite its ocular hypotensive action (Goldschmidt, E., Jensen, H., Marushak, 1985; Hosaka, 1988). The second drug to be tested in chicks was latanoprost, a PG F2-alpha analogue. However, in this earlier study, latanoprost was delivered by intravitreal injection rather than applied topically (Jin and Stjernschantz, 2000). Thus, while the study reported a positive benefit on myopia progression, the translatability of this result to the clinic is questionable, given the drug delivery route. Moreover, the underlying scleral remodelling mechanism and role of IOP in eye enlargement are likely different in the chick, which has a bilayered sclera, with a fibrous layer reinforced by an inner cartilaginous layer, compared to mammals and primates, both of which lack a scleral cartilaginous layer.

Apart from studies in chicks, the testing of IOP lowering drugs in other animal models has been limited to just one study, which tested the efficacy of brimonidine, another ocular hypotensive drug, against lens-induced myopia in guinea pigs (Liu et al., 2017). Brimonidine belongs to a different drug class than both latanoprost and timolol, being an alpha2 adrenergic agonist, with effects on both aqueous inflow and uveoscleral outflow. Nonetheless, it proved effective in stabilizing myopia progression.

Among the various ocular hypotensive drugs available today as glaucoma therapies, prostaglandin (PG) analogues are the most widely used (Jin and Stjernschantz, 2000). As a potential myopia control treatment that they have proven to be effective in lowering IOP around the clock (24 h) has considerable merit. However, their mode of action may be problematic. Specifically, PG analogues promote matrix metalloproteinase (MMP) activity and thus remodelling of the extracellular matrix (ECM) within the uveoscleral outflow pathway (Russo et al., 2008). This group of drugs has also been reported to promote scleral ECM remodelling, an action that may exacerbate rather than slow myopia progression (Kim et al., 2001), given that myopia progression per se has also been linked to increased scleral remodelling (Harper and Summers, 2015). In studies described in this dissertation, we investigated the efficacy of topical latanoprost as a myopia control therapy in the form-deprived guinea pig, as a myopia animal model.

1.2 Intraocular pressure

1.2.1 Intraocular pressure, its regulation, and aqueous humor dynamics

Intraocular pressure (IOP) reflects the relative balance of aqueous inflow and outflow, and provides the eye with its shape and rigidity.

The secretion of aqueous humor (AH) and the regulation of its outflow are physiologically critical for the normal eye function. In healthy human eyes, the flow of AH against resistance generates an average IOP of ~ 15 mmHg (Goel et al., 2010). Generally, IOP is considered normal if it is two standard deviations below and above the mean, which ranges between 10 and 21 mmHg (Asrani et al., 2000; Liu et al., 1999). Any imbalance between the production and removal of the AH in which the former dominates results in IOP elevation, which is the central problem in glaucoma.

The main ocular structures related to AH dynamics are the ciliary body, where AH production occurs, and the trabecular meshwork (TM), Schlemm's canal and uveoscleral pathway, which represent the key components of the AH outflow pathway: The conventional outflow pathway involves the passage of AH through the TM, into Schlemm's canal and finally into the episcleral veins (Ascher, 1954; Goldmann H, 1950). In a second, so-called unconventional pathway, AH passes through the suprachoroidal space after entering the connective tissue between the ciliary muscle bundles, and finally out through the sclera (Bill and Hellsing, 1965). The physiology of these two pathways differs in many important ways. For instance, unlike the conventional pathway, the unconventional pathway is relatively independent of IOP (Brubaker, 2001) and the two pathways are also differentially affected by most pharmacological IOP lowering agents (Bill, 2003). However, ECM regulation appears to influence the resistance of AH outflow in both pathways (Goel et al., 2010).

The IOP lowering (ocular hypotensive) drugs typically used to treat glaucoma, work by reducing AH production and/ or increasing aqueous outflow through TM and/ or uveoscleral routes. These effects and mechanisms of action of the different ocular hypotensive drug classes are critical determinants of their potential for controlling myopia progression, the main focus of this dissertation, the background for which is provided in section 1.3.4.

1.2.2 Diurnal intraocular pressure rhythms in animals

Diurnal rhythms in IOP have been documented in many species, including mice (Aihara et al., 2003a), rats (Krishna et al., 1995; Moore et al., 1996), chicks (Weiss and Schaeffel, 1993; Nickla et al., 1998); rabbits (Katz et al. 1975; Rowland et al. 1981; McLaren et al., 1996), monkeys (Bito et al., 1979; Liu et al., 1994; Nickla et al., 2002; Yu et al., 2009), and humans (David et al., 1992; Liu et al., 2003, 1999) with species differences in the phase and amplitude of IOP rhythms apparent (Table 1.1).

Mice

Mice have become increasingly popular as a research animal due to the similarities observed between mouse and human eye, which includes having a well-defined trabecular meshwork, Schlemm's canal, ciliary body, and uveoscleral outflow (Lindsey and Weinreb, 2002; Smith et al., 2001), and similar responses to ocular hypotensive drugs (Aihara et al., 2002; Avila et al., 2003). However, studies investigating the diurnal IOP variations in mouse eyes are limited. As mice are nocturnal animals, their activity is higher at night and so it is possible that IOP might also rise at night. One study suggested that the circadian IOP rhythm in mice is biphasic, with any exposure to light disrupting this IOP rhythm. In this same study, IOP was measured every three hours using a microneedle method. Under a 12 hr light/ 12 hr dark cycle, the diurnal IOP rhythm showed a sinusoidal pattern, with IOP being highest in the early evening (before 9 pm), and declining in the morning until noon (Aihara et al., 2003b). In another study, IOP in freely moving C57BL/6J and CBA/CaJ mice strains was recorded every 5 minutes over 24 hr using a pressure catheter for 4-13 days. As expected, in the two mice strains, IOP during the dark was significantly higher than during the light. However, the magnitude of light-to-dark IOP elevation was different for the two strains (Li and Liu, 2008). This strain related difference might reflect differences in clock genes, e.g., Cry1, Cry2, Per1, Per2, appear to be involved in the regulation of the circadian IOP rhythm.(Dalvin and Fautsch, 2015; Maeda et al., 2006). Broad variations in IOP across different strains of genetically modified mice have also been reported, making them an important resource for studying IOP regulation and glaucoma (Savinova et al., 2001). Overall, the results of these studies agree that mice have the highest IOP in the dark and lowest during the light.

Rats

Like mice, rats are nocturnal species. Therefore, IOP is expected to be elevated in the dark and be lowest in the light. This prediction is also consistent with the findings of Moore and colleagues who measured Brown Norway rats reared on 12 hrs light/ 12 hrs dark schedule, at 4-hour intervals using Tonopen XL tonometer. The lowest IOP was recorded when lights were on (19.3 ± 1.9 mm Hg) and highest (31.3 ± 1.3 mm Hg) during the dark (Moore et al., 1996). These results are consistent with those from recorded from another common strain of rat (Lewis rats) using a Tono-Pen to measure IOPs every 2 hrs between 6:00 am and midnight, and every 3 hours between midnight and 6:00 am (Krishna et al., 1995). IOPs showed a consistent trough in the early morning (6:00 am) and a peak at 8:00 pm.

In a study comparing the diurnal rhythms in IOP in Brown Norway rats housed in standard light-dark conditions versus continuous dim light conditions, a persistent, but dampened rhythm of IOP under the latter conditions (Lozano et al., 2015), highlighting the important influence of the lighting conditions used in rearing on study outcomes.

Chickens

Like most animals, chicks exhibit a diurnal IOP rhythm. However, in contrast to the findings for rodents, IOPs tend to be highest during the day and lowest in the middle of the night, with a similar phase to axial length rhythm (Weiss and Schaeffel, 1993; Nickla et al., 1998). The amplitude of IOP rhythm as reported in one study was ~ 8 mmHg (Nickla et al., 1998). The important influence of the lighting conditions on IOP in chicks has been demonstrated in a number of studies. For example, when chicks were reared in the total darkness, the IOP rhythm persisted, but with a smaller amplitude (Nickla et al., 1998), while constant light conditions have been reported to suppress the usual diurnal fluctuations in IOP in hatchling chicks (Wahl et al. 2016). Likewise, Li et al., 2003 reported that daytime IOP was lower in birds raised in constant light (Li and Howland, 2003). Finally, after 3 weeks of constant light conditions, recovery required more than 1 week in normal diurnal light conditions (Wahl et al., 2016).

Rabbits

While diurnal variations in IOP are also a consistent finding in rabbits, there are inconsistencies in results across studies. Nonetheless, it is generally agreed that rabbits have their highest IOP in the dark. One of the earliest studies in rabbits found the lowest IOP to occur at night, with IOP reaching its highest level during the day between 8:00 and 11:00 am and 4:00 and 7:00 pm (biphasic), when measured hourly by application tonometry (Katz et al. 1975). Another study that used rebound tonometer, showed that IOP was a little lower, on average, during the light phase (7 am to 7 pm) than during the dark (8 pm to 6 am), but that IOP was highest at ~10 am over the 24 hr period (Wang et al., 2013). Three studies by Liu and Dacus in 1991 also reported IOP to be elevated in the dark and low in the light. The latter group suggested that increased resistance of aqueous outflow, mediated by alpha-1 adrenergic receptors, could contribute to these findings (Liu et al., 1991; J. H K Liu and Dacus, 1991; J. H.K. Liu and Dacus, 1991). Similar results were obtained in a study using an implanted pressure transducer to measure IOP continuously in rabbits, i.e., IOP decreased after lights turned on and increased after lights turned off. However, it is possible that the implant surgery affected the IOP rhythm, which could explain why the timing of the nocturnal rise in IOP advanced gradually over approximately 2 weeks (McLaren et al., 1996).

Guinea Pigs

Although guinea pigs are considered rodents, they do not seem to share the same circadian rhythms as mice and rats. Guinea pigs are neither strictly diurnal nor nocturnal, but rather tend to be crepuscular.

One IOP study involving guinea pigs used a Tonolab to measure IOPs, which were found to exhibit a diurnal variation, peaking in the early morning when the light first came on and decreasing across the day (Lisa A. Ostrin and Wildsoet, 2016). Results from one of the studies presented in a latter chapter of this dissertation agree with these findings. However, a different study comparing rebound and applanation tonometers

reported opposite results compared to our findings. Specifically, IOP was reported to be lower during the light phase (7 am to 7 pm) than during the dark phase (8 pm to 6 am) and the lowest IOP occurred at 7 am (Rajaei et al., 2016). The origin of this difference in study outcomes is unclear, especially given that all of the above studies used a 12 h:12h light/ dark cycle for rearing, although it could reflect, at least in part, the randomly scattered periods of activity interspersed with shorter periods of sleep throughout the day and night, as is typical of guinea pig behavior.

Dogs

Diurnal variations in IOP have been also observed in dogs (Gelatt et al. 1981; Giannetto et al., 2009; Martín-Suárez et al., 2014; Piccione et al., 2010), which show similar patterns to humans, with highest values occurring in the early morning and troughs during the day.

Giannetto et al. measured IOPs in Beagle dogs every 4 hours for 48 hours using Tono-Pen applanation tonometer. Mean IOP in the first day was 17.44± 0.83 mmHg and 17.19 ± 1.14 mmHg in the second day. In another study, IOPs were recorded every 90 minutes from 8:00 am to 8:00 pm in healthy dogs using applanation tonometry. This study reported a mean IOP (± SD) of 15.2 ± 2.2 mmHg, which is very close to the average IOP of humans. Furthermore, there were no significant differences between a reading taken within the 8:00 am to 3:30 pm window, while readings taken after 3:30 pm were significantly lower (Martín-Suárez et al., 2014b).

When exposing dogs to four different artificial lighting regimes, including 12 hr light/ 12 hr dark, 12 hr dark/ 12 hr light, constant light, and constant darkness, diurnal rhythms in IOP were found in all cases except in constant light, which resulted in a loss of the IOP rhythm in constant light similar to that previously reported in mice, rats, and rabbits (Liu et al., 1994; Maeda et al., 2006; Moore et al., 1996).

Monkeys and marmosets

Several studies have shown that the diurnal rhythms of IOP in monkeys are remarkably similar to that of humans, with some but not all studies reporting differences in IOP rhythms between young and old monkeys. In one study of less than 6 years old monkeys, IOP was reported to decline between 9 am and 2 pm, while older animals showed smaller fluctuations between 8 am and 5 pm. However, it is worth noting that IOP was measured under general anaesthesia in the latter study, using a floating-tip pneumatonometer (Bito et al., 1979).

In another study, IOPs were measured in monkeys every 3 hours using TonoVet® rebound tonometer without sedation or anaesthesia. In this study, the lowest IOP was recorded at 3 am (19.8±0.4 mmHg) and highest at noon (29.3±0.9 mmHg), with similar results for young and older monkeys (Liu et al., 2011). These results contrast with those from another study using a TonoVet rebound tonometer, in which IOP measurements were measured every three hours between 9:00 am and 9:00 pm in sedated, seated

rhesus monkeys. In these animals, IOP peaked at 3:00 pm and 9:00 pm and troughed at noon and 6:00 pm (Yu et al., 2009).

Diurnal IOP rhythms were also documented in marmosets, a smaller primate, with IOPs being highest in the dark and lowest during the light period, with a mean difference of 3.6 mmHg (Nickla et al., 2002). In this study, IOPs were measured under isoflurane anaesthesia by Tono-pen applanation tonometry at 12- hour intervals, using three different measurement schedules (6 am and 6 pm in 10 animals; 12 pm, 12 am, and 12 pm in 3 animals and 6-hr intervals starting at 2 pm in 1 animal).

Humans

Traditionally, IOP in normal humans is thought to be highest in the early morning, between 6 am and 10 am (Konstas et al., 2005a; Konstas et al., 2006; Quaranta et al., 2008, 2006). This assumption is consistent with the results of a well-controlled study by Liu et al. although they reported the peak IOP to occur just before the start of the light period, around 5:30 am, with the lowest IOP recorded just before the start of the dark period, around 9:30 pm, in young healthy subjects (Liu et al., 2003, 1999).

Liu et al. also concluded that the change in posture from sitting to supine positions may contribute to both the nocturnal IOP elevation and drop in systemic blood pressure. Related change in the episcleral venous pressure in supine position could partially account for the nocturnal IOP increase (Liu et al., 2003, 1999).

Comparison across species

Rodents, including mice and rats, are considered nocturnal animals, therefore, their IOP tend to rise at night and fall in the morning. Guinea pigs do not seem to display the same IOP rhythms as mice and rats, despite branching from the rodents' family. Guinea pigs are neither strictly diurnal nor nocturnal and tend to be crepuscular, with randomly scattered periods of activity and sleep around the clock. Rabbits and marmosets are mostly nocturnal, with IOP being highest in the dark and lowest during the light period. Finally, chicks, dogs, and monkeys all have similar patterns to humans, with IOP being highest in the early morning and decreasing thereafter across the day.

As apparent from the preceding summary of the various IOP studies, it is very challenging to compare results across different studies, due to the use of different methods to measure IOP, different measurement schedules, and sometimes different light/ dark cycles in rearing. Nonetheless, diurnal variations in IOP were a consistent finding across studies and species. Thus, when measuring IOPs, it is critical to have consistency of measurement times and tools in studies involving repeated measurements. Also, as it is known that general anesthesia tends to lower IOP (Duncalf, 1975; Jantzen, 1988), it is preferable to avoid it where possible.

Table 1.1: Summary of studies that have performed diurnal intraocular pressure rhythms in different species.

Study	Species	Interval	Method	Results
Aihara 2003	Mice	Every 3 h	Microneedle	Biphasic (highest evening until 9p, declined in the morning until noon
Li 2008	Mice	Every 5 min	Pressure Catheter	Highest in dark, lowest during light
Krishna 1995	Rats	Every 2 h (6a-12a) Every 3 h (12a – 6a)	Tonopen	Trough at 6a, peak at 8p.
Moore 1996	Rats	Every 4 h	Tonopen XL	Highest in dark, lowest during light
Nickla 2002	Chicks	Every 6 h or every 12 h	Applanation tonometer	Highest during the day, lowest at night
Katz 1975	Rabbits	Every 1 h	Application tonometer	Biphasic (Lowest at night, highest 8-11a and 4-7p.
Liu 1991	Rabbits	Every 4 h	pneumatonometer	Highest in dark, lowest during light
Mclaren 1996	Rabbits	for 15 seconds every 2.5 minutes	Pressure transducer	Highest in dark, lowest during light
Wang 2013	Rabbits	Every 1 h	Rebound tonometer	Highest at 10 am, IOP 7am-7pm is little lower than 8 p- 6 a
Ostrin 2016	Guinea Pigs	Every 2 h	Tonolab	Highest in the morning and lowers throughout the day
Rajaei 2016	Guinea Pigs	Every 8 h	Rebound and applanation tonometers	Lowest 7a-7p. Highest 8p-6a
El-Nimri 2018	Guinea Pigs	Every 6 h	iCare tonometer	Highest in the morning and lowers throughout the day
Ginnetto 2009	Dogs	Every 4 h	Tonopen	Diurnal acrophase
Martin-Suarez 2014	Dogs	Every 90 min	Aplanation tonometry	Lower after 3:30p, no difference 8a -3:30p
Bito 1979	Monkeys	Every 2 h	Pneumatonometer (anesthesia)	Lowest 9a-2p, small fluctuations between 8a- 5p
Yu 2009	Monkeys	Every 3 h	Tonovet	Peak 3p-9p Trough noon- 6p
Liu 2011	Monkeys	Every 3 h	Tonovet	Lowest at 3 am, highest at noon
Nickla 2002	Marmosets	Every 6 h	Tonopen (anaesthesia)	Highest in dark, lowest during light

1.2.3 Current ocular hypotensive (anti-glaucoma) drug treatments and their mechanisms of action

There are many effective IOP lowering drugs, developed as therapies for patients with primary open-angle glaucoma and ocular hypertension. In all cases, the ocular hypotensive actions of these drugs reflect effects on aqueous humor dynamics, either decreased production or increased outflow through the trabecular meshwork or uveoscleral pathway, or by a combination of these mechanisms. The ideal ocular hypotensive drug is one that is effective at lowering IOP across 24 hr, needs to be dosed only once a day, and has no adverse side-effects. These points were kept in mind in selecting the drug for testing the efficacy of lowering IOP as an approach for controlling myopia progression. A brief summary of the current treatment options is given below, with key features of each drug group summarized in Table 1.2.

In early 1960, the only available glaucoma drugs were topical cholinergic agents that improved aqueous outflow, topical adrenergic drugs that reduced aqueous production, and systemic carbonic anhydrase inhibitors that reduced aqueous inflow (Hoyng et al., 2000). Since then, many new ocular hypotensive drug classes have appeared.

Beta-blockers

Beta-blockers lower IOP by decreasing aqueous production. They act by binding beta-adrenergic receptors on the nonpigmented epithelium of the ciliary body, thereby inhibiting the actions of endogenous sympathomimetic catecholamines,(Zimmerman, 1993). Currently available topical formulations for glaucoma therapy include non-selective beta blockers that inhibit both beta 1 and 2 adrenergic receptors, as well as one selective beta 1 blocker (Hoyng et al., 2000). Beta-blockers lower IOP by 20-27% during the daytime (Orzalesi et al., 2000a; Stewart and Castelli, 1996), while they have little to no effect on nocturnal IOP (Liu et al., 2004; Orzalesi et al., 2000). The latter profile reflects the decrease in the levels of circulating epinephrine decrease during sleep (Orzalesi et al., 2000).

As previously described, the nonselective beta-blocker, timolol, had minimal protective effect against myopia in chicks and humans (Jensen, 1992b; Schmid et al., 2000). This outcome is not surprising, given that, as predicted, timolol was found to have little effect on IOP at night (Liu et al., 2004), which is when eye growth is accelerated in myopia progression, at least in chicks (Nickla et al., 1998). Interestingly, timolol does appear to lowering IOP in guinea pigs, contrasting with the report that it is ineffective in lowering IOP during the night in humans, and possibly reflecting the crepuscular nature of guinea pigs (El-Nimri 2019, AOPT abstract).

Alpha agonists

Apraclonidine and brimonidine, which belong to the alpha2 adrenergic agonist class of drugs, were introduced in the early 1990s. These drugs work by reducing aqueous

humor production, with brimonidine also increasing uveoscleral outflow (Toris, 2007). In humans, decreases in IOP by 12.5% to 29% one-hour post administration have been reported. In the case of brimonidine, its maximum effect is reported to occur ~4-5 hours after administration, with little or no effect on night-time IOP (Katz, 1999; Liu et al., 2010; Van Der Valk et al., 2005). The latter observation is also consistent with its mechanism of action, although a study comparing the 24-hour IOP lowering profiles of brimonidine and dorzolamide/ latanoprost combination found them to be comparable (Konstas et al., 2005).

It is plausible that alpha 2 agonists will be more effective in lowering IOP at night in guinea pigs, for the same reason that beta-blockers are more effective, i.e., because of their crepuscular nature. This prediction is also consistent with results from a recent study which showed brimonidine to be effective in stabilizing myopia progression in guinea pigs using a lens-induced myopia model (Liu et al., 2017).

Carbonic anhydrase inhibitors (CAI)

There are two topical CAIs available for ocular use, dorzolamide and brinzolamide, which work by decreasing aqueous humor production. These drugs are sulfonamide derivatives that inhibit carbonic anhydrase in the nonpigmented epithelium of the ciliary body, the net effect being decreases in ion and fluid transport, thereby decreasing the secretion of aqueous humor. CAIs reduce the production of aqueous less than timolol. Therefore, they also reduce IOP to a lesser degree (Silver, 1998; Wayman et al., 1998), with effects of between 13.2% to 22% reported (Sall, 2000; Van Der Valk et al., 2005). For this reason, CAIs are best used as adjunctive therapy to other ocular hypotensive drugs (Clinechmidt et al., 1995; Tsukamoto et al., 2005). Nonetheless, they do have modest efficacy during the night (Orzalesi et al., 2000).

Due to their relatively lower efficacy, CAI were not selected for testing in our myopia control studies.

Prostaglandin analogues (PGs)

Prostaglandin analogues now represent the most widely prescribed topical glaucoma therapies. Developed at the end of the 90s, they have proven very effective in lowering IOP around the clock (24 h) and are currently considered the first line treatment for open-angle glaucoma (T. Li et al., 2016). Remodeling of the extracellular matrix (ECM) within the uveoscleral (UV) outflow pathway as reflected in increased matrix metalloproteinase (MMP-2 and 3) activity appears to be largely responsible for their enduring ocular hypotensive action (Gaton et al., 2001; Russo et al., 2008).

Three of the PG analogues (latanoprost, travoprost, and bimatoprost) are approved for use as glaucoma therapies in the United States. Reductions in IOP by 18% to 31% during the day have been reported (Diestelhorst et al., 2002; Orzalesi et al., 2000; Van Der Valk et al., 2005). Notably, IOP reductions of about 8.5% to 17% during the night

have been reported, contrasting with the negligible effect of beta blockers at night (Liu et al., 2004; Orzalesi et al., 2000b).

Latanoprost (Xalatan) is an ester prodrug of PGF2 alpha analogue, with selective FP receptor agonist activity (Toris et al., 1993). It is used as first-line therapy in POAG, because of its efficacy reducing IOP by 25-34% (Camras, 1996; Mishima et al., 1997), achievable with only once a day administration. Latanoprost is considered well-tolerated and safe with mild conjunctival hyperemia, hyperpigmentation, hypertrichosis in the lids and lashes and decreases in orbital fat (Camras, 1996; Chiba et al., 2004). Serious, but rare side-effects, include cystoid macular edema, anterior uveitis, and re-activation of herpes simplex keratitis (Fechtner et al., 1998; Morales et al., 2001; Wand et al., 2001; Warwar et al., 1998).

The effect of latanoprost on myopia progression was first tested in chicks, applied by intravitreal injection rather than topical delivery (Jin and Stjernschantz, 2000). Thus, while the study reported a positive benefit of latanoprost on myopia progression, the translatability of this result to the clinic is questionable, given the drug delivery route used. We chose to test the effect of latanoprost in controlling myopia progression in the guinea pig myopia model, because it has proven to be effective in lowering IOP around the clock (24 hr), despite some concerns related to the known effect of PG analogues on ECM remodeling (i.e. increased remodelling),,an action that may exacerbate rather than slow myopia progression (Kim et al., 2001). That being said, latanoprost proved to be effective in slowing down myopia progression in our guinea pig myopia model (El-nimri and Wildsoet, 2018).

New anti-glaucoma drugs

Latanoprostene bound (LB), a recently FDA-approved drug, is a potent nitric oxide (NO)-donating derivative of latanoprost, which promotes aqueous outflow through both the trabecular meshwork and uveoscleral routes (Kaufman, 2017; Liu et al., 2016). Interestingly, nitric oxide has been linked to choroidal thickening and ocular growth inhibition in chicks (Nickla et al., 2009, 2006; Nickla and Wildsoet, 2004) Thus given its demonstrated potency in lowering IOP around the clock in humans, it would seem a good candidate for testing as a myopia control therapy.

Rho kinase (ROCK) inhibitors, including netarsudil, represent another new class of glaucoma therapies. Their ocular hypotensive action appears to be achieved through enhanced trabecular outflow, with reductions in episcleral venous pressure through vasodilation being a contributing factor. This class also seems to have similar efficacy at lowering IOP during the night as it does during the day (24 hour effect) (Van de Velde et al., 2015), and is reported to be more effective when compared to timolol in lowering IOP in eyes that have relatively low IOPs (Serle et al., 2018). The latter observation suggests that it might be a good choice for myopia control in otherwise healthy eyes with normal IOPs, i.e., between 10 and 21 mmHg.

Table 1.2: Summary of Intraocular pressure lowering drug (anti-glaucoma) classes available

Drug Class	Drug Name	Mechanism of action	Effect	Receptor mediated or ECM remodeling	Tested for myopia control
Beta-blockers	Timolol Betaxolol Carteolol	Sympathomimetic-Block effect of epinephrine	Decrease aqueous production	Receptor	Yes
Alpha 2 agonists	Apraclonidine Brimonidine	Selective alpha 2 adrenoceptor agonists	Reduce aqueous humor production increase uveoscleral outflow	Receptor	Yes
Carbonic anhydrase inhibitors	Dorzolamide Brinzolamide	Inhibit carbonic anhydrase in the ciliary body	Decrease aqueous production	Receptor	No
Prostaglandin analogues	Latanoprost Travoprost Bimatoprost	Extracellular matrix (ECM) remodelling within the uveoscleral (UV) outflow pathway	Increase UV outflow	ECM remodeling	Yes
Latanoprostene bound	Latanoprostene bound or Vyzulta	potent nitric oxide (NO)-donating derivative of latanoprost	Increase aqueous outflow through both TM and UV routes	ECM remodeling	—
Rho kinase inhibitors	Netarsudil	Inhibit Rho kinase	increase aqueous outflow	Receptor	—

Chapter 2: Changes in diurnal intraocular pressure rhythms, scleral and optic nerve head architecture with myopia progression in the guinea pig form-deprivation model

2.1 Introduction

Many studies in experimental animal myopia investigated the role of 24-hour intraocular pressure variation in the myopic eye growth (I. Papastergiou et al., 1998b; Nickla et al., 2002; Nickla et al., 1998). Form deprivation (FD) in chicks was reported to not affect the amplitude of IOP rhythm but causes more phase variability. For example, the trough does not consistently occur at night when compared to normal eyes (Nickla et al., 1998). They also concluded that IOP rhythms influence eye elongation in chicks by inflating the eye and/or influencing scleral extracellular matrix production rhythms. In guinea pigs, there is some controversy in IOP diurnal rhythms role in normal eye growth. One study showed that IOP was lower during the light period than the dark period (Rajaei et al., 2016), while other study states the opposite (L.A. Ostrin and Wildsoet, 2016). In our study, we measured IOP in normal and myopic guinea pig eyes for a total of 10 weeks. For all of our guinea pigs, IOP peaked when lights turned on and became lower throughout the day.

The sclera plays an important role in ocular growth regulation. Increased remodelling of the scleral matrix may lead to scleral thinning and weakening, which in turn leads to myopic growth and increased risk of other ocular complications. The sclera is mainly made up of collagen type I, with fibroblasts functioning to produce and maintain the extracellular matrix. It is well established that there are structural and biomechanical changes in the myopic sclera. In myopic eyes, the sclera is thinner and its collagen is reduced and disorganized, which makes it biomechanically weaker and more unstable leading to scleral creep (irreversible scleral stretching caused by constant mechanical stress) and in its more exaggerated form, it may lead to posterior staphyloma, where there is a mechanical scleral failure (Avetisov et al., 1983; Curtin et al., 1969, 1979). These myopic structural and biomechanical changes are considered a byproduct of the scleral molecular changes. It is well known in the literature that the scleral changes in myopic eyes are related to altered genes expressions, including, but not limited to type 1 collagen, matrix metalloproteases (especially MMP2), tissue inhibitor of MMPs (TIMP), TGF beta, and integrins (Barathi and Beuerman, 2011; McBrien et al., 2006; McBrien and Gentle, 2003; Rada et al., 1999). MMP2, an enzyme associated with collagen breakdown was shown to increase and TIMP-1 to decrease in the myopic

sclera of tree shrews (Guggenheim and McBrien, 1996; J. T. Siegwart and Norton, 2001). TGF beta and alpha 1, 2 and beta 1 integrins were downregulated and FGF receptor-1 was upregulated in the myopic sclera (Gao et al., 2011; Gentle and McBrien, 2002; Jobling et al., 2004). Cyclic AMP and GMP levels were also found to increase in FD guinea pigs and injecting normal guinea pigs with inhibitors of these secondary messengers inhibited FD myopia (Fang et al., 2013; Tao et al., 2013).

The lamina cribrosa (LC) is a multilayered mesh-like network of collagen fibers that inserts into the scleral canal. The LC plays an important role in maintaining a pressure gradient and forming an interface between the intraocular pressure inside the eye and the cerebrospinal fluid pressure in the optic nerve sheath (Balaratnasingam et al., 2007; Eraslan et al., 2016; Kim et al., 2015; Yang et al., 2007a). The LC is weaker and thinner than the surrounding dense sclera. As a result, the LC is more sensitive to IOP changes and tends to displace posteriorly causing pores pinching and deformation as a response to elevated IOP. This is believed to be one of the causes of the glaucomatous optic nerve damage (Morgan-Davies, 2004).

A thinner and weaker peripapillary sclera in myopia can affect the lamina cribrosa biomechanics explaining in part the increased risk of glaucomatous damage in myopic patients (Jonas et al., 2011; Norman et al., 2011). In fact, it was found that the LC thickness decreases with longer axial length and thinner posterior sclera (including sclera at the optic disc border) in non-glaucomatous monkeys; a similar finding to humans (Jonas et al., 2016). In our study, we also examine the optic nerve head, lamina cribrosa, and scleral macro/ micro-structural changes in FD guinea pigs.

2.2 Methods

2.2.1 Animals

Pigmented guinea pigs were used in this study, with breeders obtained from the University of Auckland, New Zealand. Study animals were bred on-site and housed in a temperature-controlled room with a light/dark cycle of 12L/ 12D (on at 9.30 am, off at 9.30 pm). Pups were weaned at 5 days of age and housed as single-sex groups in 41 cm wide X 51 cm long transparent plastic wire-top cages, with free access to water and vitamin C-supplemented food, with additional fresh fruit and vegetables given five times a week as diet enrichment. All animal care and treatments in this study conform to the ARVO Statement for the Use of Animals in Ophthalmic and Vision Research. Experimental protocols are approved by the Animal Care and Use Committee of the University of California, Berkeley.

2.2.2 Treatments and monitoring

Ten guinea pigs underwent monocular FD, using white plastic diffusers worn from 14-days of age for 10-weeks to induce progressive myopia. Untreated contralateral eyes

served as controls. FD treatment was monitored every 30 minutes to 1 hour during light cycle (12 hours).

The design of the diffusers and attachment protocol were adapted from those implemented in chicks (Wildsoet and Wallman, 1995). The diffusers were made from sheets of white styrene (Midwest Products Co), hot-molded into semicircular domes and mounted on hook Velcro ring supports. Opaque diffusers were used in this study. To attach the diffusers to the guinea pigs, rings of loop Velcro were cut in halves and the two segments symmetrically affixed to the fur surrounding one of the guinea pig's eyes using gel cyanoacrylate glue (SureHold® Plastic Surgery) (Figure 2.1).

Figure 2.1: Guinea pig with a monocular detachable diffuser attached to induce form deprivation (FD) myopia.

2.2.3 Measurements: Intraocular pressure, refractive error, and axial ocular dimensional measurements

Intraocular pressures (IOP), spherical equivalent refractive errors (SE) and optical axial lengths (AL) were recorded for both eyes of each animal, immediately before the initiation of the FD treatment (baseline), with follow-up measurements made at weekly intervals over the first month and every other week thereafter. Because of well-documented circadian rhythms in both IOP and eye elongation (Nickla et al. 1998), measurements were always taken around the same time each day, early in the morning, after lights-on.

All IOP measurements were conducted in awake animals, prior to other procedures requiring anaesthesia to avoid possible confounding effects of the latter. An iCare rebound tonometer (Tonolab, Helsinki, Finland) was used along with the setting for rat eyes, for which this instrument has been calibrated and which are similar in size to those of guinea pigs. This instrument provides confidence interval information based on

successive readings; only data with a confidence interval of 5% or less were used. Three measurements were taken on each eye and the average used in data analysis.

Refractive errors were measured using streak retinoscopy on awake animals, 30 minutes after instillation of one drop of 1% cyclopentolate hydrochloride (Bausch & Lomb, Rochester, NY) for cycloplegia. Spherical equivalent refractive errors (average of results for the two principal meridians) were derived for use in data analysis.

Ocular axial dimensions were measured with a custom-built, high-frequency A-scan ultrasonography system, with an estimated resolution of ~10 μm (Nickla et al., 1998; Wildsoet and Wallman, 1995). For these measurements, animals were first placed under gaseous anaesthesia (1.5-2.5% isoflurane in oxygen), with eyelid retractors inserted to hold their eyes open. For each measurement, at least 8 traces were captured per eye and analyzed off-line. Only optical axial lengths are reported here, derived as the sum of anterior chamber depth, axial lens thickness and vitreous chamber depth.

2.2.4 Measurements: Diurnal intraocular pressure rhythms

To characterize diurnal rhythms in IOP, five measurements were made using the iCare tonometer at ~6 h intervals over 24 h, including time points just after lights-on and just before lights-off. Measurements during the lights-off hours were taken under photographic dark light conditions to minimize the possible effect of brief exposures to light on circadian rhythms. Three measurements were taken on each eye at each time point and averaged for use in data analysis.

2.2.5 Measurements: SD-OCT imaging

A high-resolution spectral-domain optical coherence tomography system (SD-OCT, Bioptigen, USA) was used to image the optic nerve head (ONH), starting one day before the diffusers are attached and once per month thereafter. Both eyes of each animal were imaged. Guinea pigs were first anaesthetized with an intramuscular injection of ketamine and xylazine (27 mg/kg, 0.6 mg/kg, respectively), then placed on a custom-made stage with x – y – z adjustments to facilitate align the optical axis of the eye being imaged with that of the instrument. A high-resolution OCT scan was generated from 500 B-scans by 400 A-scans, with a 12 by 12 mm field size, with two to three such scans, centred on the ONH, captured from each eye at each time point (Figure 2.2).

A cross-sectional 200×200 pixel image containing the ONH at its maximum horizontal dimension was selected to assess ONH diameter, using the termination in Bruch's membrane to define its boundary. Relevant points in the image were manually selected and diameter measured using a custom MATLAB (MathWorks Inc., Natick, MA) program. Values were corrected for differences in magnification related to the eye's length.

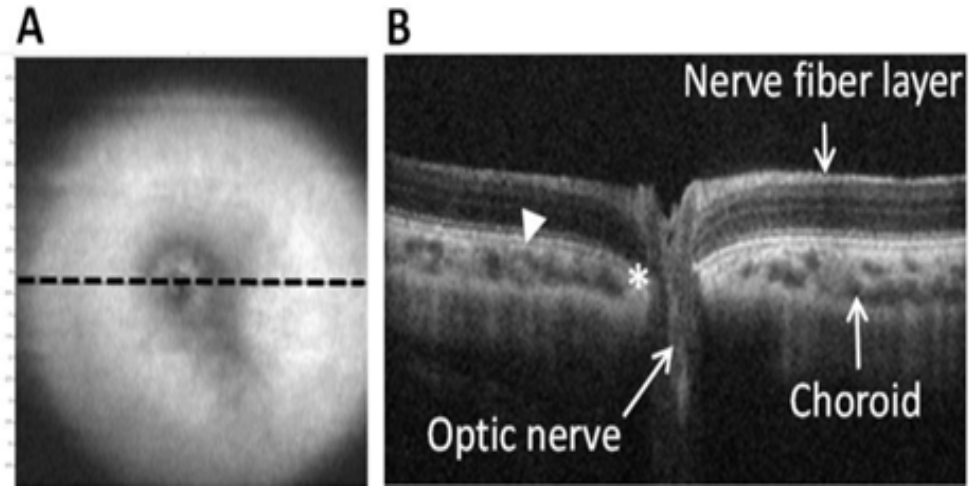

Figure 2.2: In Vivo SD-OCT images from a 2 week –old guinea pig: (A) Low resolution en face volume intensity projection, indicating location of cross-sectional image in B (dotted line), and (B) corresponding OCT image through optic nerve head (12 mm line scan, arrowhead: choroidoretinal border , asterisk, termination of Bruch's membrane).

2.2.6 Scanning electron microscopy to image lamina cribrosa

Following animals sacrifice, eyes were enucleated and ONHs excised from the posterior segment to include a 4 mm ring of surrounding sclera for scanning electron microscopy (SEM). ONH samples were first soaked in 0.2M NaOH for 30 h, to remove cellular components, leaving only collagenous structures. ONHs/ lamina cribrosa (LC) samples were then fixed in 4% glutaraldehyde in 0.1M sodium cacodylate, stained with osmium tetroxide, dried through an ethanol series, and finally subjected to critical point drying before imaging. LC samples were imaged using a Hitachi TM-1000 scanning electron microscope. Images were captured at 600X magnification (Figure 2.3).

Figure 2.3: The process of imaging the lamina cribrosa; A) processed optic nerve head and 4 mm ring of the surrounding sclera, B) Scanning electron microscope, C) lamina cribrosa electron microscopy image at 600X.

2.2.7 Transmission electron microscopy to image scleral collagen

Following animals sacrifice, eyes were enucleated and optic nerve heads (ONHs) excised from the posterior segment. A 6 mm ring of sclera surrounding the ONH was excised using disposable punchers for transmission electron microscopy (TEM). Tissue samples were first fixed in 4% glutaraldehyde in 0.1M sodium cacodylate, stained with osmium tetroxide, dried through an acetone series, infiltrated with resin and finally embedded into molds (Figure 2.4).

Figure 2.4: Resin molded blocks containing cross-sections of scleral tissue on both edges.

To section the sample blocks, the blocks containing a cross-section of the tissue were hand-cut by razorblade creating a face in the shape of a right trapezoid. Smooth faces were made using a diamond knife on a Reichert-Jung Ultracut E microtome. The tissue sections were cut into 70 nm silver and gold-colored sections (Figure 2.5).

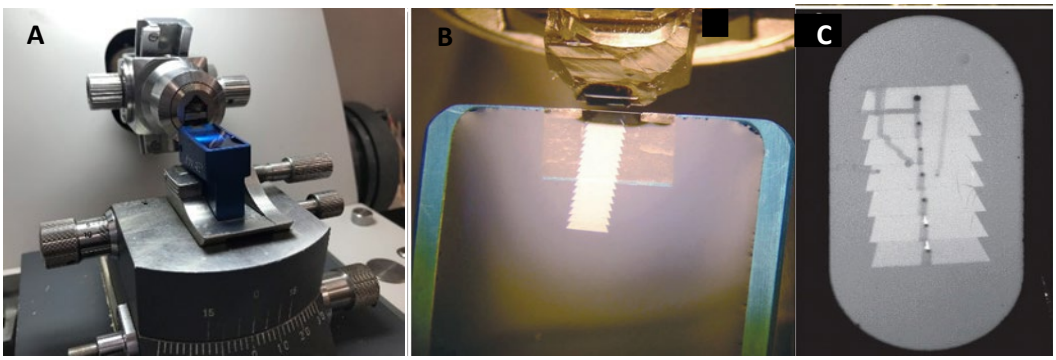

Figure 2.5: A) Scleral sample attached to a Reichert-Jung Ultracut E microtome and sectioned using a diamond knife, B) Scleral tissue cut into 70 nm silver and gold-colored sections, C) Silver sections with scleral samples in the middle.

Sections were then placed on coated copper meshed grids. The ready sections were stained with uranyl acetate and lead citrate (Figure 2.6).

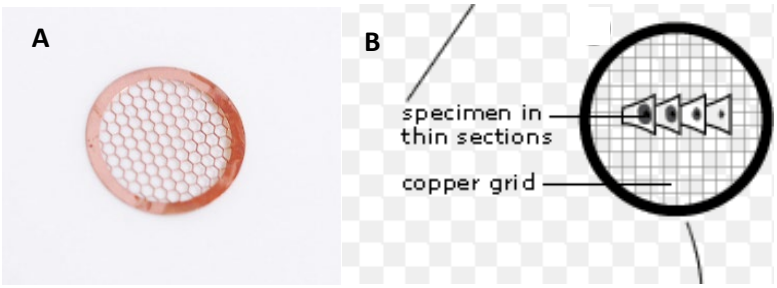

Figure 2.6: A) An example of a copper meshed grid, B) A cartoon of thinly sectioned specimens placed on top of a copper grid.

Samples were viewed using an FEI Tecnai 12 transmission electron microscope. Images were captured from three different samples of each eye at a magnification of 6800X (Figure 2.7).

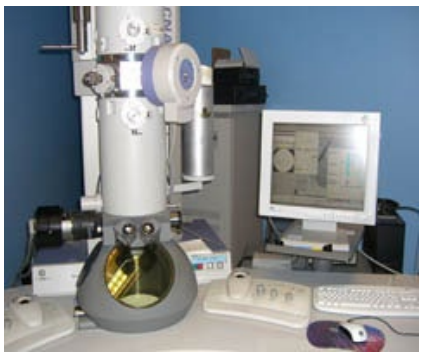

Figure 2.7: An FEI Tecnai 12 transmission electron microscope.

2.3 Results

2.3.1 Effects of myopia progression on refractive error and axial length

Our guinea pig group showed significant ocular elongation of their FD eyes and myopic shifts in spherical equivalent refractive error (RE), as reflected in the changes in interocular differences and FD eye measurements over the 10-week treatment period.

Over the first week of the FD treatment, FD eyes elongated faster than their fellows and showed myopic shifts in their spherical equivalent refractive errors. The mean interocular differences in SE and axial length (AL) at the end of this 1-week treatment period, reflect these changes, i.e., -2.9 ± 0.35 D and 0.05 ± 0.02 mm. The changes in this group recorded significantly increased interocular differences, i.e., 0.00 ± 0.015 at baseline vs. 0.29 ± 0.04 mm after 10 weeks ($p < 0.001$) and 0.025 ± 0.36 vs. -8.2 ± 0.71 D ($p<0.001$) (Figure 2.8).

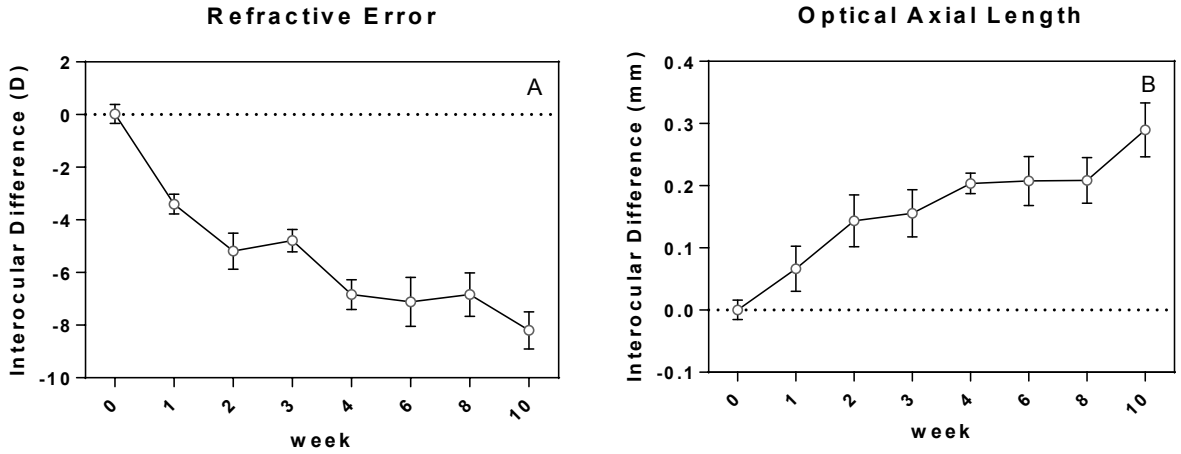

Figure 2.8: A) Mean (± SEM) interocular differences in spherical equivalent refractive error (diopters), and B) optical axial lengths (distance from the front surface of the cornea to the retina, mm) in guinea pigs that were monocularly form-deprived (FD) for 10 weeks.

2.3.2 Effects of myopia progression on intraocular pressure and diurnal rhythms

Mean IOP (±SEM) was measured in FD and fellow control eyes of 10 guinea pigs, deprived from 2 weeks of age for 10 weeks. IOPs of FD eyes significantly increased over time, from a baseline value of 22.37 ±1.21 to 28.63 ±1.59 mmHg by week 10 ($p = 0.0016$). IOPs of fellow eyes also increased with time, from 22.2 ±1.53 to 26.5 ±1.25 mmHg by week 10 ($p = 0.04$). Although not statistically significant, IOPs of FD eyes appeared to increase at a faster rate over time than IOPs of fellow eyes (Figure 2.9).

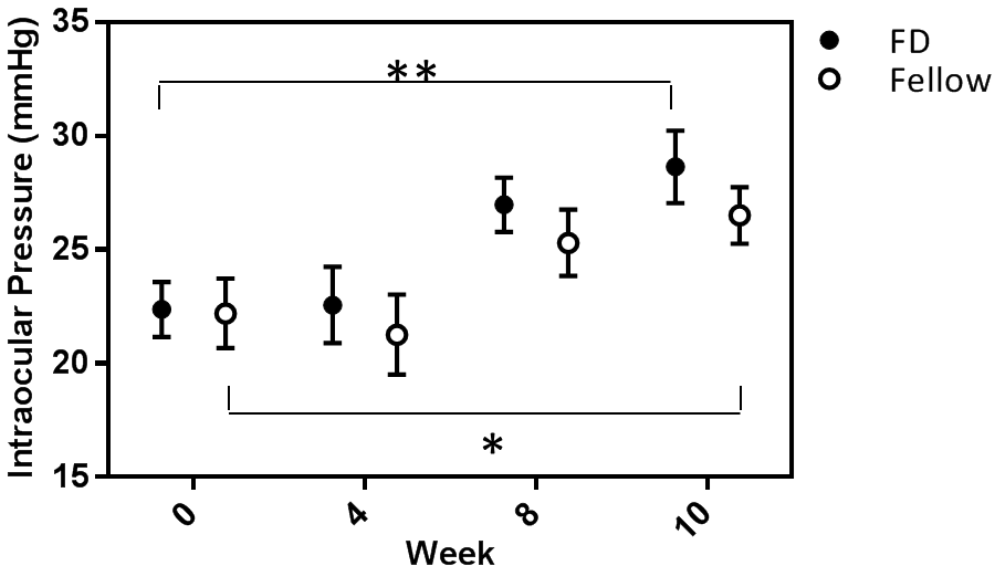

Figure 2.9: Mean IOP (±SEM) measured in FD and fellow control eyes of 10 guinea pigs, deprived from 2 weeks of age for 10 weeks. IOPs of FD eyes significantly increased over time. IOPs of fellow eyes also increased with time, although not statistically significant, IOPs of FD eyes appeared to increase at a faster rate over time than IOPs of fellow eyes.

The figure below shows the average diurnal rhythm in IOP for FD and fellow eyes derived from measurements made at 6-hour intervals over 24 hours. The timing of peak IOP was similar for the FD eyes and their fellows, around 9:35 am, just after “lights on”. The mean diurnal IOP (±SEM) at 9:35 am was 29.87 ± 1.65 mmHg in the FD eyes and 29.9 ±1.7 mmHg in the fellow eyes. No statistically significant difference was found between FD and fellow eyes at each measurement point (Figure 2.10).

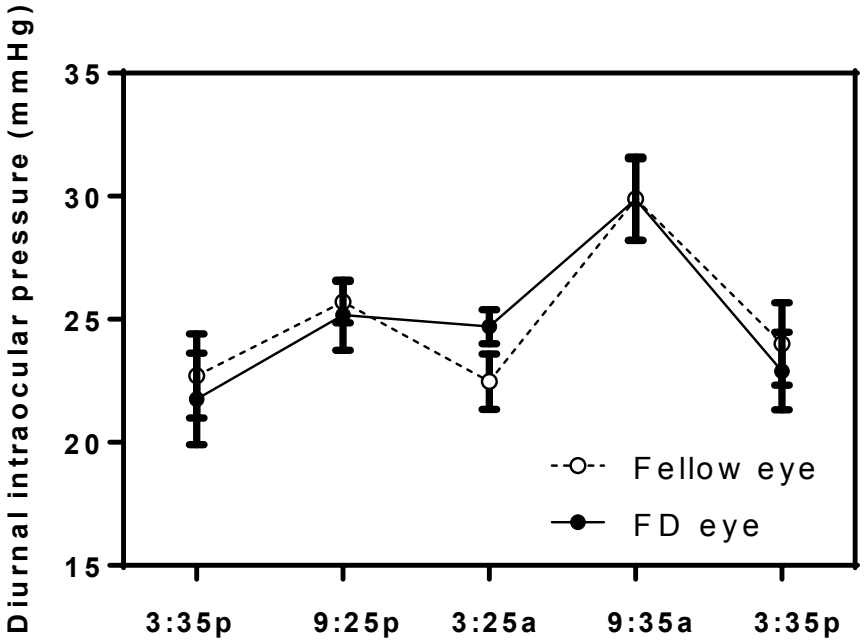

Figure 2.10: Mean IOPs (± SEM) measured at 6-h intervals over 24 h, for the form-deprived and fellow eyes of ten guinea pigs. IOPs were recorded at the end of the 10-week treatment period.

2.3.3 Optic nerve head size increases with myopia progression

The dimensions of the opening in Bruch's membrane to accommodate the exiting optic nerve fibers were used here as a surrogate for optic disc dimensions (ODDs). For the FD eyes, the mean ODDs increased from 218.8 ± 7.7 μm at the start of the study (2 weeks old) to 248.6 ± 8.9 μm by the end of the study (3 months old). For the fellow eyes, the equivalent values are 224.3 ± 7.7 μm and 238 ± 8.7 μm (Figure 2.11).

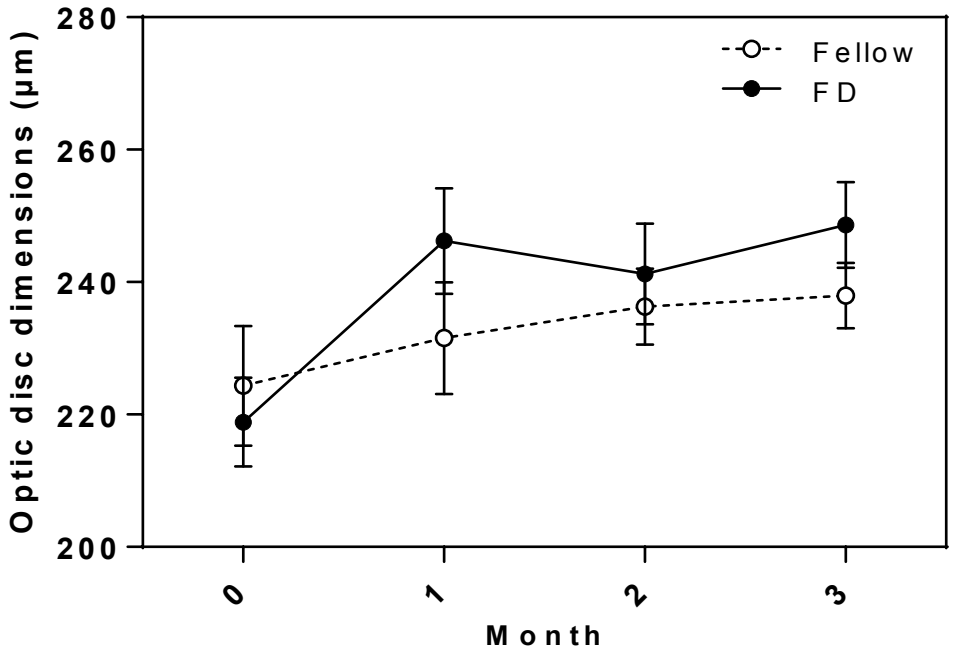

Figure 2.11: ODDs (mean ± SEM) for FD and fellow eyes of young NZ guinea pigs, recorded over a 10-week period corresponding to ages of 2 weeks to 3 months.

Optic disc dimensions (ODDs) were calculated by measuring Bruch's membrane opening, of form-deprived and fellow eyes plotted against the axial length of the same eyes (Figure 2.12). While both FD and fellow eyes showed significant linear correlations between these parameters (r^2= 0.93, p= 0.03 FD vs. r^2= 0.99, p= 0.002 fellow), FD eyes showed a more rapid increase in ODDs with axial elongation over the 10 week treatment period, as reflected in the slopes of regression lines (23.98±4.8 for FD eyes compared to 13.16 ±0.65 for fellow eyes).

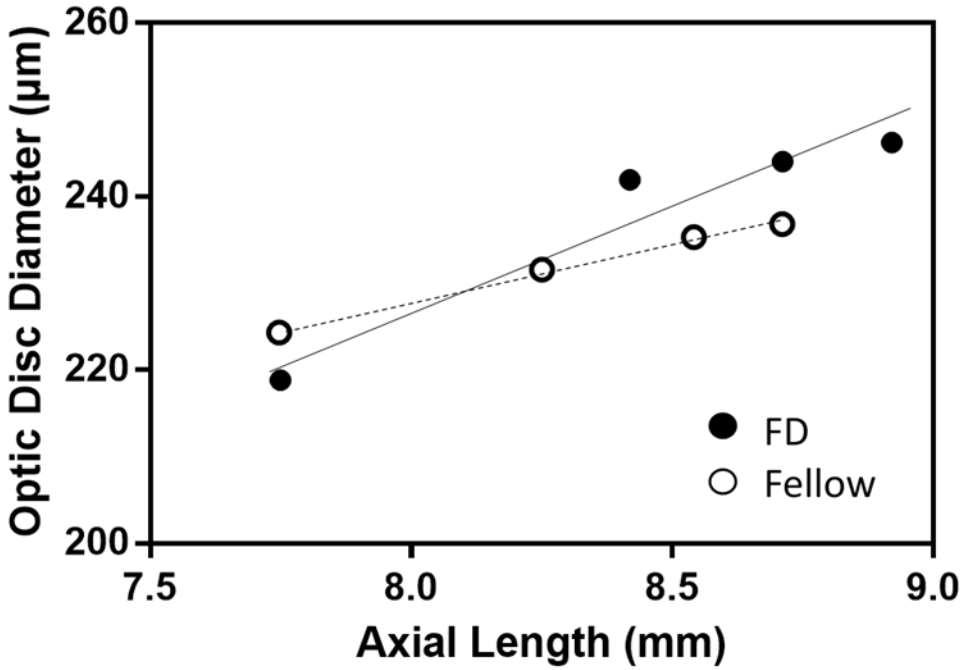

Figure 2.12: Optic disc dimensions (ODDs) of form-deprived and fellow eyes plotted against the axial length of the same eyes.

2.3.4 Effects of myopia on lamina cribrosa - scanning electron microscopy

In this study, there was no statistically significant difference in the mean of laminar pores area between FD and fellow eyes. The mean laminar area was 21.69 ± 8.88 μm^2 for the FD eyes and 22.21 ± 8.71 μm^2 for the fellow eyes (Figure 2.13). Laminar pores were further categorized based on the area into small (<15 μm^2), medium (15-30 μm^2), and large (>30 μm^2) pores area. FD and fellow eyes had the largest percentage of the smallest lamina criborsa pores area (FD; 65.3 ± 15.3 %, fellow; 63.9 ± 13.5%) and about a similar percentage of the medium (FD; 16.5 ± 5.2 %, fellow 16.6 ± 3.2%) and large pore (FD; 18.2 ± 10.9%, fellow 19.5 ± 11.5%) area. No statistically significant difference in the pore area was found between the FD and the fellow eyes (Figure 2.14).

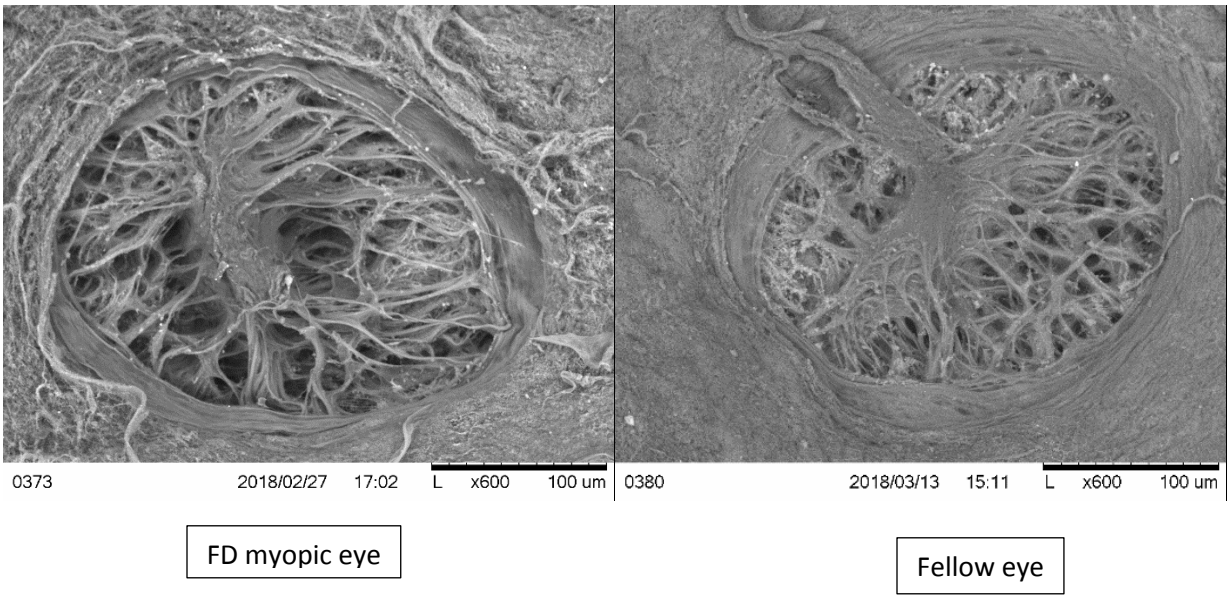

Figure 2.13: Representative image of the lamina cribrosa of a form-deprived eye and fellow eye using scanning electron microscopy (SEM) imaged at 600X.

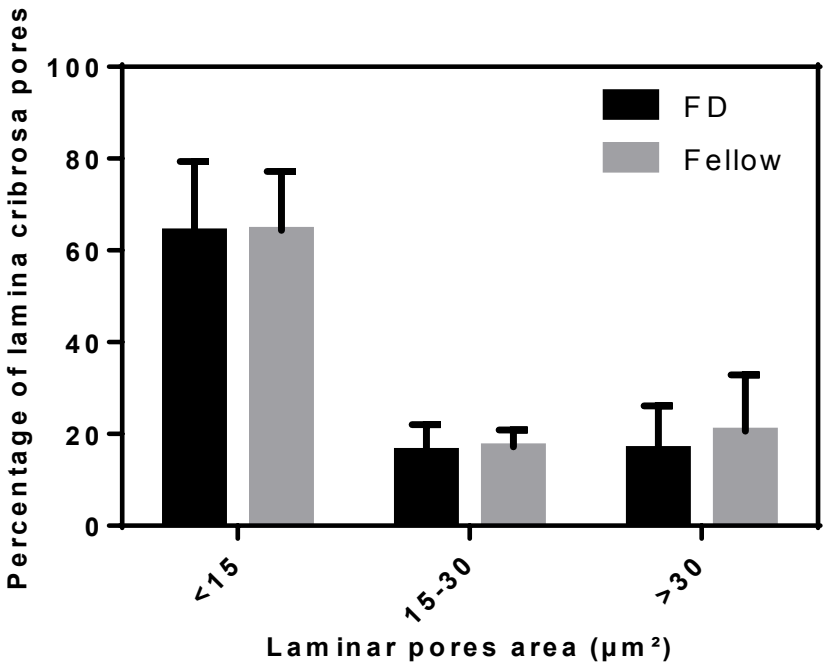

Figure 2.14: Laminar pores categorized based on the area into small (<15 μm^2), medium (15-30 μm^2), and large (>30 μm^2) pores area. FD and fellow eyes had the largest percentage of the smallest lamina cribrosa pore area and about a similar percentage of the medium and large pore areas.

2.3.5 Effects of myopia on scleral collagen - transmission electron microscopy

Both the distribution of scleral collagen fibers and their cross-sectional area dimensions were qualitatively examined. In the normal guinea pig sclera, as represented by that of fellow eyes, scleral collagen fibers were evenly spaced. In contrast, the sclera from myopic FD eyes was clearly altered, with increased spacing between the collagen fibers; there also appeared to be a higher proportion of smaller fibers (Figure 2.15). That the scleras of FD myopic eyes had smaller fibers compared to those of their fellows was confirmed statistically (0.0059 ± 0.0013 μm^2, FD-AT vs. 0.0085 ± 0.002 μm^2, fellow ($p<0.001$)).

To further compare the effects of the FD myopia on scleral collagen fibers, cross-sectional area data were categorized into one of three groups, small (<6000 nm^2), medium (6000-12,000 nm^2), and large (>12,000 nm^2). The percentage of scleral collagen fibers in each category was calculated for both FD eyes and their fellows. The FD eyes had the highest percentage of the smallest fibers (51.7 ± 9.1%), and the lowest percentage of the largest fibers (19.5 ± 6.5%) ($p= 0.02$), compared to their fellows (39.6 ±13.1%, small vs. 25.2 ± 12.7%, large; $p= 0.32$) (Figure 2.16).

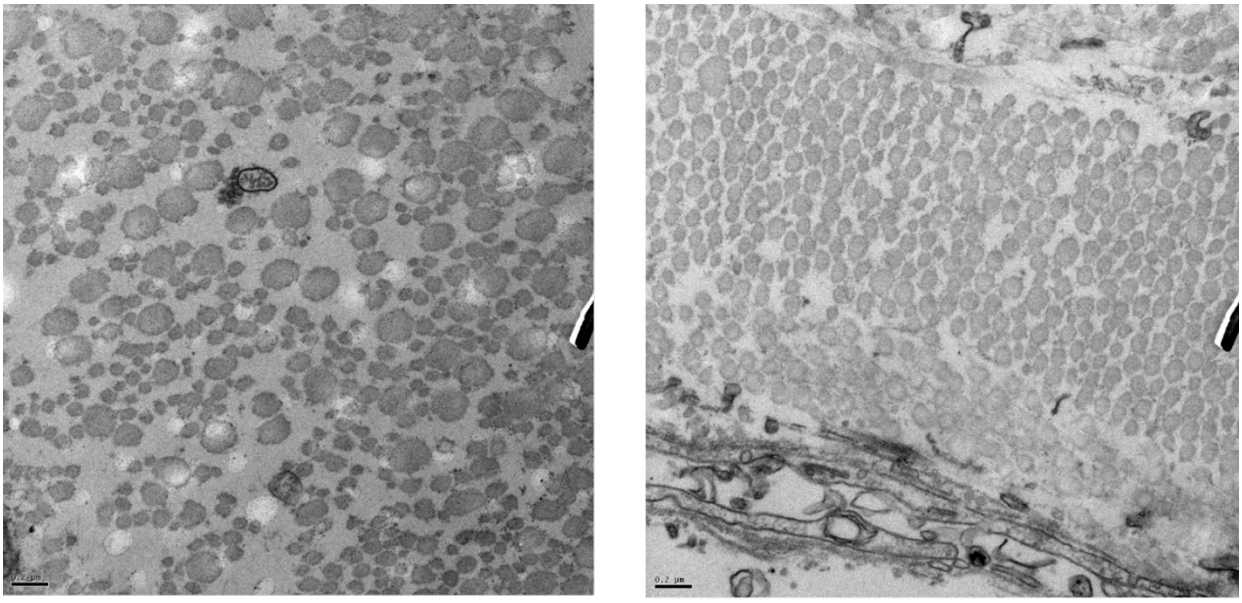

FD Myopic sclera

Fellow eye sclera

Figure 2.15: Representative image of the scleral collagen fibers of a form-deprived eye and fellow eye using transmission electron microscopy (TEM) imaged at 6800X. Note the difference in morphology of myopic sclera and fellow sclera. Myopic sclera has a higher proportion of the smaller collagen fibers with a lot more spacing between the fibers exposing the extracellular matrix. On the other hand, fellow sclera has more evenly spaced collagen fibers with predominating medium-sized fibers.

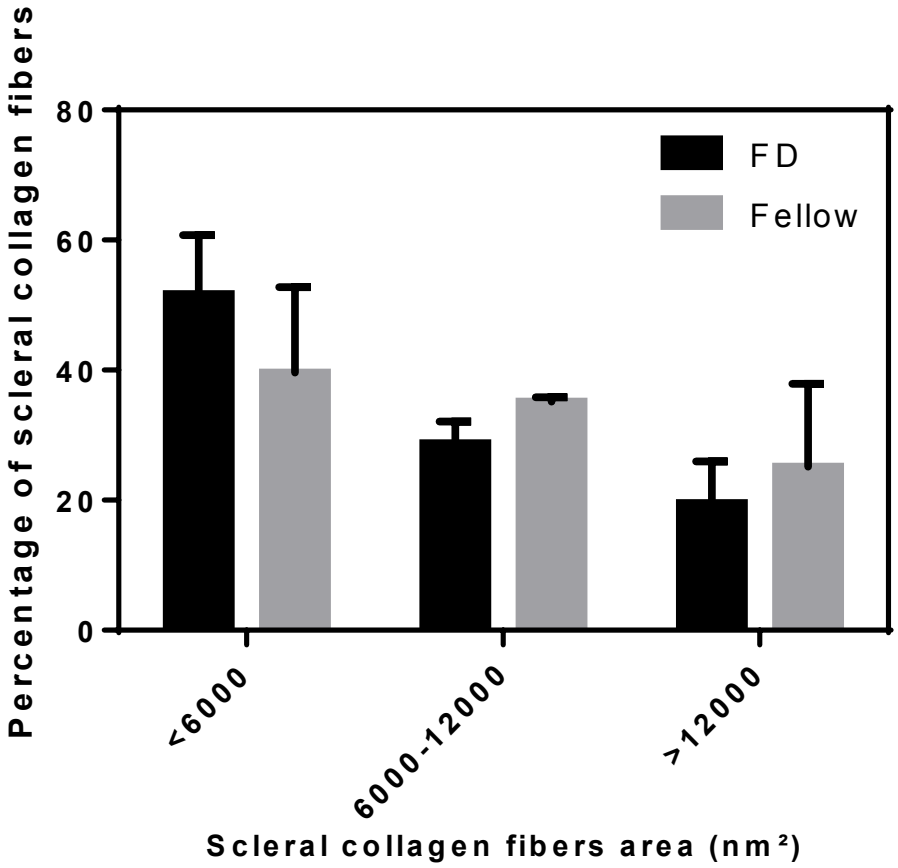

Figure 2.16: Percentage of each of three categories of scleral collagen fibers, based on cross-sectional areas (small, <6000 nm^2; medium, 6000-12,000 nm^2; large, >12,000 nm^2), shown for the FD and fellow eyes.

2.4 Discussion

2.4.1 Form-deprivation myopia-related changes in intraocular pressure and diurnal rhythms

In our study, the FD eyes showed a trend towards IOP elevation. Although this trend was not statistically significant, another study also reported an increase in IOP in lens-induced myopic guinea pig eyes receiving 0.9% saline by the end of the study (Liu et al., 2017). These findings also fit with isolated reports in humans of higher IOPs in myopes compared to emmetropes (Cahane and Bartov, 1992; Detry-Morel, 2011; Wong et al., 2003). Nonetheless, even without significant IOP elevation, for eyes with fibrous scleras, biomechanically weakening of the sclera due to the increased extracellular matrix during myopia progression, will arguably render it more vulnerable to the stretching (inflationary) influence of IOP. The possibility that structural changes in

myopic (FD) eyes can lead to IOP elevation, as a further adverse complication, is the subject of future investigations.

Diurnal rhythms in IOP have been documented in many species, including chicks (Nickla et al., 1998), rats (Arranz-Marquez and Teus, 2004; Kahane et al., 2016), rabbits (Howlett and McFadden, 2006; Smith et al., 2009), monkeys (Bito et al., 1979), and humans (Detry-Morel, 2011; Lindsey et al., 1997), with species differences in the phase and amplitude of IOP rhythms apparent, e.g., lower in rhesus monkey eyes (5 mmHg) (Bito et al., 1979) than in rat eyes (Arranz-Marquez and Teus, 2004; Kahane et al., 2016) and rabbit eyes (10 mmHg) (Howlett and McFadden, 2006; Smith et al., 2009). For our guinea pigs, the highest IOP was recorded at the first, morning time-point, just after lights-on, with IOP decreasing throughout the day. These results agree with our already published diurnal IOP patterns for normal guinea pigs (Lisa A. Ostrin and Wildsoet, 2016). The IOP rhythm amplitude for FD eyes was increased, to approximately 8 mmHg, compared to fellow eyes. However, while the latter value is comparable to the amplitude reported for FD myopic chick eyes (Nickla et al., 1998), the amplitude was reported to be not significantly affected, but phase more variable in the latter study, pointing to a possible species difference.

2.4.2 Form-deprivation myopia and macro/ micro-structural changes

In this study, optic discs tended to increase in size with increasing axial length in both FD myopic and fellow (normal) eyes, but at a faster rate in the myopic eyes, paralleling the trends reported for human myopia. IOPs also seemed to be slightly higher in myopic eyes compared to their fellows, and as a result, the scleras of the larger myopic eyes would have experienced more mechanical stress, perhaps contributing to the greater rate of elongation in these eyes.

While optic discs area generally increases with axial elongation (Hoh et al., 2006; Savini et al., 2012; Bae et al. 2016), Leung et al. found using a Heidelberg Retina Tomograph (HRT), that optic disc size was independent of axial length and refractive error between -8 and +4 D and concluded that OCT does not agree with HRT, because it may overestimate optic disc area, cup to disc area ratio, and rim area in myopic eyes (Leung et al., 2006). This discrepancy between the two instruments could be related to the different methods of measuring the disc margin. In the HRT, the disc margin is demarcated by Elschnig's ring outer boundary, whereas, the retinal pigmented epithelium ends are what is detected in OCT (Leung et al., 2006). Given that peripapillary atrophy- disruption of the retinal pigmented epithelium in the area surrounding the optic disc- is more common in myopic eyes (Ramrattan et al., 1999), the optic disc margins with the peripapillary atrophy, could have been overestimated in size in OCT. Therefore, it is crucial to account for axial length- induced ocular magnification when measuring optic nerve head size.

To date, the effect of myopia on the architecture of the lamina cribrosa has not been investigated in any animal model, although a previous study by our group used scanning electron microscopy to image the lamina cribrosa of normal pigmented and albino guinea pigs (Lisa A. Ostrin and Wildsoet, 2016). The guinea pig was shown to

have a well-organized, collagen-based lamina cribrosa, making it a promising model for investigating the relationship between myopia and glaucoma. Histomorphometric studies of human globes have found the lamina cribrosa to be thinner in highly myopic eyes when compared to eyes with normal axial length (Jonas et al., 2012, 2004), and in another study involving normal monkeys (no myopia or glaucoma), lamina cribrosa thickness was found to decrease and the posterior sclera to thin, with increasing axial length (Jonas et al., 2016). However, in the current study, no abnormalities in the lamina cribrosa architecture were identified in FD myopic eyes.

Our interest in the lamina cribrosa architecture of the myopic guinea pigs stems from *in vivo* human studies suggesting that both high myopia and glaucoma significantly increase the risk of lamina cribrosa damage, and the further suggestion that lamina cribrosa changes in highly myopic eyes with no glaucoma may partially explain the increased risk of glaucoma in these eyes (Miki et al., 2015). Eyes with tilted discs, as commonly encountered in human myopia, appear more susceptible to focal temporal lamina cribrosa defects and associated glaucomatous visual field defects, (Sawada et al., 2017). Interestingly, none of the myopic guinea pigs that were also imaged *in vivo* using SD-OCT showed tilted discs. It is plausible that this difference between the guinea pig and human eyes reflects differences in the anatomical location of the optic nerve insertion site, raising the further possibility that shearing forces on the lamina cribrosa may be less in the case of guinea pig lamina cribrosa, as reflected in our failure to detect any related structural abnormalities. Nonetheless, because the SEM technique used in this study only allows for characterization of the surface structure of the lamina cribrosa, we cannot rule out changes in the deeper layers. It is also possible that such changes as described in humans may slowly evolve over time, while our study was limited to a 10-week monitoring period.

The scleras of the myopic FD guinea pig eyes were morphologically different from those of their fellow eyes. In the scleras of untreated fellow (normal) eyes, collagen fibers were relatively evenly spaced; also, while the fibers ranged in size from quite small to quite large, medium-sized fibers dominated. In contrast, the scleras of the more myopic eyes had both a higher proportion of smaller collagen fibers and overall, the fibers were more sparsely spaced. The latter picture fits well with other descriptions of myopic scleras. For example, in 1979, Curtin (Curtin et al., 1979), in examining human myopic eyes by electron microscopy, noted the following differences in myopic sclera: predominantly lamellar, reduction in fibril diameters (below 60-70 nm), greater dispersion for the range of fibril diameters, greater prevalence of extremely small diameter fibrils, and unusual star-shaped fibrils on cross-section. With the exception of the last observation, this description also captures the changes in the scleras of our myopic guinea pigs.

Similar to human myopic scleral changes, myopia development and progression in tree shrews and mice have also been linked to changes in scleral collagen fiber spacing and diameter, as viewed by TEM. For example, in one study involving long-term (≥ 3 months) form deprivation in tree shrews, the resulting myopia was linked to an increase in the proportion of small diameter scleral collagen fibrils (McBrien et al., 2001). Similar scleral changes were also observed in a transgenic mouse model, which exhibits high myopia (Song et al., 2016). These findings are consistent with our own observation of a

higher proportion of the smaller collagen fibers in the scleras of the form-deprived myopic eyes of guinea pigs.

Chapter 3 Effect of Intraocular Pressure Reduction on Slowing Myopia Progression in the Guinea Pig Form-Deprivation Model

3.1 Introduction

Myopia (near-sightedness) has become a significant public health concern, as its prevalence continues to increase in the United States (Vitale et al., 2009) and around the world, especially Asia (Pan et al., 2015). The sclera plays an important role as a determinant of eye size and thus in the development of myopia, which reflects excessive eye elongation. Comprising mainly of collagen type I, with fibroblasts functioning to produce and maintain the extracellular matrix, the sclera is known to undergo structural and biomechanical changes in myopic eyes. These changes are a byproduct of altered gene and protein expressions, including, but not limited to type 1 collagen, matrix metalloproteases (especially MMP2), tissue inhibitor of MMPs (TIMP), TGF beta, and integrins (Barathi and Beuerman, 2011; McBrien et al., 2006; McBrien and Gentle, 2003; Metlapally and Wildsoet, 2015; Rada et al., 1999). For example, expression of MMP2, an enzyme associated with collagen breakdown, was shown to be increased and expression of TIMP-1 to be decreased, in the myopic sclera of tree shrews (Guggenheim and McBrien, 1996; J. T. Siegwart and Norton, 2001). This increased remodelling of the scleral matrix leads to altered scleral microarchitecture, collagen fibers becoming reduced in size and more disorganized, and the sclera, thinner and weaker. In highly myopic eyes, the exaggerated and sustained biomechanical instability of the thinned sclera may lead to scleral creep (irreversible scleral stretching) and posterior staphyloma, in the event of mechanical scleral failure (Avetisov et al., 1983; Curtin et al., 1969, 1979).

The role in ocular growth (enlargement) of intraocular pressure (IOP), which exerts a stretching influence on the scleral wall of the eye, has been the subject of a number of investigations making use of experimental animal models (Nickla, 2013). During myopia development and progression, when scleral remodelling is upregulated, the sclera is predicted to be more susceptible to the stretching influences of IOP, and thus eye enlargement to accelerate as a consequence (Cahane and Bartov, 1992). That the converse is also true, i.e., that ocular elongation can be slowed by decreasing IOP and so the tension experienced by the sclera, was tested in this study using the topical ocular hypotensive drug, latanoprost, and the guinea pig form-deprivation myopia (FDM) model. In this study, we reported topical latanoprost to be effective in both lowering IOP and slowing myopia progression in young guinea pigs (El-nimri and Wildsoet, 2018).

The use of IOP lowering drugs for controlling myopia progression has another potential merit. Growing evidence from a number of studies links myopia with an increased risk of primary open angle glaucoma (POAG), a leading cause of irreversible blindness (Flitcroft, 2012). Eyes with POAG typically exhibit high intraocular pressure (IOP) and altered diurnal IOP rhythms, as well as thinning of the neuroretinal rim and excavation of the optic nerve head (ONH). The latter ONH changes reflect the loss of retinal ganglion cell (RGC) axons as they pass through the lamina cribrosa (LC) (Flammer et al., 2002), a sieve-like structure bridging the scleral canal through which the axons pass to form the optic nerve, and which is also reported to be altered in glaucomatous eyes (Yang et al., 2007).

The mechanism(s) underlying the increased susceptibility of myopes to glaucoma is not well understood. Of possible contributing factors is the failure of the LC to adequately support the RGC axons as they exit the eye. As the sclera becomes progressively thinner and mechanically weaker with myopia progression, one might expect similar changes in the LC since it is continuous, at least posteriorly, with the adjacent sclera (Cahane and Bartov, 1992). A thinner and weaker peripapillary sclera in myopia could also affect the biomechanical properties of the LC, potentially explaining, at least in part, the increased risk of glaucomatous damage in myopic patients (Jonas et al., 2011; Norman et al., 2011). In fact, it was found that the LC thickness is decreased in eyes with longer axial lengths and thinner posterior scleras (including the sclera adjacent to the optic disc border) in non-glaucomatous monkeys, a similar finding to that in humans (Jonas et al., 2016).

Latanoprost is one of a number of prostaglandin (PG) analogues, which are currently considered the first-line treatment for POAG, because they reliably reduce IOP, by approximately 30%, and offer 24-hour control (Aptel et al., 2008). The IOP reduction achieved with topical PGs is associated with increased uveoscleral (UV) outflow, achieved through increases in the levels of matrix metalloproteinases (2 and 3), leading to remodelling of the extracellular matrix (ECM) within the UV pathway (Russo 2009). The latter activity profile raises the obvious question of whether the sclera is similarly remodelled, despite latanoprost's demonstrated ability to slow myopia progression in the FDM guinea pig model (See sections 1.4.3 and 1.4.4).

3.2 Methods

3.2.1 Animals

Pigmented guinea pigs were used in this study, with breeders obtained from the University of Auckland, New Zealand. Study animals were bred on-site and housed in a temperature-controlled room with a light/dark cycle of 12L/ 12D (on at 9.30 am, off at 9.30 pm). Pups were weaned at 5 days of age and housed as single-sex groups in 41 cm wide X 51 cm long transparent plastic wire-top cages, with free access to water and vitamin C-supplemented food, with additional fresh fruit and vegetables given five times a week as diet enrichment. All animal care and treatments in this study conform to the ARVO Statement for the Use of Animals in Ophthalmic and Vision Research.

Experimental protocols are approved by the Animal Care and Use Committee of the University of California, Berkeley.

A total of 20 animals were used in this study, comprising of 2 groups of 10 animals. All animals underwent monocular myopia-inducing form deprivation (FD) and the same eyes also underwent one of two topical ophthalmic treatments as summarized below (see also Tables 3.1 and 3.2 below). Untreated contralateral eyes served as controls.

3.2.2 Treatments: Myopia-generating (Form deprivation) and intraocular pressure lowering (topical latanoprost)

Form deprivation: Detachable white plastic diffusers were fitted to 14 days-old guinea pigs and worn for 10 weeks. Animals were monitored hourly during the 12 h lights-on period to ensure that the diffusers remained in place; they were also cleaned as necessary. The design of the diffusers and attachment protocol were adapted from those implemented in chicks (Wildsoet and Wallman, 1995). The diffusers were made from sheets of white styrene (Midwest Products Co), hot-molded into semicircular domes and mounted on hook Velcro ring supports. Opaque diffusers were used in this study. To attach the diffusers to the guinea pigs, rings of loop Velcro were cut in halves and the two segments symmetrically affixed to the fur surrounding one of the guinea pig's eyes using gel cyanoacrylate glue (SureHold® Plastic Surgery) (Figure 2.1).

Topical ophthalmic drug treatments: One group received one drop of latanoprost (0.005% ophthalmic solution, Akorn, Lake Forest, IL), instilled daily into their FD eyes, starting one week after the initiation of diffuser wear and continuing throughout the rest of the 10-week treatment period. The FD eyes of the second (control) group received topical artificial tears daily. The animals were randomly assigned to one of these two treatment groups (latanoprost or artificial tears) at the end of the first week of the FD treatment.

3.2.3 Measurements: Intraocular pressure, refractive error, and axial ocular dimensional measurements

Intraocular pressures (IOP), spherical equivalent refractive errors (SE) and optical axial lengths (AL) were recorded for both eyes of each animal, immediately before the initiation of the FD treatment (baseline), with follow-up measurements made at weekly intervals over the first month and every other week thereafter. Because of well-documented circadian rhythms in both IOP and eye elongation (Nickla et al., 1998), measurements were always taken around the same time each day, early in the morning, after lights-on. Diurnal IOP rhythms were also recorded at monthly intervals. All IOP measurements were conducted in awake animals, prior to other procedures requiring anaesthesia to avoid possible confounding effects of the latter. An iCare rebound tonometer (Tonolab, Helsinki, Finland) was used along with the setting for rat eyes, for which this instrument has been calibrated and which are similar in size to those of guinea pigs. This instrument provides confidence interval information based on

successive readings; only data with a confidence interval of 5% or less were used. Three measurements were taken on each eye and the average used in data analysis.

Refractive errors were measured using streak retinoscopy on awake animals, 30 minutes after instillation of one drop of 1% cyclopentolate hydrochloride (Bausch & Lomb, Rochester, NY) for cycloplegia. Spherical equivalent refractive errors (average of results for the two principal meridians) were derived for use in data analysis.

Ocular axial dimensions were measured with a custom-built, high-frequency A-scan ultrasonography system, with an estimated resolution of ~10 μm (Nickla et al., 1998; Wildsoet and Wallman, 1995). For these measurements, animals were first placed under gaseous anaesthesia (1.5-2.5% isoflurane in oxygen), with eyelid retractors inserted to hold their eyes open. For each measurement, at least 8 traces were captured per eye and analyzed off-line. Only optical axial lengths are reported here, derived as the sum of anterior chamber depth, axial lens thickness and vitreous chamber depth.

3.2.4 Measurements: Diurnal intraocular pressure rhythms.

To characterize diurnal rhythms in IOP, five measurements were made using the iCare tonometer at ~6 h intervals over 24 h, including time points just after lights-on and just before lights-off. Measurements during the lights-off hours were taken under photographic dark light conditions to minimize the possible effect of brief exposures to light on circadian rhythms. Three measurements were taken on each eye at each time point and averaged for use in data analysis.

Statistical analysis: Data analysis made use of Prism 6 (GraphPad Software, La Jolla, CA, USA). Data for treated and control eyes, as well as derived interocular differences (treated eye - control eye), are reported as mean ± SEM. For diurnal IOP data, the timing of peak IOPs was analyzed as were rhythms amplitudes, derived as the difference between the highest and lowest IOP recorded during the 24 h period, regardless of time of day. Two-way repeated measures ANOVAs, with a Bonferroni post hoc test, were applied to longitudinal data. P-values from post-hoc testing are reported in the results section and summarized in Tables 3.1 and 3.2. A two-tailed paired t-test was applied to compare the IOP rhythm amplitudes of treated and control eyes. By way of indirectly evaluating the influence of IOP on myopic growth, the relationship between latanoprost-induced reductions in IOP at week 10, relative to baseline, and the ratio of changes in optical axial length of FD eyes to changes in fellow eyes over the same time period was examined by regression analysis.

3.2.5 Measurements: SD-OCT imaging

A high-resolution spectral-domain optical coherence tomography system (SD-OCT, Bioptigen, USA) was used to image the optic nerve head (ONH), starting one day before the diffusers are attached and once per month thereafter. Both eyes of each animal were imaged. Guinea pigs were first anaesthetized with an intramuscular

injection of ketamine and xylazine (27 mg/kg, 0.6 mg/kg, respectively), then placed on a custom-made stage with x – y – z adjustments to facilitate align the optical axis of the eye being imaged with that of the instrument. A high-resolution OCT scan was generated from 500 B-scans by 400 A-scans, with a 12 by 12 mm field size, with two to three such scans, centred on the ONH, captured from each eye at each time point.
A cross-sectional 200×200 pixel image containing the ONH at its maximum horizontal dimension was selected to assess ONH diameter, using the termination in Bruch's membrane to define its boundary. Relevant points in the image were manually selected and diameter measured using a custom MATLAB (MathWorks Inc., Natick, MA) program. Values were corrected for differences in magnification related to the eye's length.

3.2.6 Scanning electron microscopy to image lamina cribrosa

Following animals sacrifice, eyes were enucleated and ONHs excised from the posterior segment to include a 4 mm ring of surrounding sclera for scanning electron microscopy (SEM). ONH samples were first soaked in 0.2M NaOH for 30 h, to remove cellular components, leaving only collagenous structures. ONHs/ lamina cribrosa (LC) samples were then fixed in 4% glutaraldehyde in 0.1M sodium cacodylate, stained with osmium tetroxide, dried through an ethanol series, and finally subjected to critical point drying before imaging. LC samples were imaged using a Hitachi TM-1000 scanning electron microscope. Images were captured at 600X magnification (See section 2.2.6).

3.2.7 Transmission electron microscopy to image scleral collagen fibers

Following animals sacrifice, eyes were enucleated and optic nerve heads (ONHs) excised from the posterior segment. A 6 mm ring of sclera surrounding the ONH was excised using disposable punchers for transmission electron microscopy (TEM). Tissue samples were first fixed in 4% glutaraldehyde in 0.1M sodium cacodylate, stained with osmium tetroxide, dried through an acetone series, infiltrated with resin and finally embedded into molds.
To section the sample blocks, the blocks containing a cross-section of the tissue were hand-cut by razorblade creating a face in the shape of a right trapezoid. Smooth faces were made using a glass knife on a Reichert-Jung Ultracut E microtome. The tissue sections were cut into 70 nm silver and gold sections.
Sections were then placed on coated copper meshed grids. The ready sections were stained with uranyl acetate and lead citrate.
Samples were viewed using an FEI Tecnai 12 Transmission electron microscope. Images were captured from three different samples of each eye at a magnification of 6800X (See section 2.2.7).

Statistical and image analysis: A custom image J program was used to measure scleral collagen fiber cross-sectional area and LC pore area from captured images after manually selecting the borders of each individual collagen fiber, as well as LC pore. Graphical data analysis made use of Prism 6 (GraphPad Software, La Jolla, CA, USA).

Data for treated and fellow eyes are reported as mean ± SEM. Two-way repeated measures ANOVAs, in combination with a Bonferroni post hoc test, were applied to compare the differences between latanoprost and AT groups in IOP, refractive error, optical axial length. Two-tailed t-tests were applied to compare the average collagen fiber areas of treated and fellow eyes for both latanoprost and AT FDM groups (paired t-tests) as well as differences between the groups (unpaired t-tests). LC pore areas were similarly compared. Two-way ANOVAs were applied to compare the differences between multiple area categories (represented in percentages) of collagen fibers and LC pores.

3.3 Results

3.3.1 Effect of latanoprost on intraocular pressure in guinea pigs

The morning IOP measurements provide convincing evidence of the effectiveness of daily topical latanoprost in lowering IOP. Specifically, the mean interocular differences in IOP changed from 0.07 ± 0.35 mmHg at baseline to -5.17 ± 0.96 mmHg after 10 weeks of latanoprost treatment ($p<0.001$). In contrast, interocular differences in IOP for the control group did not change significantly over the study period ($p= 0.53$), with the difference at the week-10 time-point being slightly but not significantly higher than the baseline value, i.e., 1.80 ± 1.16 vs. -0.30 ± 0.51 mmHg (Figure 3.1). Both eyes of control animals and the fellow (control) eyes of latanoprost-treated animals recorded higher IOPs at week 10, compared to baseline values. In contrast, the FD eyes treated with latanoprost showed relatively stable IOP over the treatment period (i.e. 24.23 ±0.87 mmHg vs. 23.4 ±1.6 mmHg) (Table 3.2). In comparing the changes in the two groups, it is of note that the mean increase in IOP for the FD eyes of the control group was also larger in absolute terms than the reduction in IOP for the FD eyes of the latanoprost group.

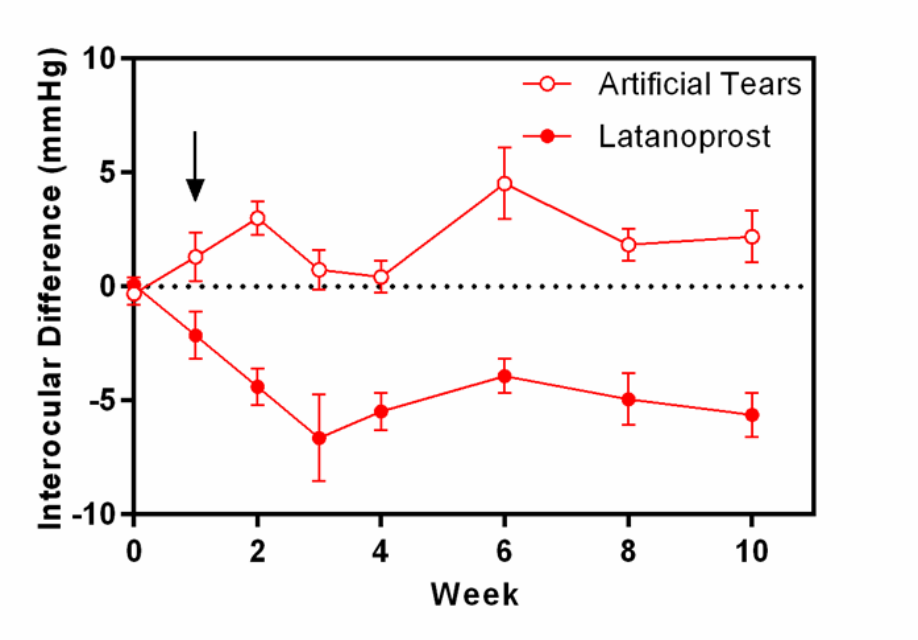

Figure 3.1: Interocular differences in IOP (mean ± SEM, mmHg) in guinea pigs treated in their FD eyes with topical latanoprost or artificial tears from week 1 of the 10-week FD treatment period. The arrow indicates the start of the topical treatments (latanoprost or artificial tears).

3.3.2 Effect of latanoprost on diurnal intraocular pressure rhythms in guinea pigs

The diurnal data offer a further perspective on the ocular hypotensive profile of latanoprost in guinea pigs. Figures 3.2 A and B show the average diurnal rhythm in IOP for FD and fellow eyes derived from measurements made at 6-hour intervals over 24 h, for both groups. As in humans, latanoprost induced a sustained drop in IOP across 24 h (Sjöquist and Stjernschantz, 2002). Thus, there were significant differences between the latanoprost and control groups in the IOPs of FD eyes, recorded in both the dark period (p=0.02) and morning (*p= 0.005*), with differences in IOPs recorded just before "lights off" being borderline significant (p= 0.051). The timing of peak IOP was similar for the FD eyes of both latanoprost and control groups, as well as for their fellows, around 9:35 am, just after "lights on". However, control FD eyes recorded a larger rhythm amplitude than their fellow eyes (8.1 versus 5.9 mmHg, p=0.045), while in contrast, latanoprost-treated FD eyes and their fellows recorded similar amplitudes (5.7 versus 5.23 mmHg, p= 0.94). There was no statistically significant difference between the amplitudes of the fellow eyes of each group.

To further analyze the effects of the latanoprost treatment on diurnal IOP rhythms, interocular difference patterns for latanoprost and control groups were compared. These data are shown in Figure 3.2 C. The interocular difference was highest in the morning, just after lights-on (-6.6 ± 1.2 mmHg) for latanoprost group, while for the control group, the largest difference was recorded in the dark phase, at approximately 3:35 am and was only small (1.67 ± 1.45 mmHg). Interocular differences for the two groups were also

significantly different at 9:25 pm, 3:25 am and 9:35 am (p-values: 0.03, 0.004, and 0.004) (Figure 3.2 C).

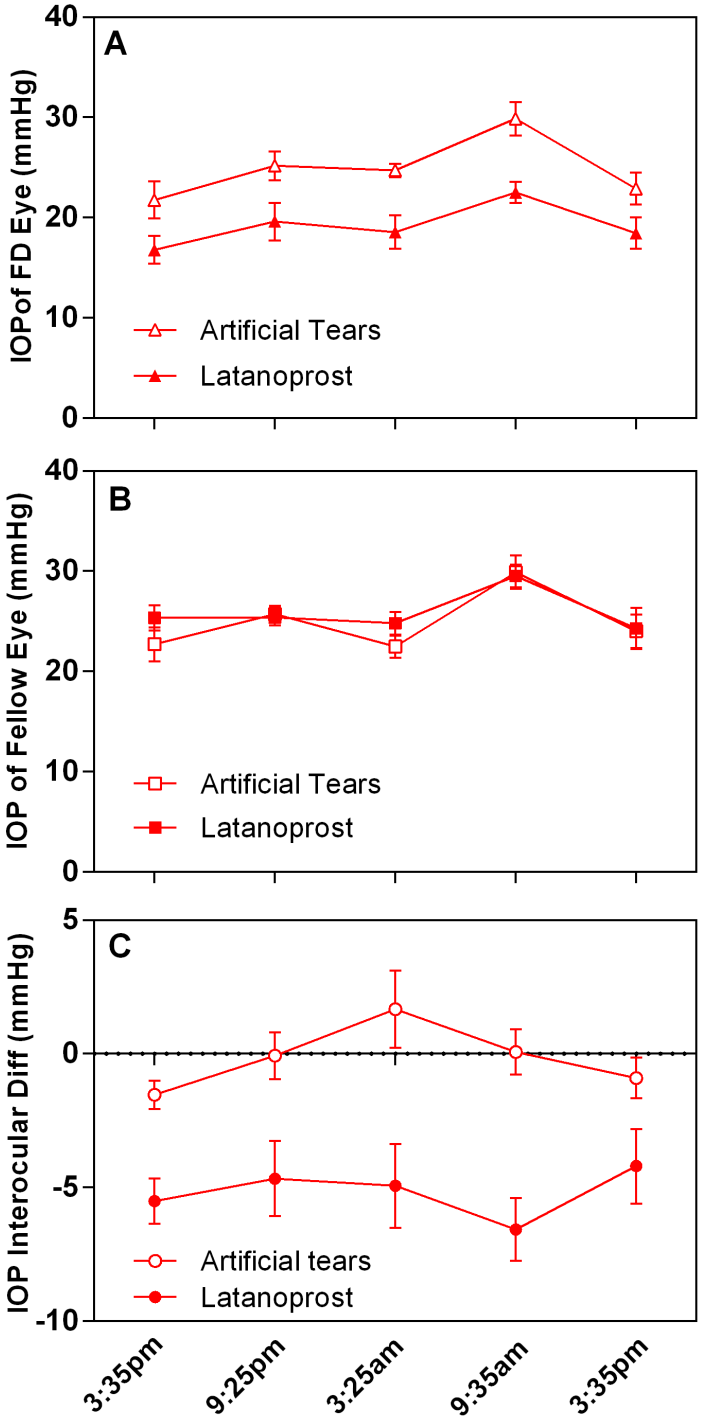

Figure 3.2: Mean IOPs (± SEM) measured at 6-h intervals over 24 h, for A) the form-deprived eyes of guinea pigs treated daily with either topical latanoprost or artificial tears, B) the fellow eyes for both

groups, and C) mean interocular (treated-control) differences; ± SEM) for the same animals. In all cases, IOPs were recorded at the end of the 10-week treatment period and both topical treatments were initiated one week after the start of the FD treatment.

3.3.3 Effect of latanoprost on slowing myopia progression and axial elongation

As expected, the control group showed significant ocular elongation of their FD eyes and myopic shifts in *spherical equivalent* refractive error, as reflected in the changes in interocular differences and FD eye measurements over the 10-week treatment period. While in contrast, the latanoprost group showed a much smaller change in these parameters over the same time period. Relevant mean baseline and week-10 interocular SE and AL difference data for both groups are summarized in Table 3.1; equivalent data for treated eyes and their fellows are also provided (Table 3.2).

Over the first week of the FD treatment, before the initiation of drug treatments, FD eyes elongated faster than their fellows and showed myopic shifts in their *spherical equivalent* refractive errors. The mean interocular differences in SE and AL at the end of this 1-week treatment period, for the two groups combined, reflect these changes, i.e., -2.9 ± 0.35 D and 0.05 ± 0.02 mm. However, over the following drug treatment period, results for the latanoprost and control groups diverged, with the FD eyes of the former group showing much slower increases in AL and smaller myopic shifts in SE. These trends are shown graphically in Figures 3.3 A and B. By the end of study period, interocular differences in AL and SE had changed minimally from baseline for the latanoprost group, i.e., 0.02 ± 0.02 vs. 0.06 ± 0.02 mm ($p= 0.202$) and -0.15 ± 0.35 vs. -2.25 ± 0.54 D ($p= 0.03$), compared to the changes in the control group, which recorded significantly increased interocular differences, i.e., 0.00 ± 0.015 vs. 0.29 ± 0.04 mm ($p< 0.001$) and 0.025 ± 0.36 vs. -8.2 ± 0.71 D ($p<0.001$). There were also statistically significant differences between the two groups in interocular differences in SE and AL at week 10 ($p<0.001$, $p<0.001$; repeated measure two-way ANOVA with a Bonferroni's post-hoc analysis, respectively). The above patterns are mirrored in the patterns of change in treated compared to fellow eyes across the 10-week treatment period (Table 3.2). For the treated and fellow eyes of the latanoprost group, the changes in AL were not significantly different ($p=0.215$), while they were for the control group ($p<0.001$). On the other hand, the AL changes in the fellow eyes of the two groups were not significantly different from each other ($p=0.275$), implying that latanoprost had no contralateral effect.

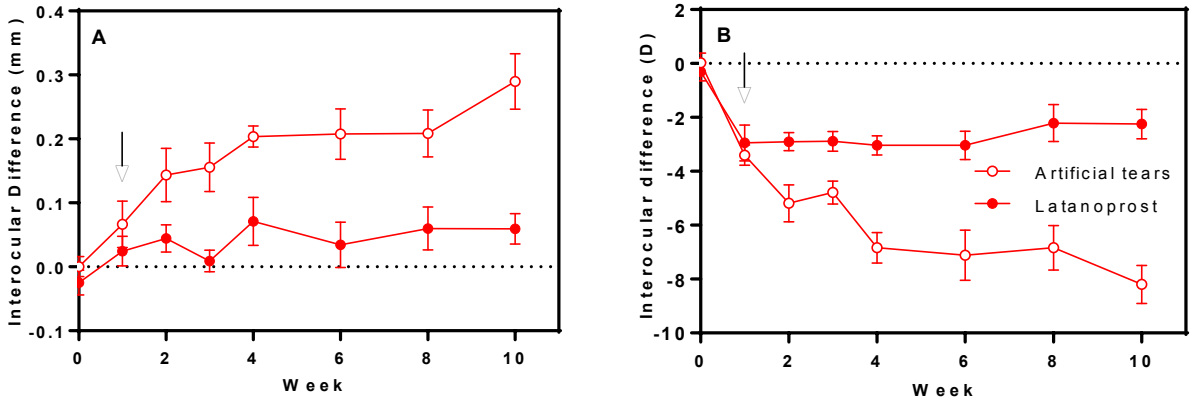

Figure 3.3: A) Mean (± SEM) interocular differences in optical axial lengths (distance from front surface of cornea to retina, mm), and B) spherical equivalent refractive error (diopters) in guinea pigs that were monocularly form-deprived (FD) for 10 weeks and treated in their FD eye with topical latanoprost or artificial tears, from week 1. The arrows indicate the start of the topical treatments (latanoprost or artificial tears).

Table 3.1: Summary of mean interocular differences in IOP, SE, and AL (± SEM) and summary statistics for monocularly form-deprived (FD) guinea pigs treated in their deprived eyes with either topical latanoprost or artificial tears (as a control treatment). Statistics indicate the significance of change over the 10-week treatment period.

Parameter	Treatment Groups	Time of measurement		Statistics (p-value)
		Baseline	Week 10	
IOP (mmHg)	FD + Latanoprost	0.07 ±0.35	-5.17 ±0.96	<0.001
	FD + Artificial tears	-0.30 ±0.51	1.80 ±1.16	0.525
Spherical Equivalent (D)	FD + Latanoprost	-0.15 ±0.35	-2.25±0.54	0.03
	FD + Artificial tears	0.025 ±0.36	-8.20 ±0.71	<0.001
Optical Axial Length (mm)	FD + Latanoprost	0.02 ±0.02	0.06 ±0.02	0.202
	FD + Artificial tears	0.00 ±0.015	0.29 ±0.04	<0.001

Table 3.2: Summary of IOP, SE, and AL for form-deprived (FD) and fellow (control) eyes (± SEM) and summary statistics for guinea pigs treated in their deprived eyes with either topical latanoprost or artificial tears (as a control treatment). Statistics indicate the significance of change over the treatment period.

Parameter	Eye	Treatment	Baseline	Week 10	Statistics (p-value)
IOP (mmHg)	**FD**	**Latanoprost**	24.23 ±0.87	23.4 ±1.6	>0.999
	Control		24.17 ±0.94	28.5 ±1.6	0.01
	FD	**Artificial tears**	22.23 ±1.0	27.33 ±1.5	0.009
	Control		22.53 ±0.92	25.53 ±1.17	0.083
Spherical Equivalent (D)	**FD**	**Latanoprost**	2.08 ±0.59	-1.32 ±0.59	<0.001
	Control		2.22 ±0.75	0.94±0.34	0.15
	FD	**Artificial tears**	2.33 ±0.73	-6.9 ±0.48	<0.001
	Control		2.3 ±0.56	1.5± 0.37	0.55
Optical Axial Length (mm)	**FD**	**Latanoprost**	7.5 ±0.05	8.5 ±0.05	<0.001
	Control		7.5 ±0.06	8.44 ±0.03	<0.001
	FD	**Artificial tears**	7.47 ±0.03	8.64 ±0.06	<0.001
	Control		7.47 ±0.03	8.35 ±0.02	<0.001

To examine the potential influence of IOP on myopia development, the ratios for individual animals of both groups, of changes over the 10-week treatment period in the ALs of FD to fellow eyes were plotted against the changes in IOP over the same period (Figure 3.4). A regression analysis undertaken on these data revealed a significant linear correlation (r^2 = 0.53, p= 0.003), providing indirect evidence for a role of IOP as an inflationary force in myopia development.

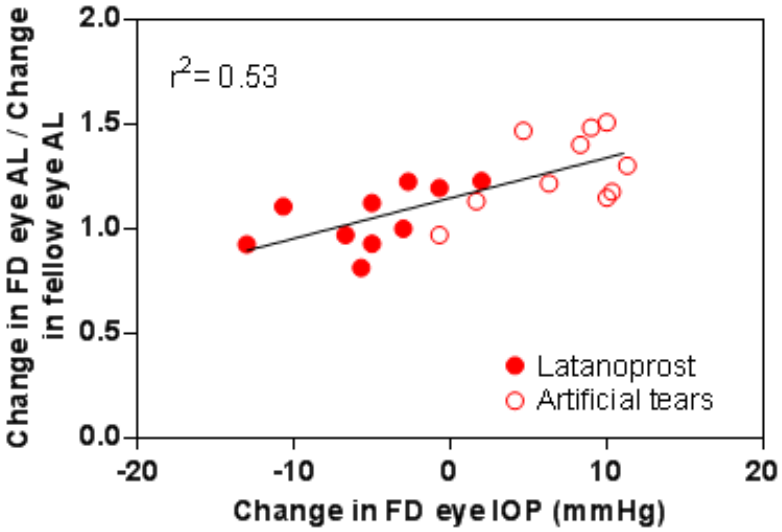

Figure 3.4: Ratio of changes over the 10-week treatment period in optical axial lengths (AL) of form deprived (FD) eyes to their fellow eyes plotted against changes in IOP, for both latanoprost and control (artificial tears) groups.

3.3.4 Effect of latanoprost on optic nerve head size

The dimensions of the Bruch's membrane opening were used here as a surrogate for optic disc dimensions (ODDs). ODDs of all eyes appeared to slightly increase over the study period (Figure 3.5), and although the ODDs of the Lat-treated and fellow eyes seemed smaller at the end of the treatment period than those of the AT group, no significant differences were found between the ODDs of Lat and AT groups at any time point. For the Lat-treated eyes and their fellows, the mean ODDs were 228.0 ± 7.8 and 225.3 ± 7.8 μm respectively at the start of the study (2 weeks old) and 244.6 ± 8.8 μm and 230.3 ± 8.7 μm by the end of the study (week 10). For the AT-treated eyes and their fellows, the mean ODDs were 218.8 ± 7.7 and 224.3 ± 7.7 μm respectively at the start of the study (2 weeks old) and 248.6 ± 8.9 μm and 238 ± 8.7 μm by the end of the study (week 10).

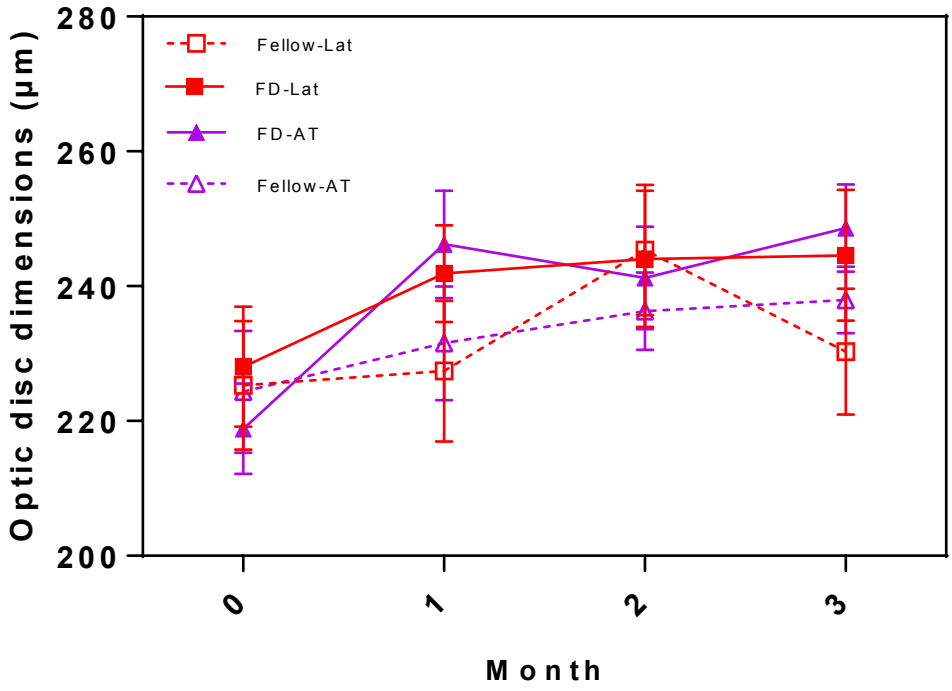

Figure 3.5: ODDs (mean ± SEM, mmHg) in NZ guinea pigs treated in their FD eye with latanoprost (Lat) or artificial tears (AT) (n= 10 per group), from week 1 of the 10-week treatment period.

ODDs of form-deprived (artificial tears (AT) or latanoprost treated) and fellow eyes was plotted against AL of the same eyes (Figure 3.6). While both FD taking AT and fellow eyes showed a trend of linear correlations between these parameters (r^2= 0.83, p= 0.08 FD vs. r^2= 0.99, p= 0.002 fellow). FD eyes seem to show a more rapid increase (steeper) in ODDs with axial elongation over the 10 week treatment period, as reflected in the slopes of regression lines (24.33 ± 7.7 for FD eyes compared to 14.45 ± 0.54 for fellow eyes) (Figures 3.6 A and B).

On the other hand, Latanoprost treated eyes showed significant linear correlations between ODDs and AL (r^2= 0.94, p= 0.03 FD) and a trend of positive linear correlation in fellow eyes (r^2= 0.36, p= 0.4 fellow). Latanoprost treated and fellow eyes had a more similar slope of regression lines (16.26 ± 3.0 for FD eyes compared to 12.84 ± 12.0 for fellow eyes) (Figures 3.6 C and D).

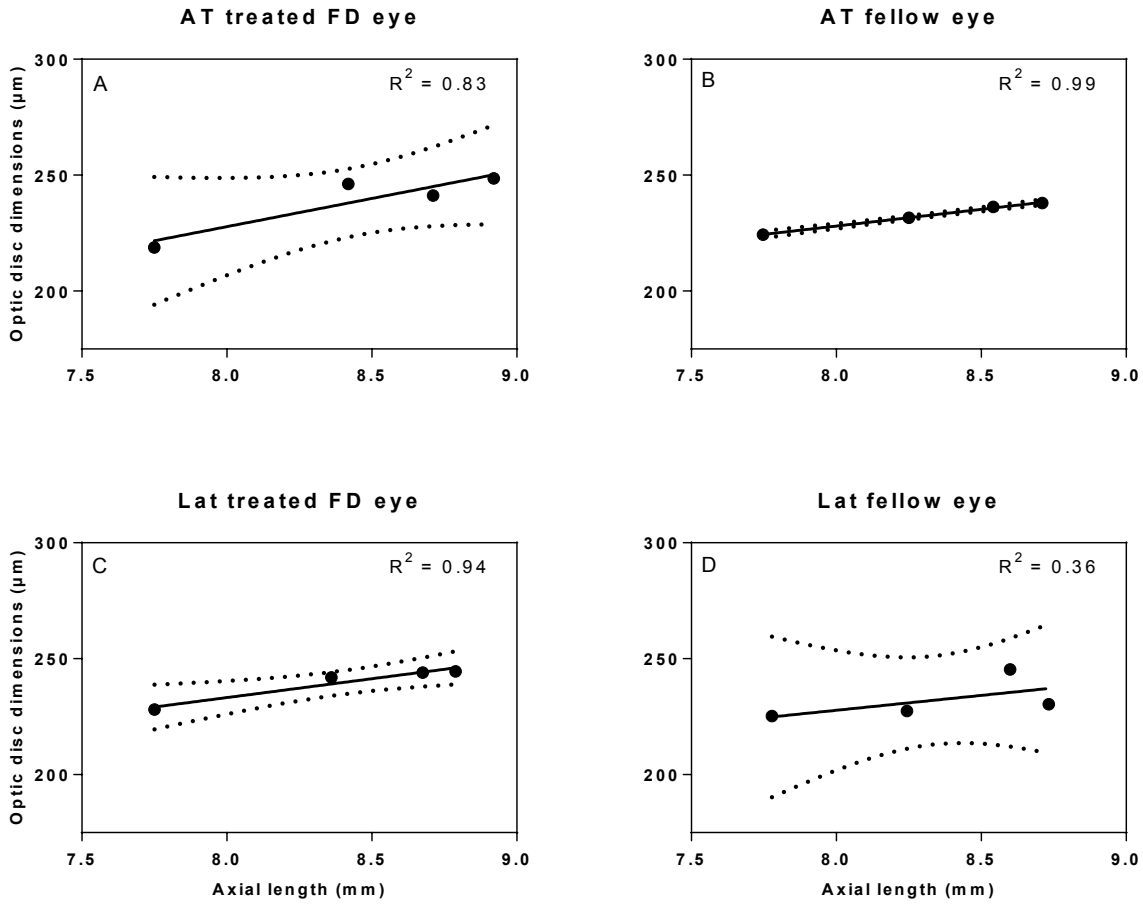

Figure 3.6: Optic disc dimensions of form-deprived and fellow eyes of artificial tears (A and B) and latanoprost groups (C and D) plotted against the axial length of the same eyes.

3.3.5 Effect of latanoprost on lamina cribrosa - Scanning electron microscopy

Latanoprost is known to remodel the extracellular matrix. To test latanoprost treatment effect and compare it to the group taking ATs, the microstructural changes of the lamina cribrosa (continuous at least posteriorly with the sclera) were evaluated by scanning electron microscopy imaging (Figure 3.7).

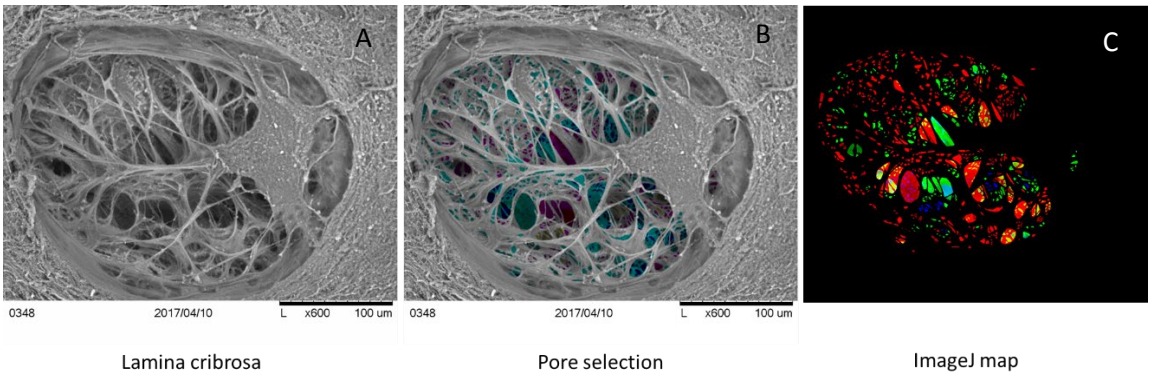

Figure 3.7: Representative image of A) the lamina cribrosa, captured using scanning electron microscopy (SEM) and imaged at 600X, B) pore selection by custom image J program, C) pore map generated by image J.

The LCs of FD-AT eyes and their fellows were very similar in appearance and this is reflected in their pore area profiles, which were not significantly different (21.69 ± 8.88 vs. 22.21 ± 8.71 μm^2; p> 0.999). Likewise, there was no difference between the LC pore area profiles of FD-Lat eyes and their fellows (18.30 ± 9.15 vs. 18.87 ± 9.33 μm^2; p> 0.999). Nonetheless, it is noteworthy that FD-Lat eyes and their fellows tended to have slightly smaller laminar pores areas, on average, than the FD-AT eyes and their fellows (Table 3.3).

Table 3.3: Mean (±SEM) laminar pore area (μm^2) in form-deprived and fellow eyes of artificial tears and latanoprost groups.

Eye	Treatment	Laminar pore area (μm^2)	Number of eyes
FD	Artificial Tears	21.69 ± 8.88	5
Fellow	Artificial Tears	22.21 ± 8.71	5
FD	Latanoprost	18.30 ± 9.15	5
Fellow	Latanoprost	18.87 ± 9.33	5

The laminar pores data were further analyzed after categorization based on size, into one of three groups, small (<15 μm^2), medium (15-30 μm^2), and large (>30 μm^2). The percentage of lamina cribrosa pores in each category was calculated for the treated and fellow eyes of both AT and Lat groups. This analysis further confirmed the lack of any significant difference between the LCs of treated eyes and their fellows. For all eyes, the smallest laminar pores accounted for the highest percentage of pores, while there were approximately equal numbers of medium and large pores, expressed in percentage terms (Table 3.4 and Figure 3.8).

Table 3.4: Laminar pores area percentages small of small (<15 μm^2), medium (15-30 μm^2), and large (>30 μm^2) pores, in form-deprived (FD)- and fellow eyes of artificial tears (AT)- and latanoprost (Lat)-treated groups. Statistics indicate significance of the difference between numbers of small and large LC pores, expressed in percentage terms; differences between numbers of small and medium LC pores, are all significant.

Eye	% of <15 μm^2	% of 15-30 μm^2	% of >30 μm^2	P-value (Small vs large)
FD-AT	65.3 ± 15.4	16.5 ± 5.2	18.2 ± 10.9	0.07
Fellow-AT	63.9 ±13.5	16.6 ± 3.2	19.5 ± 11.5	0.09
FD-Latanoprost	71.3 ± 16.7	10.7 ± 5.7	18.0 ± 11.0	0.03
Fellow-Latanoprost	68.9 ± 16.7	13.3 ± 6.1	17.7 ± 10.8	0.04

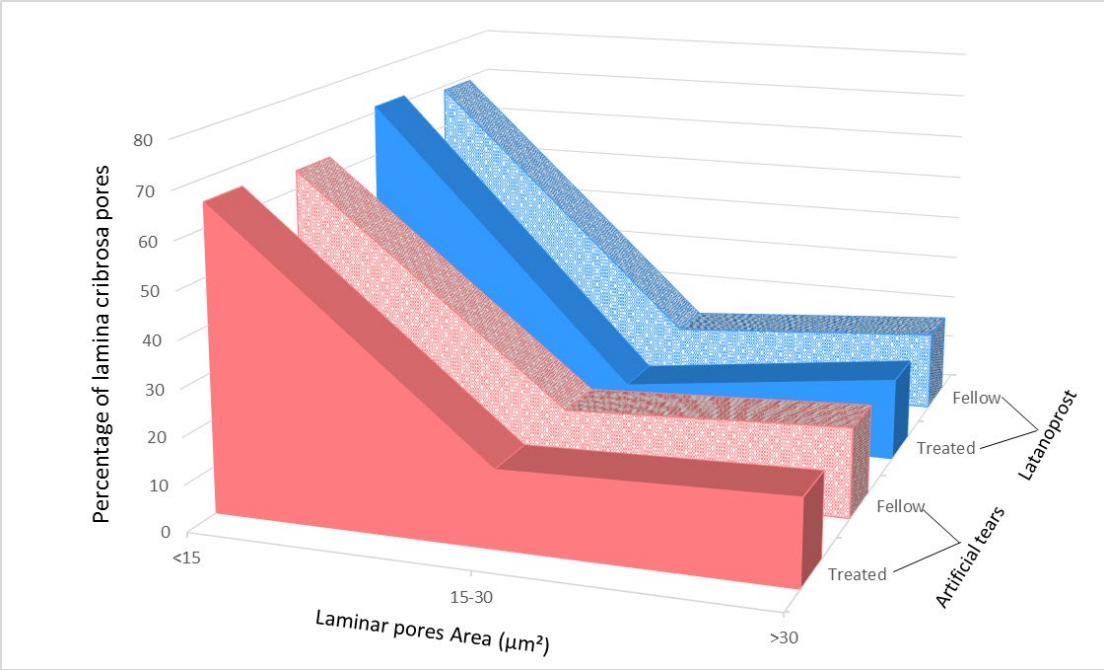

Figure 3.8: Graph showing percentage of laminar pores in each of three size categories (small, <15 μm^2; medium, 15-30 μm^2; large (>30 μm^2). for the treated and fellow eyes of artificial tear (AT) and latanoprost groups. For all eyes, the smallest laminar pores accounted for the highest percentage, while there were approximately equal numbers of medium and large pores.

3.3.6 Effect of latanoprost on scleral collagen - Transmission electron microscopy

Both the distribution of scleral collagen fibers and their cross-sectional area dimensions were qualitatively examined. In the normal guinea pig sclera, as represented by that of fellow eyes, scleral collagen fibers were evenly spaced (Figure 3.9A). In contrast, the sclera from myopic FD eyes treated with AT (FD-AT eyes), was clearly altered, with increased spacing between the collagen fibers; there also appeared to be a higher proportion of smaller fibers (Figure 3.9B). Interestingly, the FD eyes treated with Lat (FD-Lat eyes), were not only less myopic, but their scleras had more evenly spaced collagen fibers than those of the FD-AT eyes, more similar to those of the fellow eyes (Figure 3.9C).

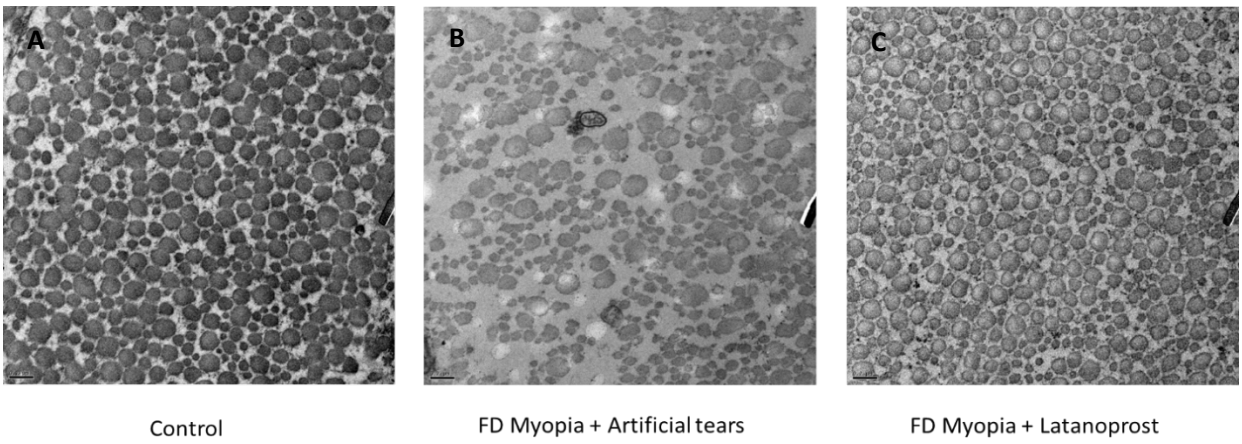

Figure 3.9: Representative TEM images of scleras from A) fellow eyes of the latanoprost group, B) FD eyes treated with artificial tears (AT), and C) FD eyes treated with latanoprost at 6800X. Compared to the sclera of the fellow eye (left panel), which shows a predominance of medium to large collagen fibers, the sclera of the AT-treated myopic eye (middle panel) has a higher proportion of smaller collagen fibers, and is less compact, contrasting with the sclera of the latanoprost-treated eye (right panel), which closely resembles that of the normal fellow sclera.

Collagen fiber cross-sectional area data for the treated and fellow eyes of both groups are summarized in Table 3.5. That the scleras of FD-AT eyes had smaller fibers compared to those of their fellows was confirmed statistically ($0.0059 \pm 0.0013\ \mu m^2$, FD-AT vs. $0.0085 \pm 0.002\ \mu m^2$, fellow ($p<0.001$)), while the scleral fiber dimensions for FD-Lat eyes and their fellows were similar to each other ($0.0083 \pm 0.002\ \mu m^2$, FD-Lat vs. $0.0078 \pm 0.0014\ \mu m^2$, fellow ($p= 0.057$). There was also a significant difference between the scleral fiber areas of FD-AT and FD-Lat eyes, being smaller on average in FD-AT eyes ($p<0.001$).

Table 3.5: Mean (±SEM) scleral collagen fiber area (μm^2) in form-deprived and fellow eyes of artificial tears and latanoprost groups.

Eye	Treatment	Scleral collagen fiber area (μm^2)	Number of eyes
FD	Artificial tears	0.0059 ± 0.0013	5
Fellow	Artificial tears	0.0085 ± 0.002	5
FD	Latanoprost	0.0083 ± 0.002	5
Fellow	Latanoprost	0.0078 ± 0.0014	5

To further compare the effects of the various treatment on scleral collagen fibers, cross-sectional area data were categorized into one of three groups, small (<6000 nm^2), medium (6000-12,000 nm^2), and large (>12,000 nm^2). For both the AT and the Lat groups, the percentage of scleral collagen fibers in each category was calculated for both treated eyes and their fellows. Results of this analysis are shown in Figure 3.10 and summarized in Table 3.6. The FD-AT eyes had the highest percentage of the smallest fibers (51.7 ± 9.1%), and the lowest percentage of the largest fibers (19.5 ± 6.5%) (p= 0.02), compared to their fellows (39.6 ±13.1%, small vs. 25.2 ± 12.7%, large; p= 0.32). On the other hand, the FD-Lat eyes and their fellows had similar percentages of small (37.6 ± 7.1%, FD-Lat; 36.8 ± 8.4%, fellow; p> 0.999), medium (32.0 ± 1.7%, FD-Lat; 36.4 ± 4.0%, fellow; p> 0.999), and large fibers (30.4 ± 5.9%, FD-Lat; 26.8 ± 8.4%, fellow; p> 0.999). The scleral collagen profiles of FD-Lat eyes and their fellows were also similar to and not significantly different from those of the fellow eyes of the FD-AT group.

Table 3.6: Scleral collagen fiber cross-sectional areas; percentages of small (<6000 nm^2), medium (6000-12,000 nm^2), and large (>12,000 nm^2) fibers in form-deprived (FD)- and fellow eyes of artificial tears (AT)- and latanoprost (Lat)-treated groups. Statistics indicate significance of difference between numbers of small and large scleral fiber areas, expressed in percentage terms; differences between other groups not significant.

Eye	% of <6000 nm^2	% of 6000-12,000	% of >12,000 nm^2	P-value (Small vs large)
FD-AT	51.7 ± 9.1	28.8 ± 3.3	19.5 ± 6.5	0.02
Fellow-AT	39.6 ±13.1	35.2 ± 0.6	25.2 ± 12.7	0.32
FD-Latanoprost	37.6 ± 7.1	32.0 ± 1.7	30.4 ± 5.9	0.91
Fellow-Latanoprost	36.8 ± 8.4	36.4 ± 4.0	26.8 ± 8.4	0.62

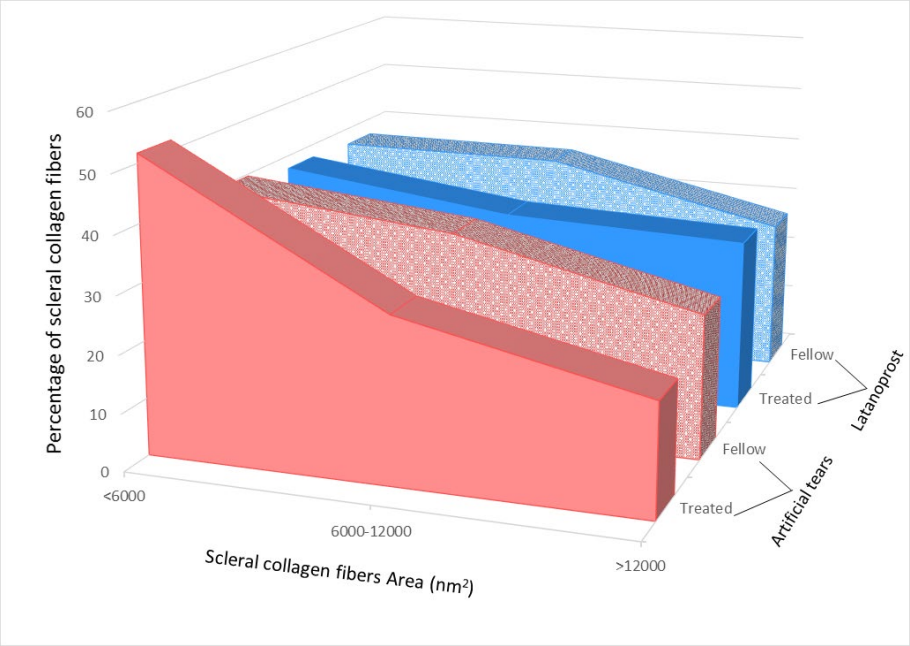

Figure 3.10: Percentage of each of three categories of scleral collagen fibers, based on cross-sectional areas (small, <6000 nm^2; medium, 6000-12,000 nm^2; large, >12,000 nm^2), shown for the treated and fellow eyes of the artificial tears and latanoprost groups.

How tightly related were the changes in scleral collagen fibers area to eye elongation? To address this question, the interocular difference of the average collagen fiber area was plotted against the interocular difference of the axial length for both AT and Lat groups. The AT group showed a negative linear correlation between axial length and collagen fiber area (r^2= 0.9, p= 0.014), while there was no significant linear correlation between these parameters for the Lat group (r^2= 0.13, p= 0.55) (Figure 3.11).

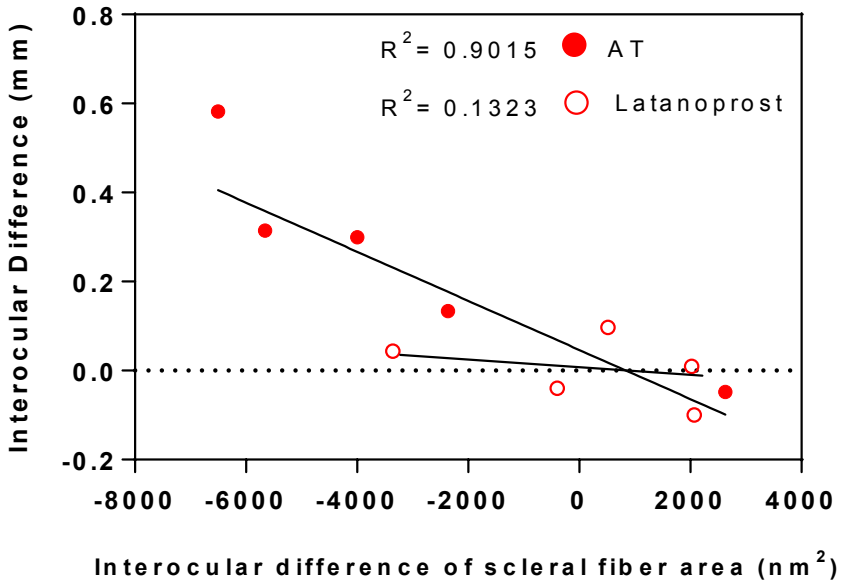

Figure 3.11: Interocular differences in average scleral collagen fiber area (nm^2) for individual animals of artificial tear (AT) and latanoprost treated groups, plotted against interocular differences of axial length for the same animals.

3.4 Discussion

3.4.1 Latanoprost and intraocular pressure, diurnal rhythms, and myopia control in guinea pigs

This study aimed to re-examine the possibility of using ocular hypotensive drugs as myopia control therapies, specifically addressing the question of whether myopia progression can be inhibited through an appropriate, sustained reduction in IOP. To this end, we examined the efficacy of topical latanoprost, as a representative prostaglandin analog, for controlling myopia progression in a form-deprived guinea pig model of myopia. We found that topically applied latanoprost was effective in both lowering IOP and slowing myopia progression in this model.

As noted in the introduction, to-date there have been three studies investigating the effects of intervention with ocular hypotensive drugs on myopia progression in animal models. Two of the studies involved form-deprived chicks and one of them also involved latanoprost, delivered by intravitreal injection (Jin and Stjernschantz, 2000). The latter study also reported attenuation of eye elongation. Intravitreal injection of 100 ng latanoprost acid twice for a week approximately halved the mean interocular difference compared to that recorded from chicks injected with isotonic saline, i.e., 0.17 ±0.12 versus 0.30 ±0.04 mm. Nonetheless, intravitreal injection of latanoprost in chicks was less effective than our longer-term topical latanoprost treatment in guinea pigs (0.06±0.02 mm latanoprost vs. 0.29 ±0.04 mm control at week 10. This is possibly

because the chick sclera has an inner cartilage layer, in addition to the more commonly found fibrous layer. Thus the underlying scleral “growth” mechanism(s) and the role of IOP in eye enlargement in the chick may be different from those in mammals and humans. The other earlier study in chicks tested timolol, a beta-blocker, which proved to have minimal effect on the development of form-deprivation myopia, even though it was found to lower IOP by approximately 18% in myopic eyes (Schmid et al., 2000). Interestingly, timolol is the only ocular hypotensive drug to have been evaluated clinically, and while a correlation between reductions in IOP and the rate of myopia progression was reported in the earliest of two studies (Goldschmidt, E., Jensen, H., Marushak, 1985), the latter effect was reported to be small, even though timolol apparently lowered IOP, by ~3 mmHg (Goldschmidt, E., Jensen, H., Marushak, 1985; Hosaka, 1988). Finally, another recent study tested the efficacy of brimonidine, another ocular hypotensive drug, against lens-induced myopia in guinea pigs (Liu et al., 2017). Brimonidine belongs to a different drug class than both latanoprost and timolol, being an alpha2 adrenergic agonist, with effects on both aqueous inflow and uveoscleral outflow. Nonetheless, it also proved effective in stabilizing myopia progression.

In our study, the FD eyes of control (artificial tears-treated) animals showed a trend towards IOP elevation. Although this trend was not statistically significant, the brimonidine study also reported an increase in IOP in lens-induced myopic eyes receiving 0.9% saline by the end of the study (Liu et al., 2017). These findings also fit with isolated reports in humans of higher IOPs in myopes compared to emmetropes (Cahane and Bartov, 1992; Detry-Morel, 2011; Wong et al., 2003). Nonetheless, even without significant IOP elevation, for eyes with fibrous scleras, biomechanically weakening of the sclera due to increased extracellular matrix during myopia progression, will arguably render it more vulnerable to the stretching (inflationary) influence of IOP. In this context, the results of our study, i.e., that latanoprost lowered IOP and slowed axial elongation in treated FD eyes relative to control FD eyes are predictable. The possibility that structural changes in myopic (FD) eyes can lead to IOP elevation, as a further adverse complication, is the subject of on-going investigations.

Why did latanoprost prove so effective relative to timolol in slowing myopia progression in our study? Apart from the differences in animal models used to test their efficacy – guinea pig versus chicks, the ocular hypotensive action of timolol is largely limited to daytime hours in comparison to latanoprost, which has an enduring (24 h) ocular hypotensive effect (Liu et al., 2004). Overall, the prostaglandin analogs also tend to be more effective in lowering IOP than beta-blockers, such as timolol (Camras, 1996). These features of latanoprost’s profile contributed to its selection for our study, along with other data showing robust ocular hypotensive effects in a variety of species, including monkeys (Takagi et al., 2004) and dogs (Kahane et al., 2016). The study reported here allows the guinea pig to be added to this list. The only previous study involving the use of topical latanoprost in guinea pigs was short-term (24 h) and the animals studied were normal and older than those used in the current study (Di et al., 2017). Nonetheless, they also reported a reduction in IOP in response to latanoprost, by 2.1±1.3 mm Hg, after one hour.

Ophthalmic research into the actions of latanoprost and closely-related PG analogs has largely been directed towards understanding their ocular hypotensive action. In this

context, they are known to increase matrix metalloproteinase (MMP) activity and thus remodelling of the extracellular matrix (ECM) within the uveoscleral outflow pathway.(Lindsey et al., 1997) Our finding that treatment efficacy, i.e., inhibition of FD myopia, was directly related to the extent to which IOP was reduced, supports a biomechanical explanation, i.e. that the reduced rate of ocular elongation reflects the reduced tension on the scleral wall, achieved by lowering IOP. However, alternative explanations cannot be ruled out, including the possibility that increased uveoscleral outflow may have contributed to the observed myopia control effect in other ways, for example, by increasing the clearance of scleral-directed myopiagenic growth factors released by the retinal pigment epithelium (Zhang et al., 2012), and/or thickening the choroid, which has been linked to inhibited eye elongation in a variety of animal models (e.g., Nickla, 2013; Takagi et al., 2004). As noted in the introduction, latanoprost has also been reported to increase scleral remodelling (Cahane and Bartov, 1992), which might exacerbate rather than inhibit myopia progression; although such effects cannot be ruled out in the current study, they clearly not dominate in terms of treatment outcome. Nonetheless, further investigation of the scleral and choroidal effects of latanoprost at the molecular, cellular and biomechanical levels, would seem warranted to better understand its myopia control effect.

Diurnal rhythms in IOP have been documented in many species, including chicks (Nickla et al., 1998), rats (Arranz-Marquez and Teus, 2004; Kahane et al., 2016), rabbits (Smith et al., 2009), monkeys (Bito et al., 1979) and humans (Detry-Morel, 2011; Lindsey et al., 1997) with species differences in the phase and amplitude of IOP rhythms apparent, e.g., lower in rhesus monkey eyes (5 mmHg) (Bito et al., 1979) than in rat eyes (Arranz-Marquez and Teus, 2004; Kahane et al., 2016) and rabbit eyes (10 mmHg) (Smith et al., 2009). For our guinea pigs, the highest IOP was recorded at the first, morning time-point, just after lights-on, with IOP decreasing throughout the day. These results agree with our already published diurnal IOP patterns for normal guinea pigs (Lisa A. Ostrin and Wildsoet, 2016). While all eyes showed daily rhythms in IOP in the current study, interestingly, the IOP rhythm amplitude for myopic eyes treated with artificial tears was increased, to approximately 8 mmHg, compared to fellow eyes. However, while the latter value is comparable to the amplitude reported for FD myopic chick eyes (Nickla et al., 1998), amplitude was reported to be not significantly affected, but phase more variable in the latter study, pointing to a possible species difference. It is noteworthy that latanoprost reduced the IOP rhythm amplitude for FD myopic eyes to a level similar to that of untreated fellow eyes (~5 mmHg), also comparable to data from normal monkeys (Bito et al., 1979). Thus, in addition to reducing IOP overall, latanoprost appears to normalize IOP rhythms in myopic eyes. In keeping with a biomechanical explanation for the slowed myopia progression with latanoprost, could the normalization of the IOP rhythm amplitude in the FD myopic eyes of the guinea pigs underlie the slowed myopia progression observed? Alternatively, it is possible that the sustained ocular hypotensive action of latanoprost, i.e., around the clock, was responsible.

Limitations: Below we summarize key weaknesses in our study. As mentioned, guinea pigs wore diffusers affixed over one of their eyes via Velcro rings. While this method successfully induced myopia, the long-term nature of these experiments carried a significant risk of the diffusers becoming detached. However, in cases of diffuser

detachment, temporary intervention using masks with diffusers attached limited the disruption to the form deprivation treatment. Also, there were no clear treatment-related biases, i.e., latanoprost versus artificial tears, in detachment events. On average, diffusers of each animal were detached once or twice a week for no longer than 1 hour each time. Accurate measurement of IOP is also critical to this study. While we did not undertake calibration measurements for the iCare rebound tonometer used in our study, it has been calibrated for rat eyes, which are similar in size to guinea pig eyes. Central corneal thickness is also known to influence IOP readings but was not measured in our study, and it is not possible to rule out an effect of latanoprost, via remodeling of the ECM of the corneal stroma, as there are no relevant published studies. Our analyses were also largely based on interocular differences, by way of reducing the effects of inter-animal variability. Lending validity to this approach, we also report no significant differences between the fellow eyes of the latanoprost and control groups; nonetheless, subtle changes in the fellows to form-deprived eyes have been reported in a number of past studies involving other animal models (Howlett and McFadden, 2006; Smith et al., 2009). Finally, we did not test the effect of latanoprost on normal (non-form deprived) eyes, leaving open the question of its effect on normal eye growth. However, data collected from older (three-months-old) animals are encouraging; monocular latanoprost significantly reduced IOP in otherwise untreated eyes (mean interocular IOP differences (± SEM): -0.44±0.48 mmHg at baseline, -2.89±1.13 mmHg after 2 weeks, p= 0.05), while neither SEs nor ALs were affected.

3.4.2 Latanoprost and macro-structural changes

Optic discs tended to increase in size with increasing axial length in both FD myopic and fellow (normal) guinea pigs eyes, but at a faster rate in the myopic eyes, paralleling the trends reported for human myopia. Latanoprost treated FD eyes and their fellow eyes also seemed to increase in size with axial elongation, but had a more similar rate of growth. Although there are not many animal studies that tracked optic disc size in relation to refractive error and axial length, there is a number of human studies that investigated the influence of refractive error and/ or axial length on the optic disc size.

While optic discs area generally increases with axial elongation (Hoh et al., 2006; Savini et al., 2012; Bae et al. 2016), Leung et al. found using a Heidelberg Retina Tomograph (HRT), that optic disc size was independent of axial length and refractive error between -8 and +4 D and concluded that OCT does not agree with HRT, because it may overestimate optic disc area, cup to disc area ratio, and rim area in myopic eyes (Leung et al., 2006). This discrepancy between the two instruments could be related to the different methods of measuring the disc margin. In the HRT, the disc margin is demarcated by Elschnig's ring outer boundary, whereas, the retinal pigmented epithelium ends are what is detected in OCT (Leung et al., 2006). Given that peripapillary atrophy- disruption of the retinal pigmented epithelium in the area surrounding the optic disc- is more common in myopic eyes (Ramrattan et al., 1999), the optic disc margins with the peripapillary atrophy, could have been overestimated in size in OCT. Therefore, it is crucial to account for axial length- induced ocular magnification when measuring optic nerve head size.

There is a lot of controversy regarding the relationship between optic disc size and refractive error. Two studies found that optic disc size was independent of refractive error between -8 and +4 D (Jonas, 2005; Wang, 2006). In contrast, another study reported an increase in the disc area for each diopter increase in the myopic direction. However, No significant correlation was found in eyes with a refractive error within the range of -4 and +4 D (Ramrattan et al., 1999). It has been reported that peripapillary atrophy increases by 1.3% for each diopter of myopic refraction increase (Ramrattan et al., 1999). Therefore, it is logical that the OCT may overestimate the optic disc area in highly myopic eyes.

3.4.3 Latanoprost and micro-structural changes

To date, the effect of myopia on the architecture of the lamina cribrosa has not been investigated in any animal model, although a previous study by our group used scanning electron microscopy to image the lamina cribrosa of normal pigmented and albino guinea pigs (Lisa A. Ostrin and Wildsoet, 2016). The guinea pig was shown to have a well-organized, collagen-based lamina cribrosa, making it a promising model for investigating the relationship between myopia and glaucoma. Histomorphometric studies of human globes have found the lamina cribrosa to be thinner in highly myopic eyes when compared to eyes with normal axial length (Jonas et al., 2012, 2004), and in another study involving normal monkeys (no myopia or glaucoma), lamina cribrosa thickness was found to decrease and the posterior sclera to thin, with increasing axial length (Jonas et al., 2016). However, in the current study, no abnormalities in the lamina cribrosa architecture were identified in either of FD groups, including the one treated with latanoprost, which is itself reassuring from a therapeutic perspective.

Our interest in the lamina cribrosa architecture of the myopic guinea pigs stems from *in vivo* human studies suggesting that both high myopia and glaucoma significantly increase the risk of lamina cribrosa damage, and the further suggestion that lamina cribrosa changes in highly myopic eyes with no glaucoma may partially explain the increased risk of glaucoma in these eyes (Miki et al., 2015). Eyes with tilted discs, as commonly encountered in human myopia, appear more susceptible to focal temporal lamina cribrosa defects and associated glaucomatous visual field defects, (Sawada et al., 2017). Interestingly, none of the myopic guinea pigs that were also imaged *in vivo* using SD-OCT showed tilted discs (unpublished data). It is plausible that this difference between the guinea pig and human eyes reflects differences in the anatomical location of the optic nerve insertion site, raising the further possibility that shearing forces on the lamina cribrosa may be less in the case of guinea pig lamina cribrosa, as reflected in our failure to detect any related structural abnormalities. Nonetheless, because the SEM technique used in this study only allows for characterization of the surface structure of the lamina cribrosa, we cannot rule out changes in the deeper layers. It is also possible that such changes as described in humans may slowly evolve over time, while our study was limited to a 10-week monitoring period.

In this study, the scleras of the myopic FD guinea pig eyes were morphologically different from those of their fellows and the latanoprost-treated eyes. In the scleras of untreated fellow (normal) eyes, collagen fibers were relatively evenly spaced; also, while the fibers ranged in size from quite small to quite large, medium-sized fibers

dominated. In contrast, the scleras of the more myopic eyes, treated only with artificial tears, had both a higher proportion of smaller collagen fibers and overall, the fibers were more sparsely spaced. The latter picture fits well with other descriptions of myopic scleras. For example, in 1979, Curtin (Curtin et al., 1979), in examining human myopic eyes by electron microscopy, noted the following differences in myopic sclera: predominantly lamellar, reduction in fibril diameters (below 60-70 nm), greater dispersion for the range of fibril diameters, greater prevalence of extremely small diameter fibrils, and unusual star-shaped fibrils on cross-section. With the exception of the last observation, this description also captures the changes in the scleras of our myopic guinea pigs.

Similar to human myopic scleral changes, myopia development and progression in tree shrews and mice have also been linked to changes in scleral collagen fiber spacing and diameter, as viewed by TEM. For example, in one study involving long-term (≥ 3 months) form deprivation in tree shrews, the resulting myopia was linked to an increase in the proportion of small diameter scleral collagen fibrils (McBrien et al., 2001). Similar scleral changes were also observed in a transgenic mouse model, which exhibits high myopia (Song et al., 2016). These findings are consistent with our own observation of a higher proportion of the smaller collagen fibers in the scleras of the form deprived myopic eyes of guinea pigs treated only with artificial tears. Furthermore, the scleral changes in these same animals were closely related to the induced changes in eye length, with the average size of collagen fibers decreasing with increased elongation.

Interestingly, in our study, latanoprost not only inhibited myopia progression but also appeared to normalize the scleral collagen mosaic in these eyes. While it is not possible to establish a causal relationship between the latter finding and the slowed myopia progression observed, it was nonetheless, an unexpected result, given that latanoprost's ocular hypotensive action has been attributed to enhanced uveal extracellular matrix remodeling (Li et al., 2016; Oh et al., 2006; Ooi et al., 2009). Should similar protein expression changes, i.e. increases and decreases expressions of matrix metalloproteinase (MMPs) and tissue inhibitor of metalloproteinase (TIMPs) respectively, occur in the nearby sclera, one would expect the myopic changes to be exaggerated. Lending weight to the latter prediction are observations involving monkey and human sclera of increased MMP expression and increased permeability after exposure to topical prostaglandins *in vivo*, (Aihara et al., 2002; Kim et al., 2001; Weinreb, 2001). That in the current study, the sclera from eyes treated with latanoprost had a similar appearance to the fellow eyes thus raises the possibility that the effect of lowering IOP outweighed any enhanced scleral remodelling effects of latanoprost. This explanation also fits with *in vitro* data showing influences of both static and dynamic stress on collagen synthesis in scleral explants (Prema O'Brien, 2010). An alternative pharmacokinetic explanation that the posterior sclera was less exposed to latanoprost than the anterior sclera, due to our use of topical drops, seems less plausible due to both the relatively small eye size of the guinea pig and evidence from *in vivo* SD-OCT imaging that the nearby posterior choroid of these eyes was structurally altered (El-Nimri et al., ARVO abstract 2018).

Chapter 4: Effect of the Ocular Hypotensive Drug, Latanoprost on Choroidal Thickness in Normal Guinea Pigs

4.1 Introduction

Intraocular pressure (IOP) is speculated to play a key role in normal ocular growth, by exerting a stretching influence (tangential tension), on the outer scleral wall of the eye, which undergoes remodeling as part of this growth process (Nickla, 2013). During development and progression of myopia, scleral remodeling is upregulated (McBrien et al., 2009; Summers Rada et al., 2006), altering the biomechanical properties of the sclera (Phillips, 1995; Siegwart and Norton, 1999), and allowing eye enlargement to accelerate. IOP likely facilitates this process, especially in larger, already myopic eyes due to the increase in tangential tension experienced (Cahane and Bartov, 1992).

The possibility that lowering IOP can slow “myopic eye elongation” led us to examine the effects of the ocular hypotensive drug, latanoprost, on “myopic” ocular growth of guinea pigs. It had been previously shown to slow myopia progression in chicks, although it was administered by intravitreal injection in this study (Jin and Stjernschantz, 2000), rather than applied topically, as is standard for glaucoma therapy. However, topical latanoprost also proved to strongly inhibit myopia progression in our guinea pig myopia model, (El-nimri and Wildsoet, 2018), raising the further question of whether the promising anti-myopia effect of latanoprost is drug-specific or a general effect of lowering IOP. As a step towards addressing the above question, it was of interest to learn more about the ocular effects of latanoprost in our guinea pig model. In this study, we specifically examined its effects on the choroid of the guinea pig.

Interest in the role of the choroid, a major component of the ocular uveal tissue, in normal and abnormal (myopic) eye growth regulation has increased in recent years, with studies across a wide range of species reporting similar trends to those of early studies in chicks, which linked choroidal thickening with slowed eye elongation and choroidal thinning with increased eye elongation (Howlett and McFadden, 2006; Hung et al., 2000; Norton and Kang, 1996; S.A. et al., 2013; Troilo et al., 2000; Wildsoet and Wallman, 1995). As a highly vascular layer lying between the retina, where growth regulatory signal are believe to be generated, and sclera, which largely determines eye size, the choroid has the potential to influence eye growth in any of a number of ways, including relaying growth regulatory signals from the retina to the sclera (Wang et al., 2015; Zhang and Wildsoet, 2015),

Latanoprost, a prostaglandin (PG) F2α isopropyl ester prodrug, has proven very effective in lowering IOP around the clock (24 h). Its pharmacological action is via FP receptors, which are widely distributed throughout the eye, including on the iris, ciliary body and choroid plexus (OCKLIND, 1998) Increased matrix metalloproteinase (MMP-

2) activity linked to remodeling of the extracellular matrix (ECM) within the uveoscleral aqueous outflow pathway appears to be largely responsible for its enduring ocular hypotensive action (Russo et al., 2008; Weinreb and Lindsey, 2002). Prostaglandin analogs have also been shown to increase choroidal thickness and improve choroidal perfusion in glaucoma patients (Akyol et al., 2017; Boltz et al., 2011).

In chapter 3 investigating the potential of latanoprost to inhibit myopia progression in guinea pigs (El-Nimri and Wildsoet, 2018), we observed a trend of choroid thinning in the form-deprived myopic eyes of animals treated with artificial tears, that was not evident in form-deprived eyes treated with latanoprost (un-reported data). However, the latter eyes were also significantly less myopic. These observations provided additional motivation for the investigation reported here into the effects of latanoprost on the guinea pig choroid.

4.2 Methods

4.2.1 Animals and treatments

Animals:

A total of 10 three-month-old, tricolored guinea pigs were used in this study, offspring of breeders obtained from the University of Auckland, New Zealand. Study animals were housed in a temperature-controlled room, with a light/dark cycle of 12L/ 12D (on at 9.30 am, off at 9.30 pm). Pups were weaned at 5 days of age and housed as single sex groups in 41 cm wide X 51 cm long transparent plastic wire-top cages, with free access to water and vitamin C-supplemented food, with additional fresh fruit and vegetables given five times a week as diet enrichment.

All animal care and treatments in this study conform to the ARVO Statement for the Use of Animals in Ophthalmic and Vision Research. Experimental protocols are approved by the Animal Care and Use committee of the University of California, Berkeley.

Topical ophthalmic drug treatments:

All animals underwent 2 weeks of daily monocular treatment with 0.005% latanoprost ophthalmic solution (Akorn, Lake Forest, IL), with the untreated contralateral eyes serving as controls. Specifically, after obtaining baseline measurements, one drop of latanoprost was instilled into the right eyes of all animals each day, at approximately 4 pm, for a total of two weeks, after which the treatment was terminated and animals followed for a further two weeks (i.e., washout period).

4.2.2 Intraocular pressure, refractive error, axial length, and choroidal thickness with A-scan ultrasonography

Intraocular pressures (IOP), spherical equivalent refractive errors (SE) and axial ocular dimensional data were recorded for both eyes of each animal, immediately before the initiation of the latanoprost treatment (baseline), with follow-up measurements made after 2 days, 1 and 2 weeks of treatment, with the same measurement schedule followed during the washout period. Because of well-documented diurnal rhythms in

IOP, choroidal thickness, and eye elongation (Nickla et al., 1998), measurements were always taken at approximately the same time each day, in the afternoon around 1:00 pm.

All IOP measurements were conducted in awake animals, prior to other procedures requiring anesthesia to avoid possible confounding effects of the latter (Duncalf, 1975). An iCare rebound tonometer (Tonolab, Helsinki, Finland) was used along with the setting for rat eyes, for which this instrument has been calibrated and which are only slightly smaller than those of guinea pigs. This instrument provides confidence interval information based on successive readings; only data with a confidence interval of 5% or less were used. Three measurements were taken on each eye and the average used in data analysis.

Refractive errors were measured using streak retinoscopy on awake animals, 30 minutes after instillation of one drop of 1% cyclopentolate hydrochloride (Bausch & Lomb, Rochester, NY) for cycloplegia. Spherical equivalent refractive errors (SERs, average of results for the two principal meridians) were used in data analysis.

Ocular axial dimensions, including choroidal thickness, were measured with a custom-built, high-frequency A-scan ultrasonography system, with an estimated resolution of ~10 μm (Nickla et al., 1998), (Schmid et al., 1996). For these measurements, animals were first placed under gaseous anesthesia (1.5-2.5% isoflurane in oxygen), with eyelid retractors inserted to hold their eyes open. For each measurement, at least 8 traces were captured per eye and analyzed off-line. Axial choroidal thickness and axial length data are reported here.

4.2.3 In vivo SD-OCT imaging

High-resolution cross-sectional images of the ocular fundus, including the choroidal layer, were captured using spectral domain-optical coherence tomography (Bioptigen SD-OCT, North North Carolina, USA). Both eyes of each animal were imaged. Animals were first anesthetized with an intramuscular injection of ketamine and xylazine (27 mg/kg, 0.6 mg/kg, respectively), then placed on a custom-made stage with x-y-z adjustments to facilitate alignment of the optical axis of the eye being imaged with that of the instrument. As the guinea pig retina is devoid of retinal blood vessels, the optic nerve head of each eye was used instead as a reference landmark for repeated imaging. OCT scans were restricted to the visual streak region, which is located approximately 2.5 optic disc diameters away from the center of the optic nerve head (~ 700 μm away from the center of the optic nerve head). The scans spanned a 2.6 by 2.6 mm-wide field of view (approx. ~ 15 deg.), and consisted of 50 B-scans by 700 A-scans, with 50 frames per B-scan (Jiang, Garcia et al., 2019). All imaging were performed around 1:00 pm, to minimize the effect of diurnal variations in choroidal thickness.

4.2.4 SD-OCT image analysis

A custom ImageJ macro program was used to measure from captured images, both overall choroidal thickness (Figure 4.1A), and the area of individual choroidal vessels (Figure 4.1B). Only the middle one-third (~ 5 deg.) of each cross-sectional image was analyzed to avoid any distortion due to lateral magnification differences at the extremities, with choroidal thickness measurements made using built-in vertical calipers at 3 different locations within this central zone and averaged. Choroidal vessels were used as reference anatomical landmarks in analyzing images collected from the same eyes on different days across the monitoring period.

Statistical analysis:

Statistical and graphical data analysis made use of Prism 6 (GraphPad Software, La Jolla, CA, USA). Data for treated and control eyes, as well as derived interocular differences (treated eye - control eye), are reported as mean ± SEM. Two-way repeated measures ANOVAs, with a Bonferroni post hoc test, were applied to data. P-values from post-hoc testing are reported in the results section.

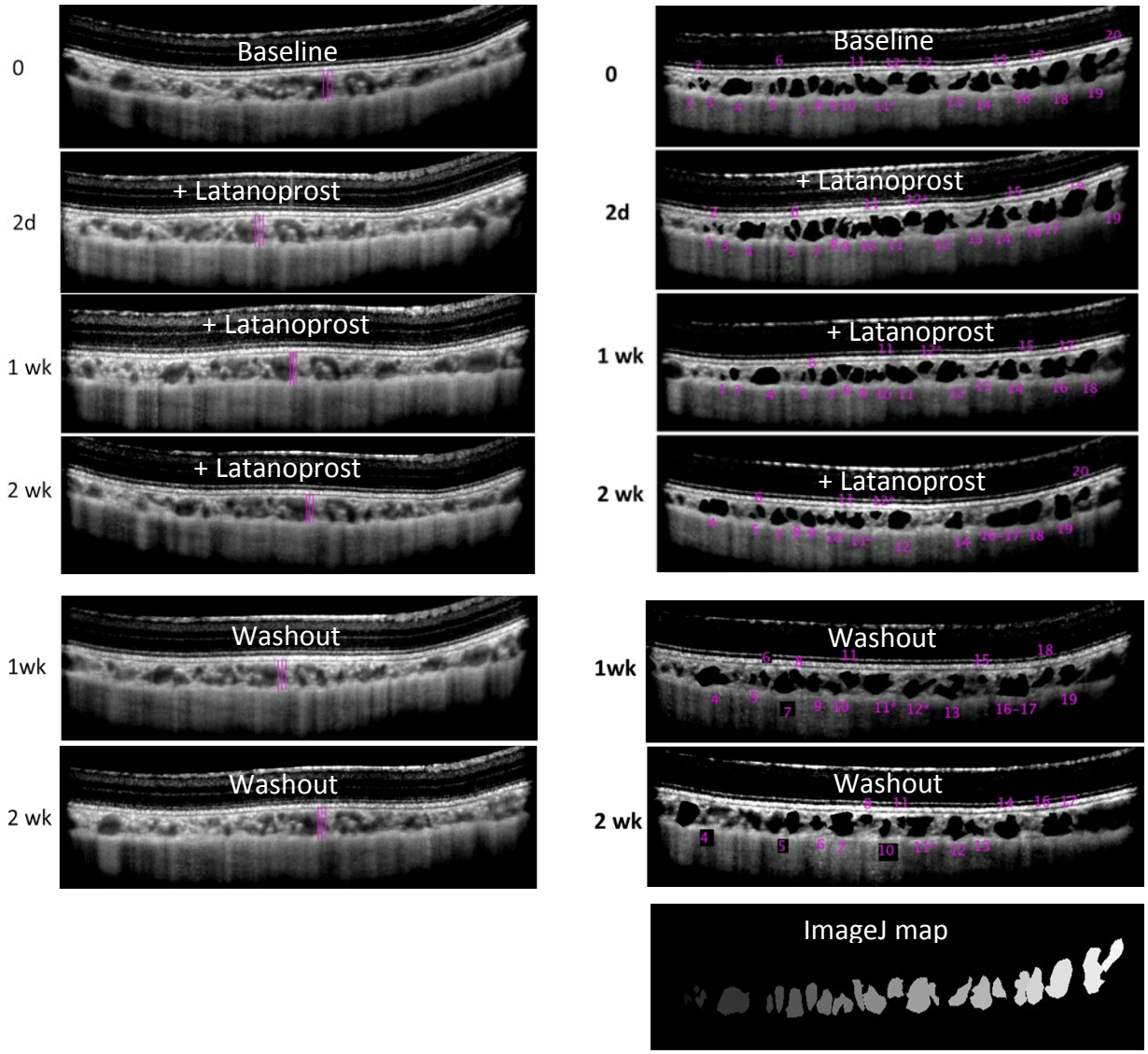

Figure 4.1: Representative SD-OCT images of fundus layers captured from the visual streak, located ~2.5 disc diameters above the optic nerve head, recorded on day 0 (pretreatment baseline), as well as day 2, week 1, week 2 of the latanoprost treatment period, and 1 and 2 weeks after termination of treatments (washout period); the visual angular subtense of the images is ~15 deg. Images were averaged to better visualize vessel margins. Bottom right image shows the choroidal vessel area map produced by the custom imageJ program.

4.3 Results

4.3.1 Effect of latanoprost on intraocular pressure, refractive error, and axial length in normal guinea pigs

Latanoprost treatment effects on IOP:

Key mean IOP data for latanoprost-treated and fellow eyes, i.e. recorded at baseline, at the end of the treatment period and the end of the washout period, are summarized in Table 4.1. Daily topical latanoprost was effective in lowering IOP in latanoprost-treated eyes. This treatment effect is evident in the graphical plots of IOPs recorded from treated and fellow eyes over the treatment period (Figure 4.2), and of the derived interocular difference data (Figure 2 inset). At baseline, IOPs recorded from the two eyes of each animal were similar, i.e., 21.63 ± 1.12 mmHg (right eyes) and 22.07 ± 0.94 mmHg (left eyes) (NS). However, thereafter, the IOPs of eyes treated with latanoprost decreased relative to the IOPs of fellow eyes (Figure 4.2), with this interocular difference reaching statistical significance after 2 weeks of latanoprost treatment, i.e., 22.23 ± 0.86 mmHg vs. 24.50 ± 0.98 mmHg (p= 0.05). However, by the end of the "no treatment" washout period, the IOPs of treated eyes were again comparable to those of fellow eyes (Figure 4.2).

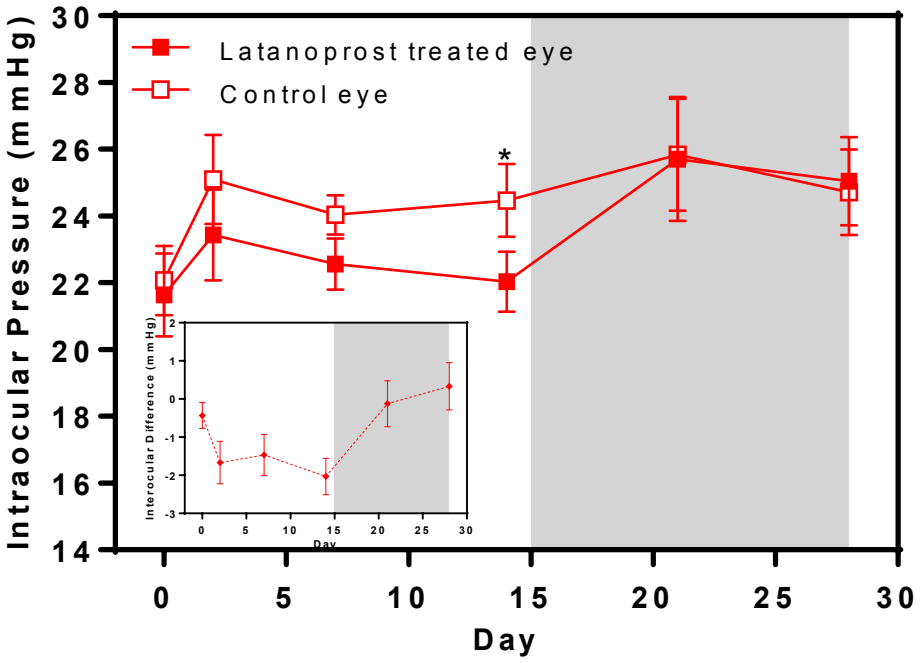

Figure 4.2: Intraocular pressures (IOP) recorded from guinea pigs treated monocularly with topical latanoprost for 2 weeks, means (± SEM, mmHg) for treated and fellow eyes plotted against time. The shaded area indicates the 2-week post-treatment washout period. Inset shows similarly plotted interocular differences in IOP. * p< 0.05.

Table 4.1 Summary of IOP, refractive error, axial length, choroidal thickness (measured using A-scan ultrasonography and SD-OCT imaging), and choroidal vessel area data for latanoprost-treated and fellow eyes (mean ± SEM), recorded at the beginning and end of 2-week latanoprost treatment and washout periods.

Parameter	Eye Treament	Baseline	Week 2 Treatment	Week 2 Washout
IOP (mmHg)	**Latanoprost**	21.63 ± 1.12	22.23 ± 0.86	25.04 ± 1.17
	Fellow	22.07 ± 0.94	24.50 ± 0.98	24.71 ± 1.13
Refractive error (D)	**Latanoprost**	0.11 ± 0.43	0.7 ± 0.36	0.34 ± 0.40
	Fellow	-0.3 ± 0.47	0.23 ± 0.28	-0.36 ± 0.47
Axial length (mm)	**Latanoprost**	8.76 ± 0.03	8.86 ± 0.03	8.99 ± 0.05
	Fellow	8.77 ± 0.02	8.87 ± 0.02	8.92 ±0.03
Choroidal Thickness (A-scan) (µm)	**Latanoprost**	180 ± 10	190 ± 10	200 ± 10
	Fellow	190 ± 10	190 ± 10	190 ± 10
Choroidal Thickness (SD-OCT) (µm)	**Latanoprost**	0.67 ± 0.03	0.65 ± 0.05	0.65 ± 0.06
	Fellow	0.66 ± 0.06	0.61 ± 0.08	0.58 ± 0.07
Choroidal Vessel Area (μm^2)	**Latanoprost**	326.2 ± 50.3	470.8 ± 43.8	500.8 ± 42.4
	Fellow	327.0 ± 46.4	370.0 ± 34.6	391.0 ± 25.8

Latanoprost treatment effects on refractive errors and axial lengths:

Key mean SER and AL data for both eyes are summarized in Table 4.1. SERs and AL were not affected by the latanoprost treatment. Neither the latanoprost-treated eyes nor their fellow eyes changed significantly over the study period, although the latter result is not surprising given that these young adult animals would have already completed their natural emmetropization and no experimental visual manipulations were used. Thus animals were approximately emmetropic at baseline (+0.11 ± 0.43 D/ 8.76 ± 0.03 mm, right eyes vs. -0.3 ± 0.47 D/ 8.77 ± 0.02 mm , left eyes), and remained so at the end of the latanoprost treatment period (+0.7 ± 0.36 D/ 8.86 ± 0.03 mm, treated eyes, vs. +0.23 ± 0.28 D/ 8.87 ± 0.02 mm , fellow eyes), and also at the end of the washout period (+0.34 ± 0.40 D/ 8.99 ± 0.05 mm, treated eyes, vs. -0.36 ± 0.47 D/ 8.92 ±0.03 mm, fellow eyes (Table 4.1 and Figure 4.3). There was also no significant difference between the SERs/ ALs of right and left eyes at any time point ($p>0.05$).

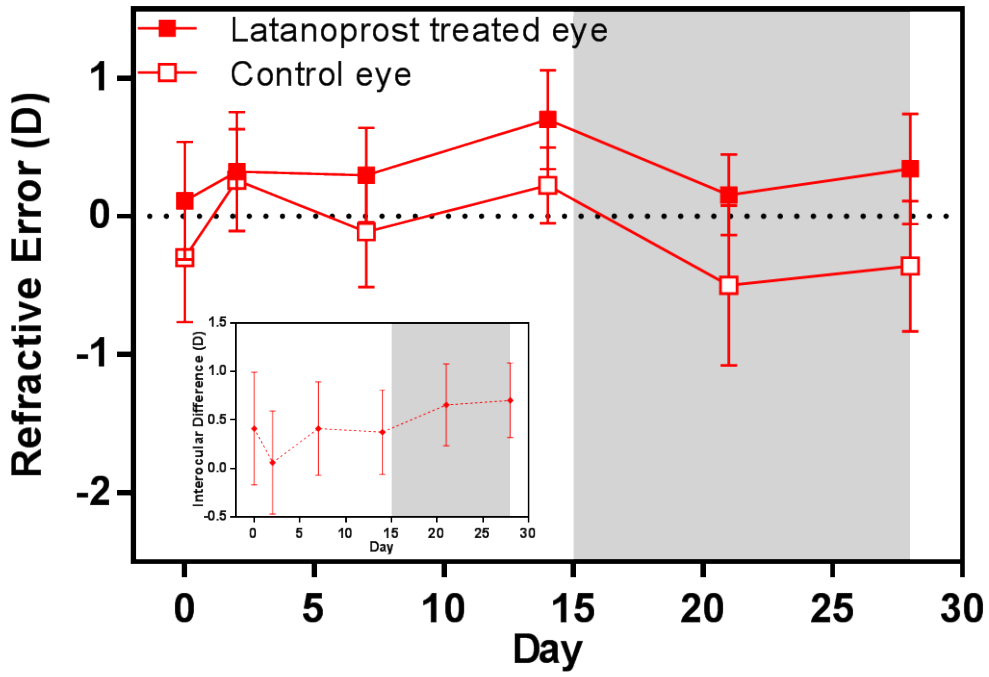

Figure 4.3: Spherical equivalent refractive error (SE) (mean ± SEM, diopters) in guinea pigs that were monocularly treated with topical latanoprost for 2 weeks. The shaded area indicates latanoprost 2-week washout period. **Inset:** Interocular differences in SE throughout latanoprost treatment and washout periods.

4.3.2 Effects of latanoprost on the choroidal thickness and vessel area

Choroidal thickness (ChT) was measured using two different techniques: high-frequency A-scan ultrasonography (on-axis only), and SD-OCT imaging. Both approaches failed to detect any significant effect of latanoprost on choroidal thickness. Key mean ChT data obtained with both techniques are summarized in Table 4.1. On-axis choroidal thicknesses, as measured by ultrasonography, were 180 ± 10 and 190 ± 10 µm for latanoprost-treated and fellow eyes respectively at baseline and not significantly different from each other ($p>0.05$); choroidal thickness also changed minimally thereafter, both over the latanoprost treatment period (e.g., 190 ± 10 µm, treated eyes vs. 190 ± 10 µm, fellow eyes, after 2 weeks of latanoprost), and over the washout period (200 ± 10 µm, right eyes vs. 190 ± 10 µm, left eyes).

The SD-OCT data show comparable trends to those just described, although in absolute value, the SD-OCT-derived thicknesses are smaller. Thus baseline ChTs were 0.67 ± 0.03 and 0.61 ± 0.08 µm for right and left eyes respectively, compared to 0.65 ± 0.05 versus 0.65 ± 0.06 µm after 2 weeks of latanoprost treatment, and 0.66 ± 0.06 versus 0.58 ± 0.07 µm at the end of the 2 weeks washout period (Figure 4.4 top).

Although no treatment-related changes in choroidal thickness were observed, choroidal vessels appeared to undergo sustained dilatation under the influence of latanoprost (Figures 4.4 bottom & Figure 4.5). Thus while there was no significant difference in choroidal vessel area between treated and fellow eyes at baseline (326.2 ± 50.3 vs. 327.0 ± 46.4 μm^2 for right and left eyes respectively ($p>0.05$), by the end of the latanoprost treatment period, the choroidal vessels of treated right eyes had increased in area to 470.8 ± 43.8 μm^2 compared to 370.0 ± 34.6 μm^2 for the fellow eyes ($p=0.04$). The increase in vessel area for fellow eyes was both much smaller and not statistically significant. This treatment effect was also enduring, being still evident at the end of the two-week washout period, i.e., 500.8 ± 42.4 μm^2 versus 391.0 ± 25.8 μm^2 for treated vs. fellow eyes ($p= 0.01$) (Figure 4.4 bottom & Table 4.1; also see Figure 4.5).

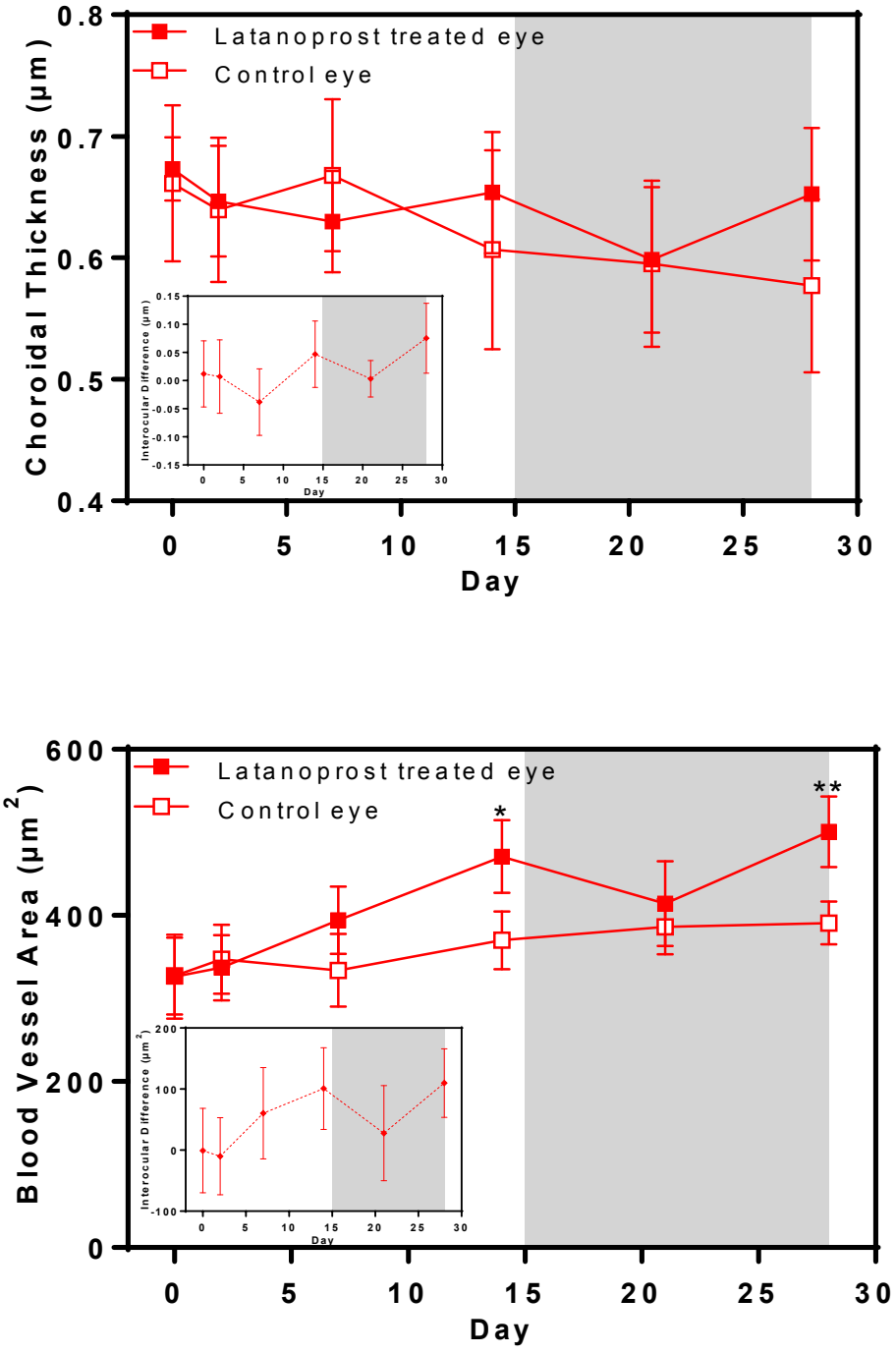

Figure 4.4: Choroidal thickness (ChT, Top) and choroidal vessel area, Bottom) (mean ± SEM), for latanoprost-treated and fellow eyes, derived from captured SD-OCT images and plotted against time. Latanoprost treatment period of 2 weeks followed by a 2-week post-treatment washout period (shaded area). Insets show similarly plotted interocular differences. * p< 0.05, ** p<0.01.

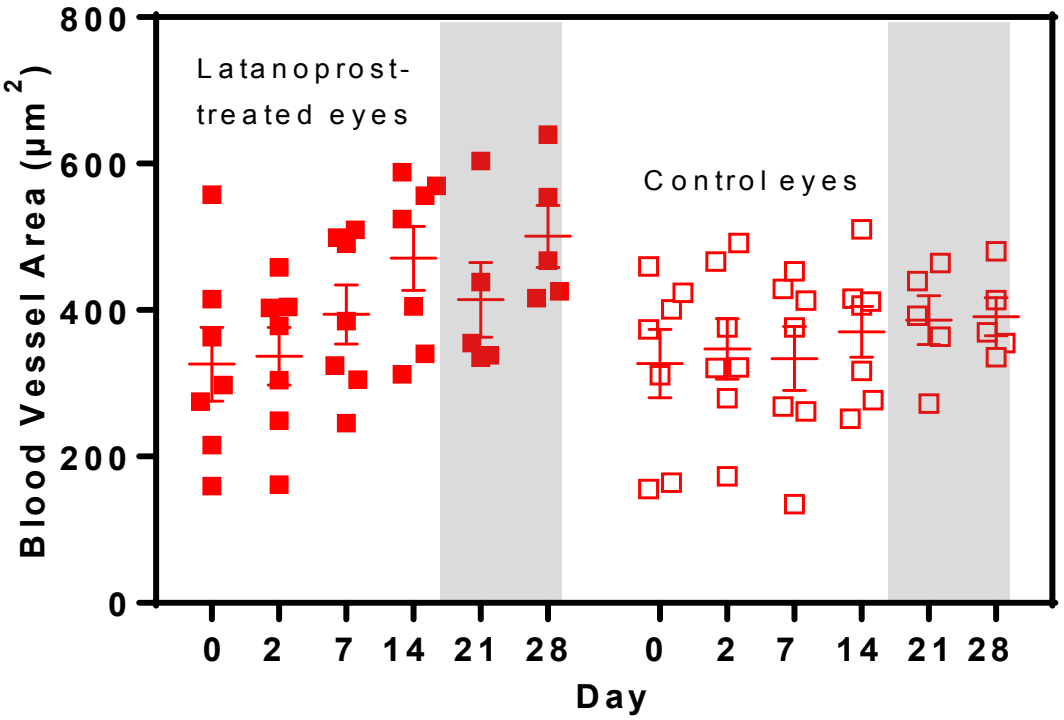

Figure 4.5: Choroidal vessel areas (mean ± SEM, µm^2), for individual guinea pigs, measured from SD-OCT images from their latanoprost-treated and fellow (control) eyes, plotted against time over the 2-week treatment and washout periods; shaded area demarcates the washout period.

4.4 Discussion

In chapter 3, we examined the efficacy of topical latanoprost, as a representative prostaglandin analog, for controlling myopia progression in a form-deprived guinea pig model of myopia. We found that topically applied latanoprost was effective in both lowering IOP and slowing myopia progression in this model. In the study described here, we confirmed the ocular hypotensive action of latanoprost in otherwise untreated young adult guinea pigs and also report latanoprost-induced changes in the choroidal vasculature, independent of choroidal thickness, the lack of effect on the latter also consistent with the lack of effect on refractive error.

The choroid, which represents a major component of the uvea, plays an important role in the aqueous humor drainage, via the so-called uveoscleral pathway. Latanoprost is known to increase the uveoscleral outflow in both normal and ocular hypertensive patients (Dinslage et al., 2000; Toris et al., 2001). Interestingly, an increase in choroidal thickness in glaucomatous eyes has also been reported with a close relative of latanoprost, specifically bimatoprost, (Akyol et al., 2017), although in contrast, no significant change in choroidal thickness was found with latanoprost used to treat newly diagnosed glaucoma and ocular hypertensive patients (Sahinoglu-Keskek 2018). In the

current study involving young healthy guinea pigs, topical latanoprost also did not increase choroidal thickness. It is possible that subtle differences in the actions of these two drugs underlies their different effects on choroidal thickness, since bimatoprost is known to lower IOP in humans by increasing both conventional (Bimatoprost activities receptors in trabecular meshwork) and uveoscleral aqueous humor outflow (Daniel Stamer et al., 2010). Furthermore, the decrease of choroidal extracellular matrix after latanoprost treatment may have cancelled the increase in choroidal blood flow and resulted in no change in choroidal thickness (Sahinoglu-Keskek 2018).

The effect of latanoprost on vascular beds appears to be site-specific, with reports of both vasodilation and vasoconstriction, depending on the site of action (USKI et al., 1984; USKI and ANDERSSON, 1984; Wendling and Harakal, 1991). In relation to the eye, there has been debate over whether latanoprost causes vasoconstriction in the posterior pole of the eye, potentially exacerbating glaucoma, or increases blood flow, which would be beneficial for eyes with glaucoma (Stjernschantz, 1999). Its action also appears to be both concentration-dependent (ASTIN, 1998; Astin and Stjernschantz, 1997), and variable across animal species (Kimura et al., 1992; MAIGAARD et al., 1986; SCHERER et al., 1986; YOUSUFZAI et al., 1996).

In the current study, we observed apparent enlargement of the choroidal vessels with latanoprost. Increased choroidal perfusion has been reported in latanoprost-treated patients, up to 56% in one study (Vetrugno et al., 1998), and others have argued that latanoprost enhances choroidal blood flow regulation (Boltz et al., 2011). However, it is alternatively possible that the improvement in choroidal blood flow regulation is a secondary effect of the latanoprost-induced decrease in IOP (Polska et al., 2007). We did not measure choroidal blood flow in the current study, to either accept or rule ut this explanation for the apparent increases in vessel areas. However, latanoprost-induced increase in MMP1 within the choroid (Wang et al., 2001), would logically lead to a reduction in extracellular matrix, which may in of itself, allow vessels to enlarge. The contribution of such choroidal vessel changes to the observed inhibitory effect of latanoprost on myopia progression, as reported in our previous study (El-nimri and Wildsoet, 2018), requires further investigation, but one could speculate that such changes may help to clear myopia-generating growth factors, released from the retina, assuming that choroidal blood flow is also increased.
Interestingly, the choroidal vessels remained enlarged at the end of the 2-week, latanoprost-washout period. It is not clear whether this reflects the time needed to recover from the extracellular matrix remodeling effect of latanoprost treatment, or whether some permanent structural change had been induced in these relatively young eyes. In humans, the maximum IOP reduction is reached within 8-12 h after a single topical dose of latanoprost and IOP remains low for at least 24 h (Lindén and Alm, 2007). It is unclear whether the extracellular matrix remodeling recovers after discontinuing latanoprost.

The results of this study should be interpreted with some limitations in mind. First, this study was not performed on myopic guinea pigs, so we can only speculate on the likely effects of latanoprost on the choroid of myopic eyes. Second, we did not use segmentation to analyze choroidal thickness using SD-OCT. Third, with the *in vivo* imaging methodology, we cannot distinguish between different types of blood vessels

(arteries and veins), or between blood vessels and lymphatic vessels. Well-developed lymphatic-like vessels have been well documented in the choroid of chicks, in which they have been linked to choroidal thickening and slowed eye growth (Wallman et al, 1995). Although there are no lymphatic vessels in the human and primates choroid, a lymphatic-like system, outside of the choroiocapillaries fenestrated vessels has been reported and might also be linked to choroidal thickness changes (Koina et al., 2015; Schroedl et al., 2014, 2008).

Chapter 5: Myopia-Insensitive Guinea Pig Strain and Effect of Latanoprost

5.1 Introduction

As noted in previous chapters, guinea pigs have become an important, now widely used animal model of myopia, reflecting the facts that they share similar features of primate eyes (e.g., fibrous-only sclera), are generally responsive to myopia-inducing visual manipulations, such as form-deprivation with diffusers (Howlett and McFadden, 2006; Lu et al., 2006) and imposed hyperopic defocus with negative lenses (Howlett and McFadden, 2009; Jiang et al., 2014), but are much easier to house and breed than primates. Their eyes are also significantly larger than mice, another commonly used model, whose eyes have a much larger depth-of-focus, rendering them less sensitive to imposed optical defocus, one of the commonly used strategies for inducing myopia. The visual acuity of guinea pigs is about 1.0 cycle per degree, also significantly better than that of mice (Ostrin L, Mok-Yee J, Wildsoet C, 2011). Finally, guinea pigs are born with their eyes open and well-developed vision (precocial) (Edwards et al., 1974), unlike tree shrews and monkeys. These various features have also contributed to their increasing popularity as a model in myopia studies.

Inter-animal variability and strain-dependent differences in ocular dimensions and responsiveness to visual manipulations are well documented in myopia research involving chicks (Chen et al., 2011; Schmid and Wildsoet, 1996; Troilo et al., 1995). More recently, our group reported on related strain-dependent differences in guinea pigs. Specifically, the Elm Hill (EH) pigmented guinea pig strain used in this study was found to be novel in three ways. Compared to another pigmented strain obtained from New Zealand, which was used in studies reported in Chapters 2 and 3, the EH animals 1) remained more hyperopic at the end of the normal emmetropization phase, 2) proved to be unresponsive to myopia-inducing negative lenses and diffusers, and 3) had thicker choroids (Jiang, L., Garcia M. et al., 2019). Although this strain has been partly characterized by our research group, this chapter will describe further important ocular features of this strain, including diurnal rhythms in intraocular pressure, and scleral and lamina cribrosa ultrastructures. In addition, in the study described here, we examined the effect of latanoprost on normal eye growth in this strain. As appropriate, we draw comparisons between findings for this EH strain reported here and those described previously for the NZ strain (Chapters 2 and 3).

5.2 Methods

5.2.1 Animals and treatments

A strain of pigmented guinea pigs, obtained from Elm Hill (EH) labs (Chelmsford, MA), was used in this study. Study animals were bred on-site and housed in a temperature-controlled room with a light/dark cycle of 12L/12D (on at 9.30 am, off at 9.30 pm). Pups were weaned at 5 days of age and housed as single-sex groups in transparent plastic wire-top cages, with free access to water and vitamin C-supplemented food, with additional fresh fruit and vegetables given five times a week as diet enrichment. All animal care and treatments in this study conform to the ARVO Statement for the Use of Animals in Ophthalmic and Vision Research. Experimental protocols are approved by the Animal Care and Use Committee of the University of California, Berkeley.

A total of 10 animals were used to track intraocular pressures, refractive errors, and optical axial lengths during normal ocular development in this strain over 10 weeks.

5.2.2 Measurements: Longitudinal intraocular pressure, refractive error, and axial ocular dimensional measurements

Intraocular pressures (IOP), refractive errors (RE) and optical axial lengths (OAL) were measured for both eyes of each animal. Measurements were made at weekly intervals over the first month and every other week thereafter. Because of well-documented diurnal rhythms in both IOP and eye elongation (Nickla et al., 1998), measurements were always taken around the same time each day, early in the morning, after lights-on.

All IOP measurements were conducted on awake animals and prior to any other procedure requiring anaesthesia, to avoid possible confounding effects of the latter. An iCare rebound tonometer (Tonolab, Helsinki, Finland) was used along with the setting for rat eyes, for which this instrument has been calibrated and which are similar in size to those of guinea pigs. This instrument provides confidence interval information based on successive readings; only data with a confidence interval of 5% or less was used. Three measurements were taken on each eye and the average used in data analyses.

Refractive errors were measured using streak retinoscopy on awake animals, 30 minutes after instillation of 1% cyclopentolate hydrochloride (Bausch & Lomb, Rochester, NY) for cycloplegia. Spherical equivalent refractive errors (REs, average of results for the two principal meridians) were derived for use in data analysis.

Ocular axial dimensions were measured with a custom-built, high-frequency A-scan ultrasonography system, with an estimated resolution of ~10 μm Nickla et al., 1998; Wildsoet and Wallman, 1995). For these measurements, animals were first placed under gaseous anaesthesia (1.5-2.5% isoflurane in oxygen), with eyelid retractors inserted to hold their eyes open. For each measurement, at least 8 traces were captured per eye and analyzed off-line. Only optical axial lengths (OALs) are reported here, derived as the sum of anterior chamber depth, axial lens thickness and vitreous chamber depth.

5.2.3 Measurements: Diurnal intraocular pressure rhythms

To characterize diurnal rhythms in IOP, five measurements were made at ~6 h intervals over 24 h, including time points just after lights-on and just before lights-off. The mid-night measurements during the lights-off hours were taken under photographic dark light conditions to minimize the possible effect of brief exposures to light on circadian rhythms. Three measurements were taken on each eye at each interval and the average used in data analysis. Diurnal IOP rhythms were recorded at monthly intervals.

5.2.4 Measurements: SD-OCT imaging of optic nerve head

A high-resolution spectral-domain optical coherence tomography system (SD-OCT, Bioptigen, USA) was used to image the optic nerve head (ONH) once per month for a total of 10 weeks. Both eyes of each animal were imaged. Guinea pigs were first anaesthetized with an intramuscular injection of ketamine and xylazine (27 mg/kg, 0.6 mg/kg, respectively), then placed on a custom-made stage with x – y – z adjustments to facilitate alignment of the optical axis of the eye being imaged with that of the instrument. A high-resolution OCT scan was generated from 500 B-scans by 400 A-scans, with a 12 by 12 mm field size, with two to three such scans, centred on the ONH, captured from each eye at each time point.

A cross-sectional 200×200 pixel image containing the ONH at its maximum horizontal dimension was selected to assess ONH diameter, using the termination in Bruch's membrane to define its boundary. Relevant points in the image were manually selected and diameter measured using a custom MATLAB (MathWorks Inc., Natick, MA) program. Values were corrected for differences in magnification related to the eye's length.

5.2.5 Scanning electron microscopy imaging of lamina cribrosa

At the end of the study, representative animals were sacrificed, their eyes enucleated and ONHs excised from the posterior segments to include a 4 mm ring of surrounding sclera for scanning electron microscopy (SEM). ONH samples were first soaked in 0.2M NaOH for 30 h, to remove cellular components, leaving only collagenous structures. ONHs/lamina cribrosa (LC) samples were then fixed in 4% glutaraldehyde in 0.1M sodium cacodylate, stained with osmium tetroxide, dried through an ethanol series, and finally subjected to critical point drying before imaging. LC samples were imaged using a Hitachi TM-1000 scanning electron microscope**.** Images were captured at 600X magnification.

5.2.6 Transmission electron microscopy to image scleral collagen fibers

For transmission electron microscopy (TEM), a 6 mm ring of sclera surrounding the ONH was excised from the posterior segments of enucleated eyes using disposable punchers. Tissue samples were first fixed in 4% glutaraldehyde in 0.1M sodium cacodylate, stained with osmium tetroxide, dried through an acetone series, infiltrated with resin and finally embedded in molds. Three scleral samples per eye embedded and

Before sectioning the sample blocks, they were trimmed by hand with a razorblade to create a face in the shape of a right trapezoid. A glass knife on a Reichert-Jung Ultracut E microtome was then used to cut 70 nm silver and gold-colored sections. Sections were then placed on coated copper meshed grids, stained with uranyl acetate and lead citrate and then imaged using an FEI Tecnai 12 transmission electron microscope. Images were captured from three different (superior) scleral samples from each eye at a magnification of 6800X.

5.2.7 Effects of topical latanoprost

Twenty animals were randomly allocated one of two monocular topical drug treatments, either latanoprost (0.005% ophthalmic solution, Akorn, Lake Forest, IL), or artificial tears (AT [same animals used to track normal eye growth above]), starting one week after the first baseline measurements and continuing for 9 weeks. Untreated contralateral eyes served as controls in both cases.

IOPs, REs and OALs were measured for both eyes of each animal, before the initiation of treatments (baseline), with follow-up measurements made at weekly intervals over the first month and every other week thereafter. Diurnal IOP data and SD-OCT images of the ONH were collected, one week before the initiation of topical treatment and once per month thereafter. ONH and scleral samples were processed for SEM and TEM, respectively as described above. See sections 5.2.2 to 5.2.6 for additional details related to measurement protocols.

5.3 Results

5.3.1.1 Intraocular pressures, refractive errors, and optical axial lengths

The IOPs of the EH guinea pigs appeared to fluctuate over the 10-week study duration, with the highest values being recorded near the beginning of the study (age 21 days), and end of the study (Figure 5.1). Thus, for right eyes, the mean IOP was 18.27 ± 0.70 mmHg at the start of the study and 20.20 ±0.86 mmHg by the end of the study (week 10). The IOPs of left eyes were also comparable (18.80 ± 0.81 mmHg, baseline; 20.50 ±0.99 mmHg, week 10), and there was no significant difference between the IOPs recorded at beginning and end of the study, for either eye, or between the IOPs of right and left eyes

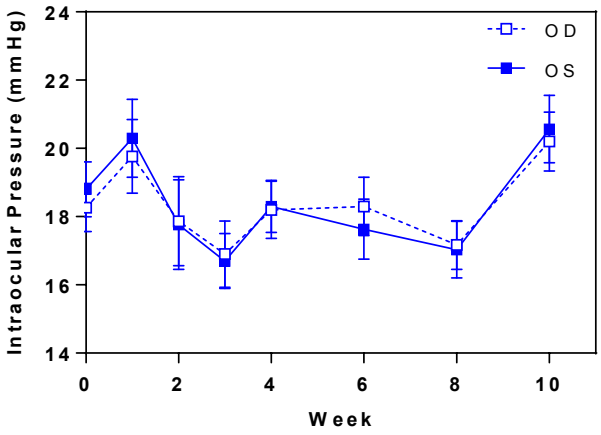

Figure 5.1: IOPs (mean ± SEM) for right (OD) and left (OS) eyes of young EH guinea pigs, recorded over a 10-week period corresponding to ages of 2 weeks (week 0) to 3 months (week 10).

The OALs of both right and left eyes of the guinea pigs showed a steady increase from over the same 10-week study period (Figure 5.2A, Table 5.1), reflecting normal development, with all animals also showing a steady increase in body weight over this period. For right eyes, OALs increased from a mean of 7.41 ± 0.026 mm to 8.45 ± 0.034 mm ($p < 0.0001$), with left eyes showing comparable OALs (7.39 ± 0.040 mm & 8.43 ± 0.04 mm; $p < 0.0001$). Changes in REs over the study period were consistent with OAL changes, being most hyperopic initially (Figure 5.2B & Table 5.1). Thus, for right eyes, the mean RE was +2.35 ± 0.50 D at age 2 weeks, decreasing to +0.73 ± 0.21 D by week 10 ($p=0.0002$), and for left eyes, equivalent values are +2.85 ± 0.52 D and +1.24 ± 0.16 D ($p= 0.0002$).

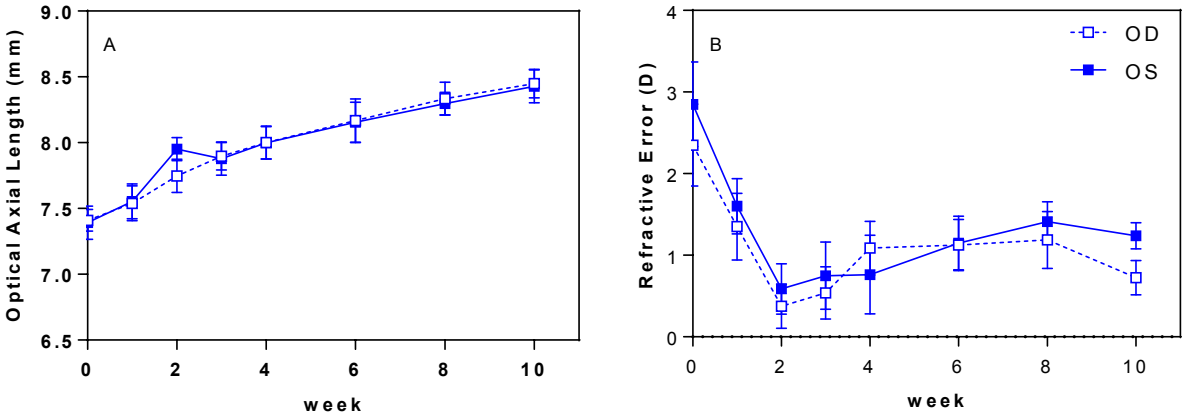

Figure 5.2: Means (± SEM) for (A) optical axial lengths and (B) refractive errors recorded from right (OD) and left (OS) eyes of young EH guinea pigs over a 10 week period, from 2 weeks of age (week 0) to 3 months (week 10) of age (n=10).

Table 5.1: Summary of mean IOP, RE, and OAL data (± SEM) recorded from right (OD) and left (OS) eyes of young EH animals and related summary statistics.

Parameter	Eye	Age		Statistics
		2 weeks (week 0)	3 months (week 10)	(p-value)*
IOP (mmHg)	OD	18.27 ± 0.70	20.20 ±0.86	0.43
	OS	18.80 ± 0.81	20.50 ±0.99	0.61
Refractive Error (RE, D)	OD	2.35 ± 0.50	0.73 ± 0.21	0.0002
	OS	2.85 ± 0.52	1.24 ± 0.16	0.0002
Optical Axial Length (OAL, mm)	OD	7.41 ± 0.026	8.45 ± 0.034	< 0.0001
	OS	7.39 ± 0.040	8.43 ± 0.04	< 0.0001

* P-values refers to differences between week 0 & week 10 results (two-tailed paired t-test).

5.3.1.2 Diurnal variations in IOP

Young EH guinea pigs exhibited diurnal variations in their IOP, with the patterns for right and left eyes being very similar (Figure 5.3). IOP consistently peaked in the morning, as reflected in the readings recorded just after lights on at 9:35 am. Left and right eyes also recorded similar rhythm amplitudes (the difference between the highest and lowest IOP recorded each day, regardless of time of day), with means estimated as 7.4 mmHg and 5.9 mmHg for left and right eyes (p= 0.054, two-tailed paired t-test). No statistically significant difference was found between either IOPs of right and left eyes at any time point or between diurnal variations in IOP recorded in week 0 (2 weeks old) and week 10 (3 months old) (repeated measures ANOVA).

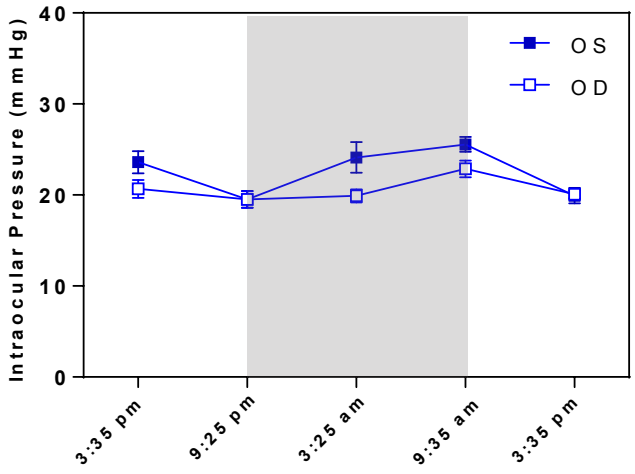

Figure 5.3: Mean IOPs (± SEM) recorded at 6-h intervals over 24 h in week 10, for right (OD) and left (OS) eyes of young EH guinea pigs (3 months old). Peak IOPs were recorded just after lights-on at 9:35 AM in all cases. Shaded area, when lights are off.

5.3.1.3 Optic disc dimensions, derived from SD-OCT images

The dimensions of the opening in Bruch's membrane to accommodate the exiting optic nerve fibers were used here as a surrogate for optic disc dimensions. The EH guinea pigs imaged all had approximately spherical optic discs and therefore only one parameter, the horizontal optic disc diameter (ODD), is reported. Although ODDs slightly increased with development in these young EH guinea pigs, none showed disc tilting. For the right eyes, the mean ODDs increased from 225.7± 15.6 µm at the start of the study (2 weeks old) to 264 ± 8.7 µm by the end of the study (3 months old). For the left eyes, the equivalent values are 226.5 ± 7.6 µm and 248.6 ± 8.7 µm (Figure 5.4). While there was also no significant difference between the ODDs of right and left eyes, the changes with development were significant only for right eyes (p= 0.008).

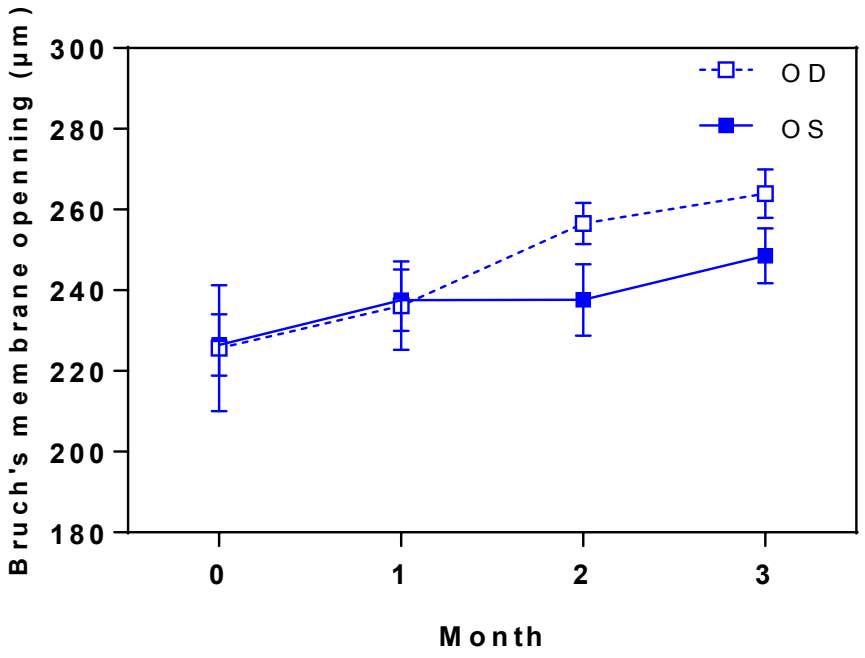

Figure 5.4: ODDs (mean ± SEM) for right (OD) and left (OS) eyes of young EH guinea pigs, recorded over a 10-week period corresponding to ages of 2 weeks to 3 months.

To examine how closely the dimensions of optic nerve heads were tied to eye size, the ODDs of left and right eyes were plotted against AL (Figure 5.5), and correlation analyses undertaken. Although the correlation between ODDs and OALs reached statistical significance for only right eyes, positive trends were observed in both cases. (OD: r^2= 0.95, p= 0.02, slope= 40.6 ± 6.4; OS: r^2= 0.85, p= 0.08, slope= 17.6 ± 5.3; Fig. 5.5).

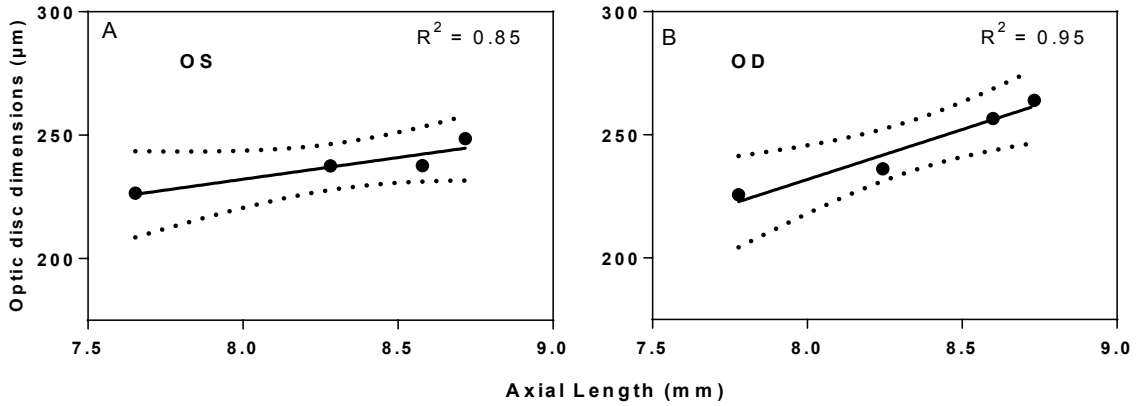

Figure 5.5: Optic disc dimensions for left (OS) and right (OD) eyes (A and B) plotted against the axial length of the same eyes recorded over the study period, from its beginning (age 2 weeks old) to its end (age 3 months old).

5.3.1.4 Lamina cribrosa and scleral ultrastructure

SEM images of the lamina cribrosa (LC) revealed a multilayered, mesh-like network of collagen fibers that inserts into the scleral canal (Figure 5.6A, B). Qualitative examination of the images also revealed a range of pore sizes, but apparently little differences in the patterns between right and left eyes. Subsequent quantitative analysis of the images confirmed this interpretation; the mean laminar pore area (± SEM) was 3.59 ± 0.52 µm² for right eyes and 3.66 ± 0.76 µm² for left eyes and there was no significant difference between results for left and right eyes.

The sclera surrounding the LC was also imaged by TEM in these animals. Morphologically, scleral collagen fibers were found to approximately uniformly spaced, with a predominance of medium-sized fibers, although smaller and larger fibers were also evident in samples from left and right eyes (Figure 5.6C, D). The mean scleral collagen fiber cross-sectional area (± SEM) was 0.01 ± 0.003 µm² for right eyes and 0.009 ± 0.0005 µm² for left eyes and there was no significant difference between values for left and right eyes.

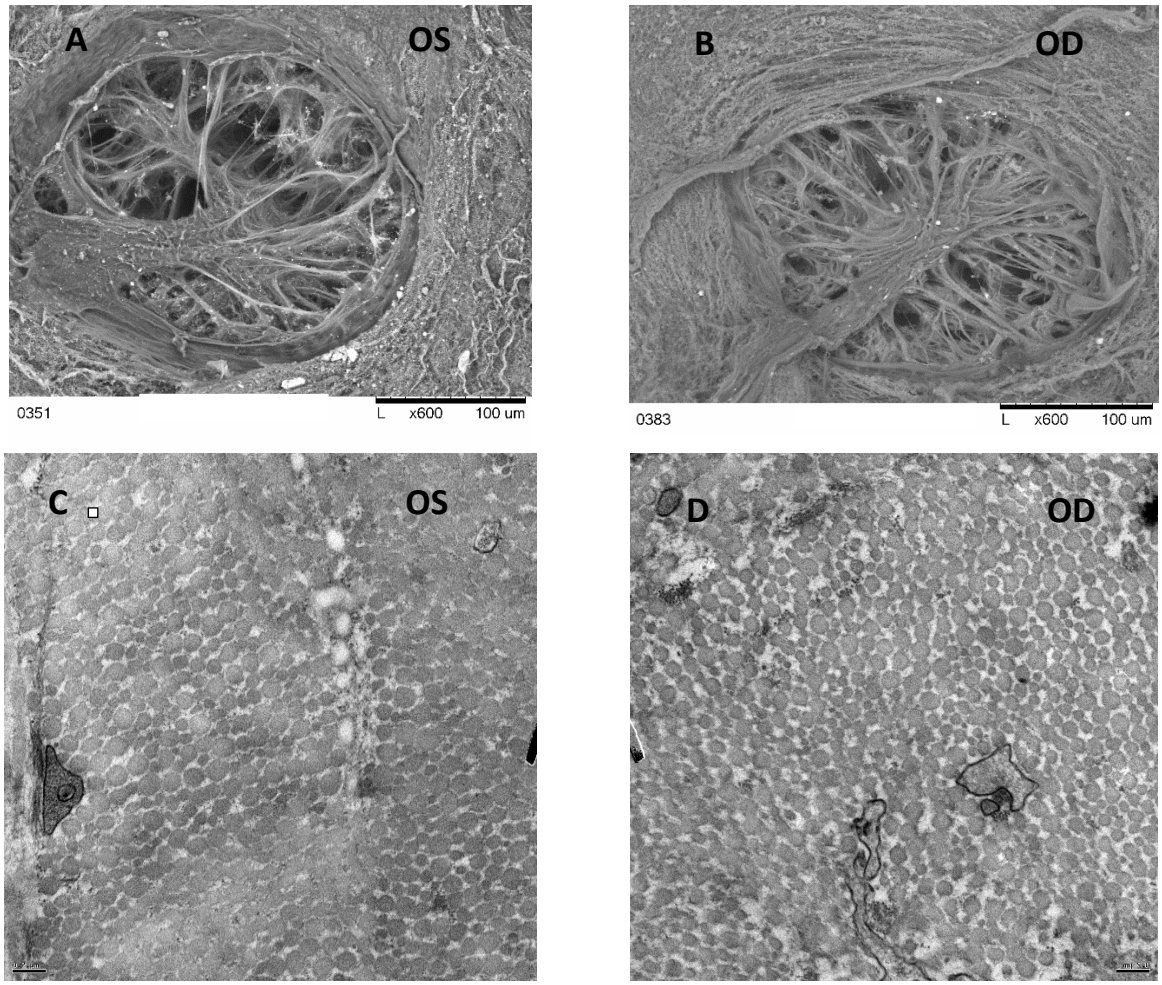

Figure 5.6: Representative lamina cribrosa images (SEM, 600X) (top panel; A, B), and scleral images (TEM, 6800X) (bottom panel; C, D), from right (OD) and left (OS) eyes of EH guinea pigs.

5.3.2.1 Effect of latanoprost on intraocular pressure, refractive error and axial length

Daily topical latanoprost (Lat) significantly reduced IOP and the IOP lowering effect progressively increased over time in these EH animals (Figure 5.7; Table 5.2). This effect is reflected in the significant increase in interocular differences in IOP for the Lat group, from 0.4 ± 0.31 mmHg at baseline to -2.83 ± 0.59 mmHg by week 10 ($p= 0.0001$, repeated measures ANOVA). In contrast, the equivalent values for the control artificial tear (AT) group were very similar to each other and there was no significant change with time, i.e., 0.53 ± 0.74 and 0.3 ± 0.25 mmHg ($p= 0.99$).

Despite the decrease in IOP achieved with the Lat treatment, it had no significant effect on either the REs or OALs of these otherwise untreated animals (Figs. 5.8A, 5.8B; Table 5.2), as reflected in the close correspondence for both Lat and AT groups in not only baseline interocular differences, but also end-of-treatment interocular differences in both REs and OALs (0.15 ± 0.30 vs. 0.9 ± 0.34 D, -0.27 ± 0.049 vs. -0.016 ± 0.017 mm

(Lat); 0.51 ± 0.32 vs. 0.5 ± 0.20 D & -0.018 ± 0.029 vs. -0.017 ± 0.02 mm (AT) (Table 5.2). The OAL changes are consistent with the RE data, with none of the groups showing significantly altered patterns of elongation in their treated eyes relative to their fellows.

To further examine the Lat treatment effects for these EH animals and the potential influence of reduced IOP, the ratio of week-10 OALs of left to right eyes (normalized to baseline), were plotted against the change in IOP over the treatment period (Fig. 5.9), and regression analyses were undertaken. There was no significant correlation between these parameters (r^2= 0.04, p=0.40).

Table 5.2: Summary of mean interocular differences in IOP, RE, and OAL (± SEM) and summary statistics for the Elm Hill (EH) animals treated with monocular latanoprost (Lat) or artificial tears (AT).

Parameter	Treatment	Time of measurement		Statistics
		Baseline (Week 0)	Week 10	(p-value)*
IOP (mmHg)	Lat only	0.40 ±0.31	-2.83 ±0.59	0.0001
	AT only	+0.53 ±0.74	0.30 ±0.25	0.9999
Refractive Error (D)	Lat only	0.15 ±0.30	0.90 ±0.34	0.0855
	AT only	0.51 ±0.32	0.50 ±0.20	0.9999
Optical Axial Length (mm)	Lat only	-0.27 ±0.049	-0.016 ±0.017	0.9999
	AT only	-0.018 ±0.029	-0.017 ±0.02	0.9999

* P-values refers to differences between baseline & week 10 results (Paired t-test).

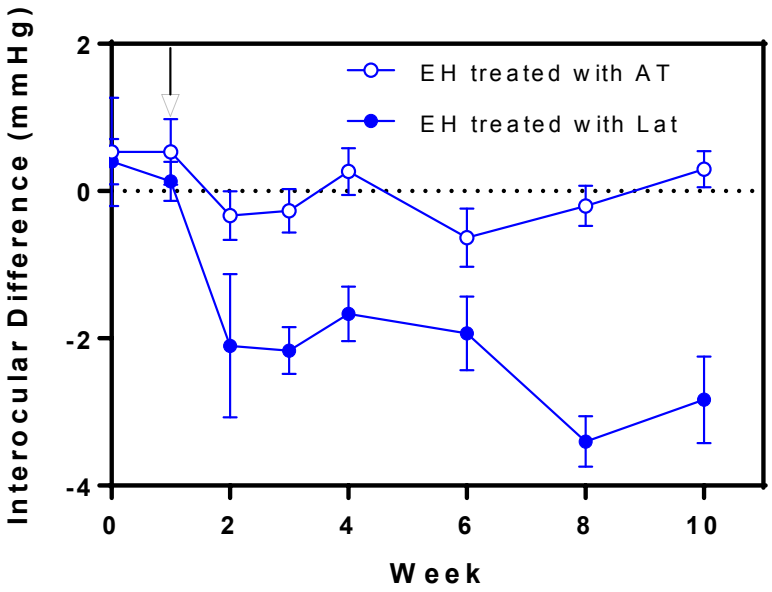

Figure 5.7: Interocular differences in IOP (mean ± SEM, mmHg) in EH guinea pigs treated in their left eye with latanoprost (Lat) or artificial tears (AT) (n= 10 per group), from week 1 of the 10-week treatment period. The arrow indicates the start of the treatment (Lat or AT).

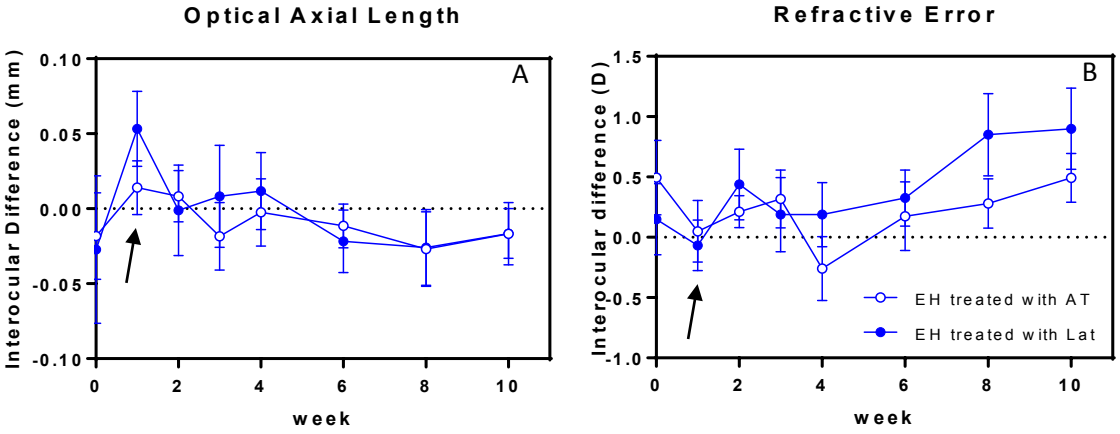

Figure 5.8: (A) Mean (± SEM) interocular differences in optical axial lengths (mm) and (B) refractive errors (D) in EH guinea pigs treated in their left eye with latanoprost (Lat) or artificial tears (AT)(n=10 per group), from the end of week 1. The arrows indicate the start of the treatment period (Lat or AT).

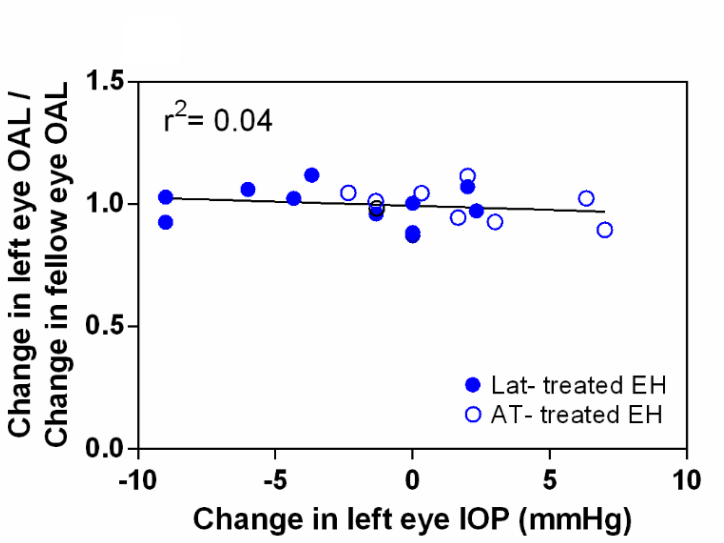

Figure 5.9: Ratio of changes over the 10-week treatment period in optical axial lengths (OAL) of left to right eyes plotted against changes in IOPs of left eyes, for both latanoprost (Lat) and artificial tears (AT) treated groups.

5.3.2.2 Effect of latanoprost on diurnal intraocular pressures

IOP data collected at week 10 over 24 h for both Lat-treated eyes and their fellow, as well as comparable data for AT-treated animals, are shown in Figures 5.10 A and B.

For these EH animals, there were statistically significant differences between the IOPs of the treated eyes of the Lat and AT groups at both 3:35 am ($p= 0.01$) and 9:35 am ($p= 0.03$). However, the IOPs recorded from the fellow eyes of the Lat and AT groups were not significantly different at any time point. Peak IOPs were consistently recorded in the morning, at 9:35 am for all eyes, and for both groups, treated eyes recorded similar rhythm amplitudes to their fellow eyes (Lat: 5.3 vs. 5.73 mmHg, $p= 0.95$; AT: 7.4 vs. 5.9 mmHg, $p= 0.054$, two-tailed paired t-test)(Table 5.3 & Figure 5.10).

To further analyze the effect of the Lat treatment on diurnal IOP rhythms, interocular difference patterns for Lat- and AT-treated groups were compared statistically and graphically (Figure 5.10). The largest interocular differences occurred for the Lat-treated guinea pigs at 9:35 am (-2.8 ± 0.72; $p= 0.006$). In contrast, interocular differences over the 24 h monitoring period never reached statistical significance for the AT-treated guinea pigs (Figure 5.11).

Table 5.3: Mean IOPs (± SEM) measured at 6-h intervals over 24 h at week 10, for fellow control eyes and left eyes treated with latanoprost (Lat) or artificial tears (AT). IOPs were significantly different at 3:35 pm versus 9:25 pm for Lat-treated eyes (p= 0.03) and for AT treated eyes at 3:35 pm (second reading) versus 9:25 pm (p= 0.007) and between IOPs at the beginning and end of cycle (3:35 pm, p=0.017).

Eye	Treatment	3:35 pm	9:25 pm	3:25 am	9:35 am	3:35 pm
Treated	Artificial tears	23.6±1.2	19.5 ± 0.9	24.1 ± 1.7	25.6 ± 0.8	20.0 ± 0.8
Fellow	Artificial tears	20.7±0.98	19.5 ± 0.90	19.9 ± 0.71	22.9 ± 0.90	20.1 ± 0.44
Treated	Latanoprost	20.4±1.0	17.0 ± 0.6	19.8 ± 0.8	21.8 ± 0.8	20.2 ± 0.5
Fellow	Latanoprost	20.2±1.1	17.9 ± 0.78	22.5 ± 1.7	22.8 ± 0.56	17.9 ± 0.6

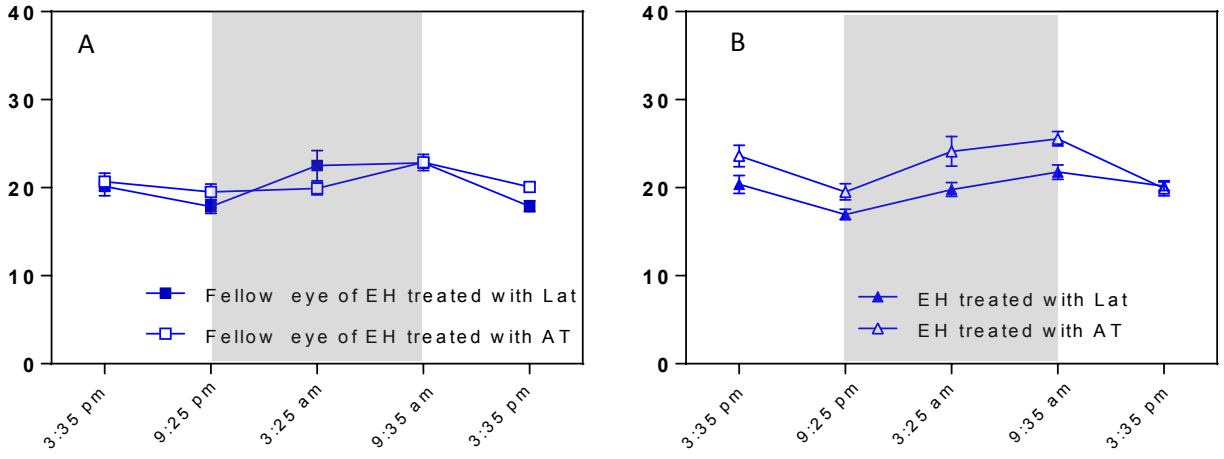

Figure 5.10: Mean IOPs (± SEM) measured at 6-h intervals over 24 h, for fellow control eyes (A) and left eyes treated with latanoprost (Lat) or artificial tears (AT)(B) at week 10. Peak IOPs were recorded just after lights-on at 9:35 AM in all cases. Shaded area, when lights are off.

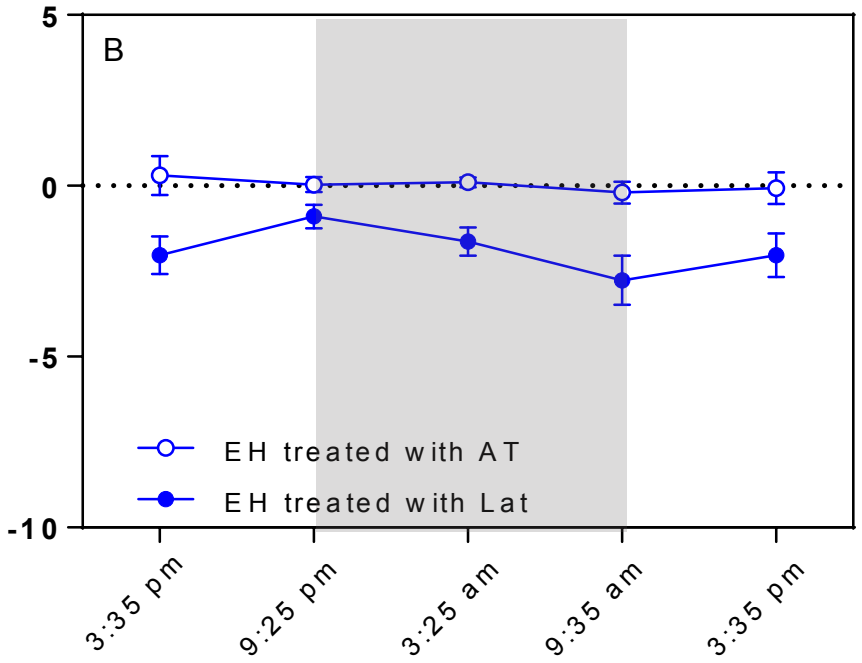

Figure 5.11: Mean interocular differences (treated-control; ± SEM), in IOPs recorded at the end of the 10-week treatment period from EH guinea pigs treated in their left eye with latanoprost (Lat) or artificial tears (AT)(n=10 each group).

5.3.2.3 Effect of latanoprost on optic nerve head size

The dimensions of the Bruch's membrane opening were used here as a surrogate for optic disc dimensions (ODDs). ODDs of all eyes appeared to slightly increase over the study period (Figure 5.12), and although the ODDs of the Lat-treated and fellow eyes tended to be smaller at the end of the treatment period than those of the AT group, no significant differences were found between the ODDs of Lat and AT groups at any time point. For the Lat-treated eyes and their fellows, the mean ODDs were 221.5 ± 7.7 and 234.6 ± 7.7 µm respectively at the start of treatment (week 1; 2 weeks old) and 251 ± 8.8 µm and 258.3 ± 8.8 µm by the end of the study (week 10; 3 months old). For the AT-treated eyes and their fellows, the mean ODDs were 226.5 ± 7.6 and 225.7 ± 15.6 µm respectively at the start of treatment and 248.6 ± 8.7 µm and 264 ± 8.7 µm by the end of the study.

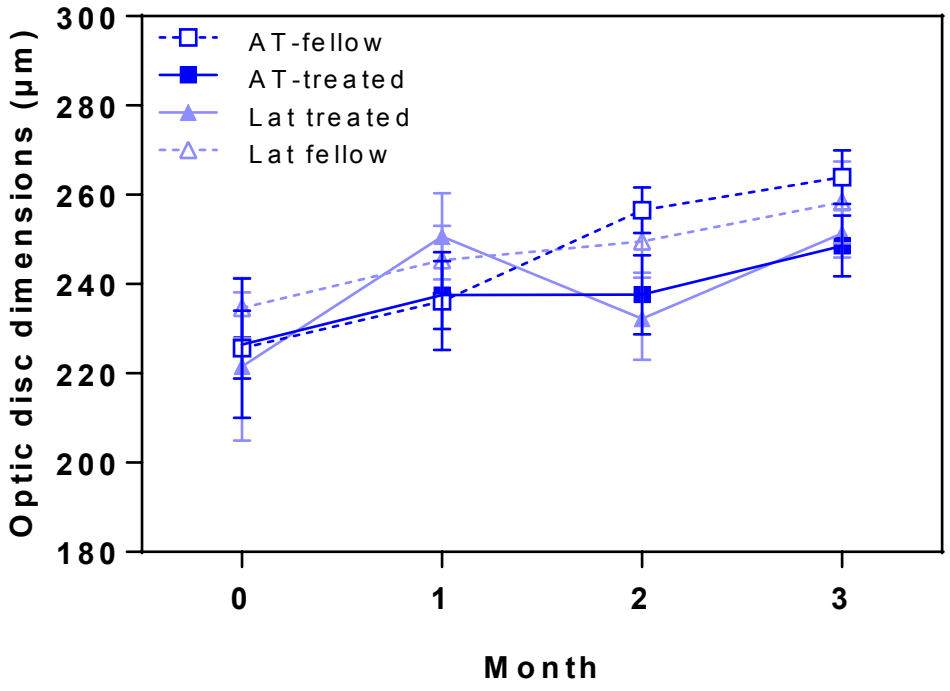

Figure 5.12: ODDs (mean ± SEM, mmHg) in EH guinea pigs (control) treated in their left eye with latanoprost (Lat) or artificial tears (AT) (n= 10 per group), from week 1 of the 10-week treatment period.

ODDs of Lat- and AT-treated eyes and their fellows are plotted against AL of the same eyes in Figure 5.13. For the fellow eyes of both treatment groups, a strong positive linear correlation between these parameters was observed (AT: r^2= 0.95, p= 0.02, slope= 40.6 ± 6.4; Lat: r^2= 0.96, p= 0.02, slope= 20.2 ± 3.0)(Fig. 5.13 B & D). However While similar trends between these parameters are evident in the data from Lat- and AT-treated eyes, they did not reach statistical significance (AT: r^2= 0.85, p= 0.08, slope= 17.6 ± 5.3; Lat: r^2= 0.52, p= 0.3, slope= 22.1 ± 14.9). (Figure 5.13 A & C).

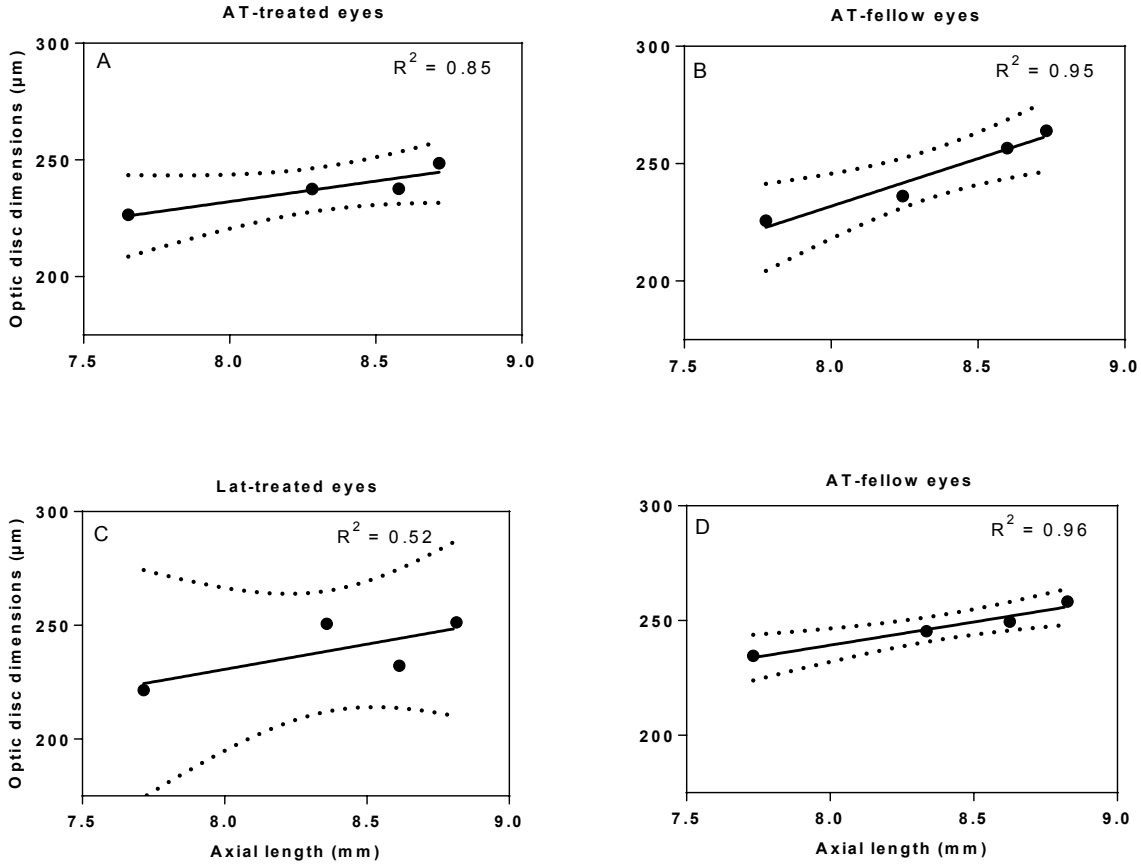

Figure 5.13: Optic disc dimensions of treated and fellow eyes of artificial tears (A and B) and latanoprost groups (C and D) plotted against the axial lengths of the same eyes.

5.3.2.4 Effect of latanoprost on lamina cribrosa and scleral ultrastructure

The effect of latanoprost (Lat) and the control artificial tears (AT) treatments on the microstructural organization of the LC and posterior sclera were evaluated by SEM and TEM imaging respectively.

Table 5.4: Mean (±SEM) laminar pore area (µm^2) in treated and fellow eyes of artificial tears and latanoprost groups. No significant difference was found between AT and Lat groups.

Eye	Treatment	Laminar pore area mean ± SEM (µm²)	Number of eyes
Treated	Artificial tears	3.66 ± 0.76	5
Fellow	Artificial tears	3.59 ± 0.52	5
Treated	Latanoprost	4.04 ± 0.54	5
Fellow	Latanoprost	3.53 ± 0.67	5

LC pore area was compared between the two EH treatment groups. No statistically significant difference in the mean laminar pores area (μm^2) was found between either AT-treated eyes and their fellows, or between Lat-treated eyes and their fellow (Table 5.4).

The laminar pores data were further categorized based on their area into small (<15 μm^2), medium (15-30 μm^2), and large (>30 μm^2), and the percentage of lamina cribrosa pores in each category was calculated for the treated and fellow eyes of both treatment groups. The smallest laminar pores area accounted for the highest percentage for all eyes (~99%) (Figure 5.14).

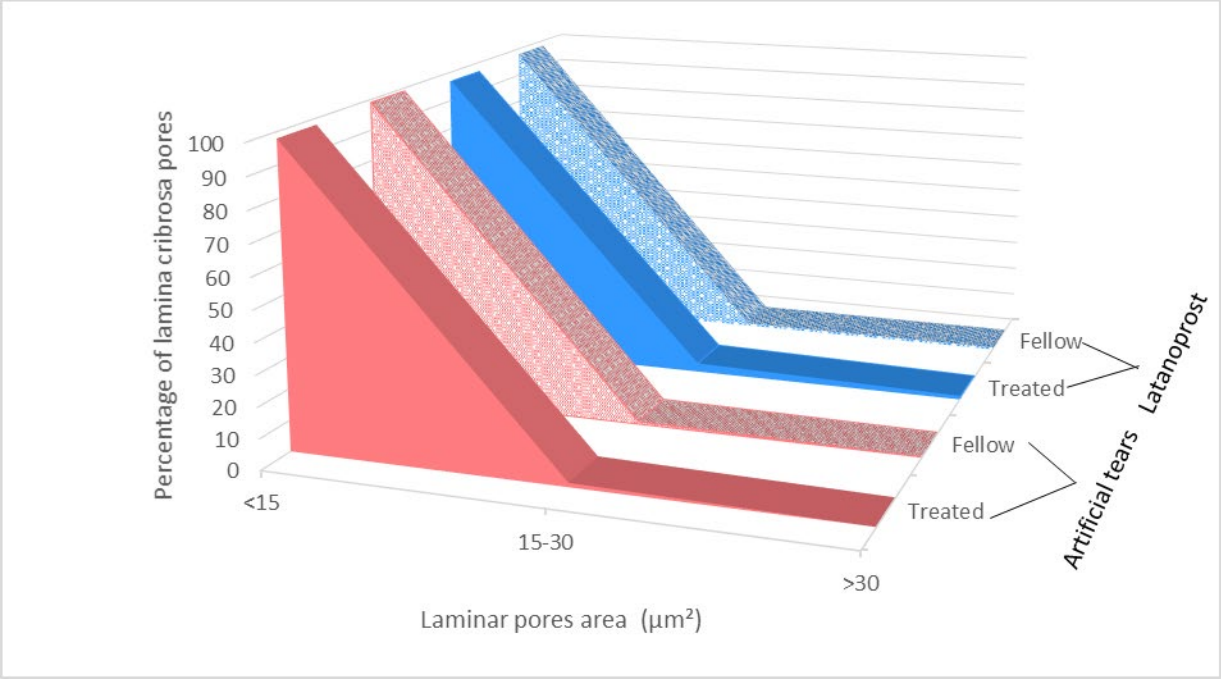

Figure 5.14: Percentage of laminar pores in each of three size categories (small, <15 μm^2; medium, 15-30 μm^2; large (>30 μm^2) for the treated and fellow eyes of artificial tear (AT) and latanoprost (Lat) treated groups. For all eyes, the smallest laminar pores accounted for most of them and there was no significant difference between AT and Lat groups or between the treated and fellow eyes of each group.

In relation to scleral ultrastructure, evenly spaced collagen fibers spanning a range of sizes (small, medium, and large) characterized the scleras of all eyes (Figure 5.15 A/B and 5.15 C/D). However, the scleras of Lat-treated eyes and their fellows seemed to have less spacing between collagen fibers, with less exposed extracellular matrix and slightly larger collagen scleral fibers overall compared to the scleras of AT-treated and fellow eyes although the latter differences were not statistically significant (Table 5.5).

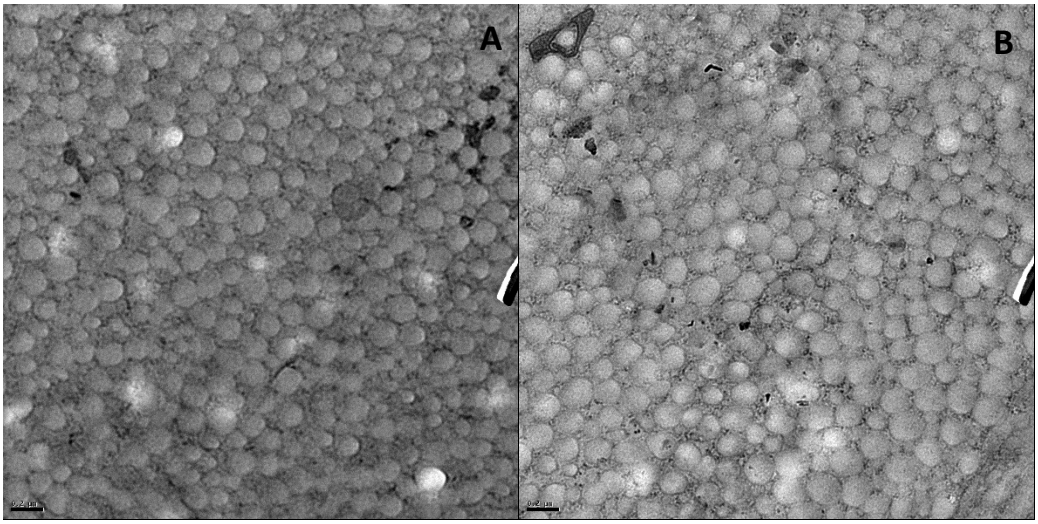

Latanoprost treated Fellow (untreated)

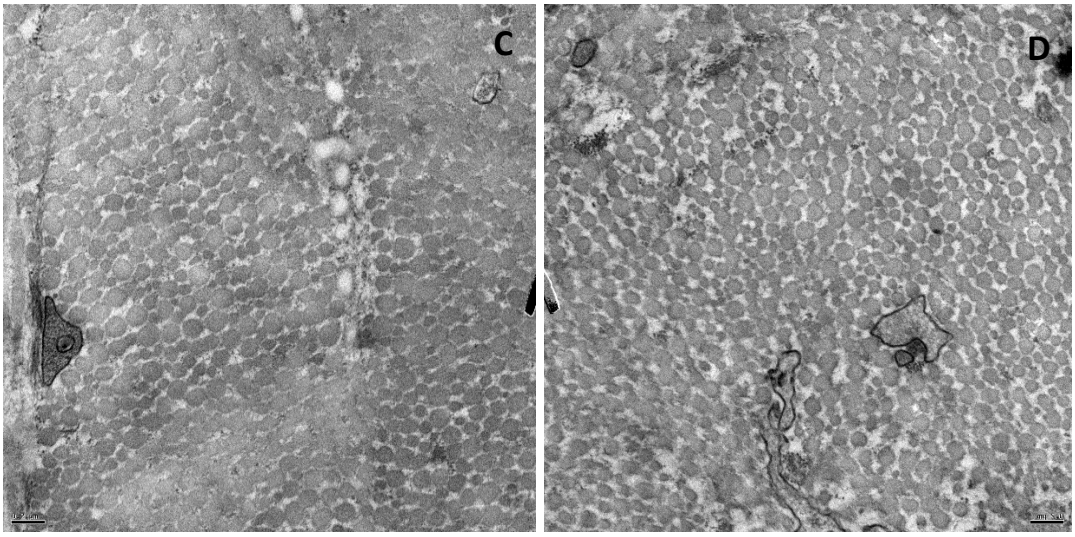

Artificial tears treated Fellow (untreated)

Figure 5.15: Representative transmission electron microscopy (TEM) images of scleras of A) a latanoprost treated eye, B) its fellow eye, C) an eye treated with artificial tears, and D) its fellow eye, showing collagen fiber organization in cross-section for EH animals; imaging at 6800X.

Table 5.5: Mean (±SEM) collagen fiber cross-sectional area (μm^2) in scleras of treated and fellow eyes of artificial tears- and latanoprost-treated EH animals.

Eye	Treatment	Scleral collagen fiber area (μm^2)	Number of eyes
Treated	Artificial tears	0.0085 ± 0.0005	3
Fellow	Artificial tears	0.012 ± 0.003	3
Treated	Latanoprost	0.014 ± 0.0004	3
Fellow	Latanoprost	0.011 ± 0.003	3

For all eyes (treated and fellow eyes of AT and Lat-treated groups), scleral collagen fibers were further categorized based on cross-sectional area into small (<6000 nm^2), medium (6000-12,000 nm^2), and large (>12,000 nm^2), and the percentage of fibers in each category calculated. Surprisingly, Lat-treated eyes had the highest percentage of the largest fibers and the lowest percentage of the smallest fibers (p=0.03), compared to their fellows and AT-treated eyes (Table 5.6 and Figure 5.16).

Table 5.6: Percentage of scleral collagen fibers categorized based on cross-sectional area into small (<6000 nm^2), medium (6000-12,000 nm^2), and large (>12,000 nm^2) for treated and fellow eyes of AT and Lat-treated groups. Statistics indicate significance of the difference between the percentage of small and large scleral fiber areas; only the difference for Lat-teated eyes was significant; differences for the other groups, including the percentages between small and medium scleral fiber areas/ medium and large scleral fiber areas were not significant.

Eye	% of <6000 nm^2	% of 6000-12,000	% of >12,000 nm^2	P-value (Small vs large)
AT-treated	38.4 ± 0.19	45.6 ± 3.0	15.9 ± 3.2	0.4
AT Fellow-	27.4 ± 9.4	33.4 ± 8.9	39.3 ± 18.3	0.96
Lat-treated	9.8 ± 2.8	30.6 ± 4.5	59.7 ± 1.7	0.03
Lat-Fellow	26.6 ± 12.1	34.4 ± 5.3	39.0 ± 17.3	0.92

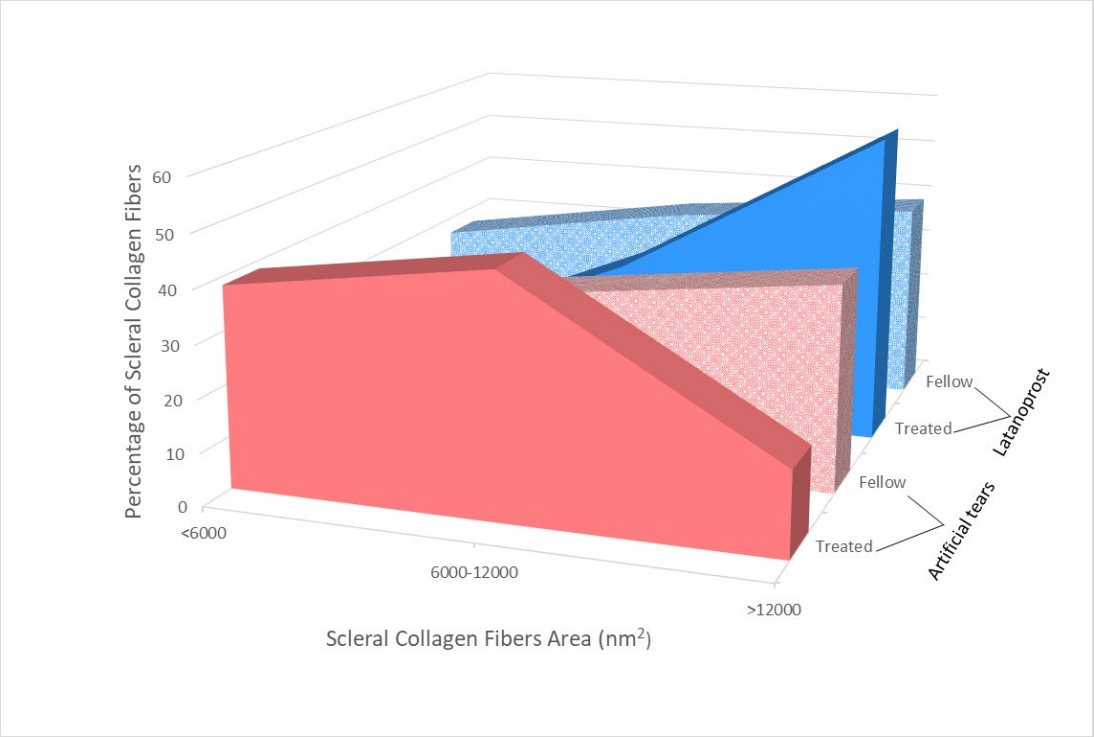

Figure 5.16: Percentage of each of three categories of scleral collagen fibers, based on cross-sectional areas (small, <6000 nm^2; medium, 6000-12,000 nm^2; large, >12,000 nm^2), shown for the treated and fellow eyes of the Artificial tears- and Latanoprost-treated EH groups.

We also examined the relationship between interocular differences in scleral collagen fiber area to eye elongation (Figure 5.17). Although there was a trend of negative correlation, no significant linear correlation was found between these parameters for the Lat group (r^2= 0.976, p= 0.099) or the AT group (r^2= 0.958, p= 0.13). However, this lack of statistical significance could be due to the smaller number of animals per group (n= 3 per group).

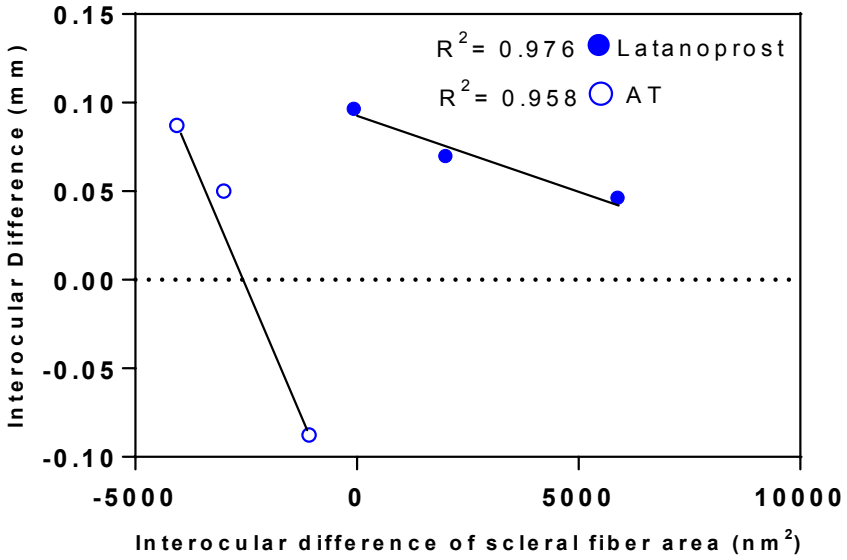

Figure 5.17: Interocular differences in mean scleral collagen fiber area (nm^2) for individual animals of artificial tear (AT) and latanoprost-treated EH groups, plotted against interocular differences in axial length for the same animals.

5.4 Discussion

5.4.1.1 Strain-dependent differences in guinea pigs

In this chapter, we characterized further important ocular features of the EH strain, including the diurnal rhythm in its intraocular pressure, and scleral and lamina cribrosa ultrastructure. We also made comparisons, as appropriate, regarding these ocular features between this EH strain and the NZ strain described in chapters 2 and 3.

Our group recently reported significant ocular differences between these EH and NZ guinea pig strains. The specific focus of the latter report was the difference in sensitivity to myopia-inducing stimuli and the role of the choroid, which appears to play an important role in normal and myopic ocular growth regulation. The current study focused on normal as opposed to “myopic” ocular growth in the EH strain, which was also profiled in terms of its diurnal IOP rhythm, and scleral and the lamina cribrosa ultrastructure. In addition, we examined the effect of the ocular hypotensive drug, latanoprost, on normal ocular growth in the EH strain. The data thus collected from the EH strain are compared with equivalent data from the NZ strain in the following discussion.

Table 5.7A below summarizes differences in IOP, RE, and OAL between the untreated right eyes of the EH strain and the fellow eyes of the AT group in the NZ strain (Chapter 3). LC pore and scleral collagen fiber dimensions, recorded from EM images of tissues samples collected at the end of the study are also compared.

Interestingly, the EH strain not only had naturally lower IOP compared to the NZ strain, but their LC pore area appeared to be significantly smaller than those of the NZ. The LC is thought to help maintain the pressure gradient between the interior of the eye and the surrounding tissues (Jonas et al., 1991). Given that the LC is typically thinner and structurally weaker than the surrounding sclera, it is more sensitive to IOP changes and tends to react to any increase in IOP through an anterior to posterior displacement, which causes the pores to deform (Morgan-Davies, 2004; Quigley et al., 2017). It is thus logical to assume that the lower IOP in the EH strain reduced LC displacement compared to that in the NZ strain and thus the deformation of its pores, which might contribute to the strain-related differences in LC pore areas.

The EH strain also recorded a larger mean peripapillary scleral collagen fiber area than the NZ strain. It is known that the scleral mechanical load is mainly derived from IOP-related strain and stress (Jia et al., 2016). Additionally, IOP-generated stress can lead to regional thinning, stretching and deformation of the LC and the peripapillary sclera (Yang et al., 2009). Others have argued that the biomechanical scleral response to increases in IOP is mainly centered on the ocular tissue immediately surrounding the ONH (Coudrillier et al., 2012). Thus as the IOP increases, the sclera deforms and these deformations, when transmitted to the ONH, in turn lead to LC displacement (Agoumi et al., 2011; Yang et al., 2009, 2007b). The results of these studies suggest that the sclera, ONH, and LC behave as a unified biomechanical system when responding to IOP elevation. The converse relationship might also apply in the case of our EH guinea pigs. Specifically, reduced ONH/LC deformation is compatible with their smaller LC pores. It is also plausible that its scleral profile is a product of the naturally lower IOP of our EH guinea pigs.

IOP-related stress in the sclera is inversely related to scleral thickness (Jia, Xu, Yu, Juan, Liao, Sheng-Hui, Duan, 2016). While we did not measure scleral thickness per se, nonetheless, one might expect the scleras of the EH animals to be more resistant to the stretching influence of IOP. If we also assume that larger collagen fibers are linked to thicker scleral walls, this combination would result in IOP-related stress being further reduced. It is also noteworthy that diurnal IOP rhythms were consistently lower around the clock in the EH strain (Table 5.7B). This finding is particularly important because of the reported interplay between IOP and ocular growth rhythms (Nickla, 2013). A comparison of scleral thickness between the two strains and more comprehensive investigations of their ocular growth rhythms are warranted to obtain additional insight into the resistance to myopia of this EH strain.

Table 5.7A: Summary of mean IOP, RE, and OAL (± SEM) at baseline and week 10, and mean lamina cribrosa pore and scleral collagen fiber areas at week 10 for the untreated right eyes of the EH animals and untreated fellow eyes of NZ animals receiving artificial tears in their other eye.

Parameter	Strain	Week		EH vs. NZ at baseline*	EH vs. NZ at week 10*
		Baseline (0)	Week 10		
IOP (mmHg)	EH	18.27 ± 0.70	20.20 ±0.86	0.037	0.002
	NZ	22.53 ±0.92	25.53 ±1.17		
Refractive Error (D)	EH	2.35 ± 0.50	0.73 ± 0.21	>0.999	0.38
	NZ	2.3 ±0.56	1.5± 0.37		
Optical Axial Length (mm)	EH	7.41 ± 0.026	8.45 ± 0.034	0.32	0.10
	NZ	7.47 ±0.03	8.35 ±0.02		
Lamina Cribrosa Pore Area (μm^2)	EH	–-	3.59 ± 0.52	–-	<0.0001
	NZ	–-	22.21 ± 8.7		
Scleral Collagen Fiber Area (μm^2)	EH	–-	0.012 ± 0.003	–-	0.42
	NZ	–-	0.0085±0.002		

* P-values refer to differences between EH and NZ strains at baseline and week 10

Table 5.7B: Mean IOPs (± SEM) measured at 6-h intervals over 24 h at week 10, for the right eyes of the EH strain and the fellow eyes treated with artificial tears (AT) in the NZ strain. IOPs recorded for the two strains were significantly different at 9:25 pm (p= 0.002) and at 9:35 am (p= 0.0003).

Strain	Eye	3:35 pm	9:25 pm	3:25 am	9:35 am	3:35 pm
EH	Right eye	20.7±0.98	19.5 ± 0.90	19.9 ± 0.71	22.9 ± 0.90	20.1 ± 0.44
NZ	Fellow of AT	22.7±1.7	25.7±0.84	22.5±1.1	29.9±1.7	24±1.7

5.4.2.1 Latanoprost and its effect on intraocular pressure, refractive error, and axial elongation

In this study, EH guinea pigs were treated with latanoprost, without any additional visual manipulation to evaluate its effects on “normal” ocular development. Daily topical latanoprost significantly reduced IOP in EH animals, consistent with already published data showing its ocular hypotensive action in guinea pigs of an unknown strain (Di et al., 2017). However, despite its ocular hypotensive action in the EH animals, refractive error and ocular axial elongation were unaffected by latanoprost. In contrast, latanoprost significantly slowed axial elongation in NZ form-deprived, myopic eyes (Chapter 3), suggesting that different mechanisms underlie normal and “myopic” eye elongation. The latter difference in the effect of latanoprost on normal and myopic eyes, and specifically

its lack of effect on normal eye growth, raises the possibility of its use prophylactically, before the onset of myopia in children, without adverse effects.

5.4.2.2 Latanoprost and macro/micro-structural changes

Latanoprost did not seem to have any negative influence on the ODDs. Both Lat and AT groups seemed to have relatively larger ODDs throughout the duration of the study when compared to baseline, however, no clear trend in the correlation between ODDs and axial length and/or refractive error was found in either group.

Although the influence of latanoprost treatment on ODDs appears not to have been investigated, either in any animal model or humans, there are a few animal and several human studies that have examined the influence of refractive error and/ or axial length on optic disc size. A recent guinea pig study derived Bruch's membrane opening (BMO) areas and diameters (Same as our ODDs measurement) from OCT images collected on 2.5 years old untreated EH guinea pigs. The mean BMO diameter reported in this study was 493.79 ± 31.89 μm (Jnawali et al., 2018), which is significantly larger than the ODDs recorded in our 3 months-old EH guinea pigs (264 ± 8.7 μm OD/ 248 ± 8.7 μm OS). This difference is mostly due to the younger age and the shorter eyes of our guinea pigs compared to those in the previous study (ALs: 8.45 ± 0.034 mm (OD) and 8.43 ± 0.04 mm (OS) vs. 10 ± 0.12 mm).

No difference was found in laminar pore size area in AT- and Lat-treated EH eyes as well as between those of treated eyes and their fellows. To date, there have only been limited studies of the LC ultrastructure in animals. A previous study by our group used scanning electron microscopy to image the lamina cribrosa of normal EH and albino guinea pigs (Lisa A. Ostrin and Wildsoet, 2016). The guinea pig was shown to have a well-organized, collagen-based lamina cribrosa, making it an attractive model for us to investigate the effect of latanoprost on the LC architecture. In an unrelated study involving normal monkeys (no myopia or glaucoma), lamina cribrosa thickness was found to decrease and the posterior sclera to thin, with increasing axial length (Jonas et al., 2016). However, in the current study, no abnormalities in the lamina cribrosa architecture were identified in either the AT, or Lat groups, as AL increased with age. This finding is itself reassuring from a therapeutic perspective. However, it is important to note that, as expected, none of the EH guinea pigs showed tilted discs, although none were myopic. Thus, the shearing forces on the lamina cribrosa may be less in the case of guinea pig lamina cribrosa compared to that experienced in the case of titled discs in human myopic eyes, and as reflected in our failure to detect any structural deviations. It is plausible that this difference between the guinea pig and human eyes may also reflect, at least in part, differences in the anatomical location of the optic nerve insertion site and the temporal location of the eyes of the guinea pig.

The IOP reduction achieved with topical latanoprost is attained through increases in the levels of matrix metalloproteinases, leading to remodelling of the extracellular matrix within the uveoscleral pathway (Russo 2009). In our study, scleral extracellular matrix remodeling was not evident, based on the findings of our TEM scleral study. However, the latanoprost-treated eyes had the highest proportion of the largest scleral collagen fibers and the lowest proportion of the smallest fibers compared to the fellow and AT-

treated eyes. It is possible that this difference is a byproduct of the IOP lowering effect of latanoprost, specifically of the reduced tension on the sclera. It was demonstrated through theoretical modelling that the higher the IOP, the higher the scleral wall tension, which is also more pronounced in longer eyes. Conversely, lowering IOP would have reduced the tension on the scleral wall (Cahane and Bartov, 1992).

Overall, the studies described in this chapter offer additional insights into the ocular differences between the EH and NZ strains of guinea pigs (Section 5.4.1.1). Results with latanoprost complement those reported for myopic eyes and the NZ strain, indicating a negligible effect on normal ocular growth, which is critical to treating otherwise healthy eyes prior to their development of myopic refractive error (Sections 5.4.2.1 and 5.4.2.2).

Chapter 6: Conclusion Chapter

The research reported in this dissertation was driven by two main goals, as summarized below along with main research outcomes.

6.1 Characterize changes with myopia in diurnal IOP rhythms, as well as scleral and optic nerve head macro- and micro-architecture in myopia-sensitive New Zealand guinea pigs

Myopia progression in humans is reported to adversely affect both scleral and optic nerve head architecture and biomechanical properties. As a myopia model, guinea pigs were monocularly form deprived (FD) and advanced imaging tools applied to track eye length and optic disc changes *in vivo,* after which ocular tissue was harvested for analysis of structural changes, e.g., in the architecture of sclera, including scleral collagen organization and lamina cribrosa (LC) pore size. Fellow untreated eyes served as controls. Like primates, including humans, and mammals, guinea pigs have a fibrous sclera, which makes them a good animal myopia model for studies focused on the sclera.

Key findings are as follows:

- Although there was no significant difference in diurnal IOP rhythms between form-deprived myopic and fellow eyes, form-deprived eyes showed a faster increase in IOP over time compared to the developmental increases in fellow eyes.

- Optic discs increased in size with increasing axial length in both form-deprived myopic and fellow (normal) eyes, but at a faster rate in myopic eyes, paralleling the trends reported for human myopia.

- No effects of myopia on the LC ultrastructure were not detected in this study. In contrast, studies in humans have reported significant changes in the LC in highly myopic eyes, which may contribute to the increased risk of glaucoma in myopic eyes (Miki et al., 2015). That the guinea pig study was comparatively short in duration as a partial explanation for this difference warrants further investigation.

- The scleras of myopic FD eyes were morphologically different compared to the scleras of fellow eyes. In latter scleras, collagen fibers ranged in size from quite small to quite large and were evenly spaced. In contrast, the scleral collagen fibers were more widely spaced, with a higher proportion of the smaller sized collagen fibers in myopic eyes. The latter description matches the typical

appearance of the myopic sclera, including human myopic sclera described by Curtin in 1979.

6.2 Investigate whether sustained reductions in IOP can slow myopia progression and if so, also reduce/minimize myopia-related changes in scleral and optic nerve head macro-/micro-architecture.

Latanoprost is now widely used to treat primary open-angle glaucoma, with the benefit of offering 24-hour control of IOP in humans. We used it to retest the hypothesis that lowering IOP could slow myopia progression. Timolol, which has been used in previous related studies, failed to do so. Our novel finding is that latanoprost slows myopic progression, at least in our mammalian (guinea pig) model of myopia.

Key findings are as follows:

- Daily topical latanoprost both lowered IOP, as expected, and significantly inhibited myopia progression.

- Latanoprost achieved a sustained IOP lowering effect over 24 hours, perhaps contributing to its inhibitory effect on myopia progression, which is reported to be fastest at night.

- The IOP lowering action of latanoprost has been linked to remodelling of the extracellular matrix in the uveoscleral pathway. Myopia has been linked to increased scleral extracellular matrix modelling, the net result being smaller collagen fibers in the myopic sclera compared to normal healthy (control) sclera. Unexpectedly, latanoprost not only inhibited myopia progression, but also normalized the scleral collagen mosaic in myopic eyes. The sclera from form-deprived eyes treated with latanoprost had a similar appearance to the control/ fellow eyes.

- The lamina cribrosas of latanoprost-treated, form-deprived eyes were similar in appearance to those of fellow eyes.

Other important findings:

- Daily topical latanoprost administered to otherwise untreated NZ guinea pigs resulted in apparent choroidal vasodilation, with no significant increase in choroidal thickness.

- While latanoprost lowered IOP in otherwise untreated ElmHill guinea pigs, ocular axial elongation was unaffected, contrasting with its inhibitory effect on “myopic” eye growth, suggesting that different mechanisms underlie these two patterns of ocular elongation.

Bibliography

Abdalla, M.I., Hamdi, M., 1970. Applanation ocular tension in myopia and emmetropia. Br. J. Ophthalmol. 54, 122-5.

Agoumi, Y., Sharpe, G.P., Hutchison, D.M., Nicolela, M.T., Artes, P.H., Chauhan, B.C., 2011. Laminar and prelaminar tissue displacement during intraocular pressure elevation in glaucoma patients and healthy controls. Ophthalmology. 118, 52-9.

Aihara, M., Lindsey, J.D., Weinreb, R.N., 2003. Aqueous Humor Dynamics in Mice. Investig. Opthalmology Vis. Sci. 44, 5168.

Aihara, M., Lindsey, J.D., Weinreb, R.N., 2002. Reduction of intraocular pressure in mouse eyes treated with latanoprost. Investig. Ophthalmol. Vis. Sci. 43,146-50.

Akyol, N., Kalkisim, A., Turk, A., Kola, M., Imamoglu, H.I., 2017. Evaluation of the effects on choroidal thickness of bimatoprost 0.03% versus a brinzolamide 1.0%/timolol maleate 0.5% fixed combination. Cutan. Ocul. Toxicol. 36, 397–403.

Aller, T.A., Wildsoet, C., 2008. Bifocal soft contact lenses as a possible myopia control treatment: A case report involving identical twins. Clin. Exp. Optom. 91, 394–399.

Anstice, N.S., Phillips, J.R., 2011. Effect of dual-focus soft contact lens wear on axial myopia progression in children. Ophthalmology 118, 1152–1161.

Aptel, F., Cucherat, M., Denis, P., 2008. Efficacy and Tolerability of Prostaglandin Analogs. J. Glaucoma 17, 667–673.

Arranz-Marquez, E., Teus, M.A., 2004. Relation between axial length of the eye and hypotensive effect of latanoprost in primary open angle glaucoma. Br. J. Ophthalmol. 88, 635–637.

Ascher, K., 1954. Veins of the aqueous humor in glaucoma. Boll Ocul 33, 129–44.

Ashby, R.S., Schaeffel, F., 2010. The effect of bright light on lens compensation in Chicks. Investig. Ophthalmol. Vis. Sci. 51, 5247-53.

Asrani, S., Zeimer, R., Wilensky, J., Gieser, D., Vitale, S., Lindenmuth, K., 2000. Large diurnal fluctuations in intraocular pressure are an independent risk factor in patients with glaucoma. J. Glaucoma 9, 134–142.

ASTIN, M., 1998. Effects of Prostaglandin E 2 , F 2α , and Latanoprost Acid on Isolated Ocular Blood Vessels In Vitro. J. Ocul. Pharmacol. Ther. 14, 119–128.

Astin, M., Stjernschantz, J., 1997. Mechanism of prostaglandin E2-, F2α- and latanoprost acid-induced relaxation of submental veins. Eur. J. Pharmacol. 340, 195–201.

Avetisov, E.S., Savitskaya, N.F., Vinetskaya, M.I., Iomdina, E.N., 1983. A study of biochemical and biomechanical qualities of normal and myopic eye sclera in humans of different age groups. Metab. Pediatr. Syst. Ophthalmol. 7, 183–8.

Avetisov, S.E., Fisenko, V.P., Zhuravlev, A.S., Avetisov, K.S., 2018. Atropine use for the prevention of myopia progression. Vestn. oftal'mologii 134, 84.

Avila, M.Y., Mitchell, C.H., Stone, R.A., Civan, M.M., 2003. Noninvasive assessment of aqueous humor turnover in the mouse eye. Investig. Ophthalmol. Vis. Sci. 44, 722-7.

Balaratnasingam, C., Morgan, W.H., Bass, L., Matich, G., Cringle, S.J., Yu, D.-Y., 2007. Axonal Transport and Cytoskeletal Changes in the Laminar Regions after Elevated Intraocular Pressure. Investig. Opthalmology Vis. Sci. 48, 3632.

Baltussen, R., Naus, J., Limburg, H., 2009. Cost-effectiveness of screening and correcting refractive errors in school children in Africa, Asia, America and Europe. Health Policy (New. York). 89, 201-15.

Barathi, V.A., Beuerman, R.W., 2011. Molecular mechanisms of muscarinic receptors in mouse scleral fibroblasts: Prior to and after induction of experimental myopia with atropine treatment. Mol. Vis. 17, 680–92.

Bartmann, M., Schaeffel, F., Hagel, G., Zrenner, E., 1994. Constant light affects retinal dopamine levels and blocks deprivation myopia but not lens-induced refractive errors in chickens. Vis. Neurosci. 11, 199-208.

Bedrossian, R.H., 1979. The Effect of Atropine on Myopia. Ophthalmology. 86, 713-9.

Benavente-Perez, A., Nour, A., Troilo, D., 2014. Axial Eye Growth and Refractive Error Development Can Be Modified by Exposing the Peripheral Retina to Relative Myopic or Hyperopic Defocus. Invest. Ophthalmol. Vis. Sci. 55, 6765–6773.

Bill, A., 2003. Some Thoughts on the Pressure Dependence of Uveoscleral Flow. J. Glaucoma 12, 88–89.

Bill, A., Hellsing, K., 1965. Production and drainage of aqueous humor in the cynomolgus monkey (Macaca irus). Invest. Ophthalmol. Vis. Sci. 4, 920-6.

Bito, L.Z., Merritt, S.Q., DeRousseau, C.J., 1979. Intraocular pressure of rhesus monkey (Macaca mulatta). I. An initial survey of two free-breeding colonies. Invest. Ophthalmol. Vis. Sci. 18, 785–93.

Boltz, A., Schmidl, D., Weigert, G., Lasta, M., Pemp, B., Resch, H., Garhöfer, G., Fuchsjäger-Mayrl, G., Schmetterer, L., 2011. Effect of Latanoprost on Choroidal Blood Flow Regulation in Healthy Subjects. Investig. Opthalmology Vis. Sci. 52, 4410.

Brubaker, R.F., 2001. Measurement of Uveoscleral Outflow in Humans. J. Glaucoma 10, S45–S48.

Cahane, M., Bartov, E., 1992. Axial Length and Scleral Thickness Thickness Effect on Susceptibility to Glaucomatous Damage: A Theoretical Model Implementing Laplace's Law. Ophthalmic Res 24, 280–284.

Camras, C.B., 1996. Comparison of latanoprost and timolol in patients with ocular hypertension and glaucoma: a six-month masked, multicenter trial in the United States. The United States Latanoprost Study Group. Ophthalmology 103, 138–47.

Chakraborty, R., Read, S.A., Collins, M.J., 2011. Diurnal variations in axial length, choroidal thickness, intraocular pressure, and ocular biometrics. Investig. Ophthalmol. Vis. Sci. 52, 5121–5129.

Chen, Y.-P., Hocking, P.M., Wang, L., Považay, B., Prashar, A., To, C.-H., Erichsen, J.T., Feldkaemper, M., Hofer, B., Drexler, W., Schaeffel, F., Guggenheim, J.A., 2011. Selective Breeding for Susceptibility to Myopia Reveals a Gene–Environment Interaction. Investig. Opthalmology Vis. Sci. 52, 4003.

Chia, A., Chua, W.H., Cheung, Y.B., Wong, W.L., Lingham, A., Fong, A., Tan, D., 2012. Atropine for the treatment of childhood Myopia: Safety and efficacy of 0.5%, 0.1%, and 0.01% doses (Atropine for the Treatment of Myopia 2). Ophthalmology. 119, 347-54.

Chia, A., Lu, Q.-S., Tan, D., 2016. Five-Year Clinical Trial on Atropine for the Treatment of Myopia 2. Ophthalmology 123, 391–399.

Chiba, T., Kashiwagi, K., Ishijima, K., Furuichi, M., Kogure, S., Abe, K., Chiba, N., Tsukahara, S., 2004. A Prospective Study of Iridial Pigmentation and Eyelash Changes Due to Ophthalmic Treatment with Latanoprost. Jpn. J. Ophthalmol. 48, 141–147.

Cho, P., Cheung, S.-W., 2012. Retardation of Myopia in Orthokeratology (ROMIO) Study: A 2-Year Randomized Clinical Trial. Investig. Opthalmology Vis. Sci. 53, 7077.

Cho, P., Cheung, S.W., Edwards, M., 2005. The longitudinal orthokeratology research in children (LORIC) in Hong Kong: A pilot study on refractive changes and myopic control. Curr. Eye Res. 30, 71–80.

Choh, V., Lew, M.Y., Nadel, M.W., Wildsoet, C.F., 2006. Effects of interchanging hyperopic defocus and form deprivation stimuli in normal and optic nerve-sectioned chicks. Vision Res. 46, 1070–1079.

Chua, W.H., Balakrishnan, V., Chan, Y.H., Tong, L., Ling, Y., Quah, B.L., Tan, D., 2006. Atropine for the Treatment of Childhood Myopia. Ophthalmology 113, 2285–2291.

Clineschmidt, C.M., Strahlman, E.R., Anderson, K., 1995. Comparison of a Fixed Combination of Dorzolamide and Timolol to Concomitant administration of Dorzolamide plus Timolol in Patients with Open-Angle Glaucoma for 3 Months. Invest. Ophthalmol. Vis. Sci.

Coudrillier, B., Tian, J., Alexander, S., Myers, K.M., Quigley, H.A., Nguyen, T.D., 2012. Biomechanics of the human posterior sclera: Age- and glaucoma-related changes measured using inflation testing. Investig. Ophthalmol. Vis. Sci. 53, 1714-28.

Curtin, B.J., Iwamoto, T., Renaldo, D.P., 1979. Normal and staphylomatous sclera of high myopia. An electron microscopic study. Arch. Ophthalmol. (Chicago, Ill. 1960)

97, 912–5.

Dalvin, L.A., Fautsch, M.P., 2015. Analysis of circadian rhythm gene expression with reference to diurnal pattern of intraocular pressure in mice. Investig. Ophthalmol. Vis. Sci. 56, 2657-63.

Stamer, DW., Piwnica, D., Jolas, T., Carling, R.W., Cornell, C.L., Fliri, H., Martos, J., Pettit, S.N., Wang, J.W., Woodward, D.F., 2010. Cellular basis for bimatoprost effects on human conventional outflow. Investig. Ophthalmol. Vis. Sci. 51, 5176-81.

David, R., Zangwill, L., Briscoe, D., Dagan, M., Yagev, R., Yassur, Y., 1992. Diurnal intraocular pressure variations: an analysis of 690 diurnal curves. Br. J. Ophthalmol. 76, 280–283.

del Buey, M.A., Lavilla, L., Ascaso, F.J., Lanchares, E., Huerva, V., Cristóbal, J.A., 2014. Assessment of Corneal Biomechanical Properties and Intraocular Pressure in Myopic Spanish Healthy Population. J. Ophthalmol. 2014, 1–6.

Detry-Morel, M., 2011. [Is myopia a risk factor for glaucoma?]. J. Fr. d'ophtalmologie 34, 392–5.

Di, Y., Luo, X.-M., Qiao, T., Lu, N., 2017. Intraocular pressure with rebound tonometry and effects of topical intraocular pressure reducing medications in guinea pigs. Int. J. Ophthalmol. 10, 186–190.

Diestelhorst, M., Nordmann, J.-P., Toris, C.B., 2002. Combined Therapy of Pilocarpine or Latanoprost with Timolol Versus Latanoprost Monotherapy. Surv. Ophthalmol. 47, S155–S161.

Dinslage, S., Diestelhorst, M., Kuhner, H., Krieglstein, G.K., 2000. The effect of latanoprost 0.005% on pupillary reaction of the human eye. Ophthalmologe. 97, 396-401.

Duncalf, D., 1975. Anesthesia and intraocular pressure. Bull. N. Y. Acad. Med. 51, 374-81.

Edwards, M.H., 1996. Animal models of myopia. A review. Acta Ophthalmol Scand. 74, 213-9.

Edwards, M.H., Brown, B., 1993. Intraocular pressure in a selected sample of myopic and nonmyopic Chinese children. Optom Vis Sci 70, 15–17.

Edwards, M.J., Penny, R.H.C., Lyle, J., Jonson, K., 1974. Brain growth and learning behaviour of the guinea-pig following prenatal hyperthermia. Experientia 30, 406–407.

El-nimri, N.W., Wildsoet, C.F., 2018. Effects of Topical Latanoprost on Intraocular Pressure and Myopia Progression in Young Guinea Pigs. Invest Ophthalmol Vis Sci 59, 2644–2651.

El-Nimri, N.W., Wildsoet, C.F., 2018. Effects of Topical Latanoprost on Intraocular Pressure and Myopia Progression in Young Guinea Pigs. Investig. Opthalmology Vis. Sci. 59, 2644.

Eraslan, M., Cerman, E., Yildiz Balci, S., Celiker, H., Sahin, O., Temel, A., Suer, D., Tuncer Elmaci, N., 2016. The choroid and lamina cribrosa is affected in patients with Parkinson's disease: Enhanced depth imaging optical coherence tomography study. Acta Ophthalmol. 94, e68-75.

Fan, D.S.P., Lam, D.S.C., Chan, C.K.M., Fan, A.H., Cheung, E.Y.Y., Rao, S.K., 2007. Topical atropine in retarding myopic progression and axial length growth in children with moderate to severe myopia: A pilot study. Jpn. J. Ophthalmol. 51, 27–33.

Fang, F., Pan, M., Yan, T., Tao, Y., Wu, H., Liu, X., Qu, J., Zhou, X., 2013. The Role of cGMP in Ocular Growth and the Development of Form-Deprivation Myopia in Guinea Pigs. Investig. Opthalmology Vis. Sci. 54, 7887.

Fechtner, R.D., Khouri, a S., Zimmerman, T.J., Bullock, J., Feldman, R., Kulkarni, P., Michael, a J., Realini, T., Warwar, R., 1998. Anterior uveitis associated with latanoprost. Am. J. Ophthalmol. 26, 37-41.

Flammer, J., Orgül, S., Costa, V.P., Orzalesi, N., Krieglstein, G.K., Serra, L.M., Renard, J.P., Stefánsson, E., 2002. The impact of ocular blood flow in glaucoma. Prog. Retin. Eye Res. 21, 359–393.

Flitcroft, D.I., 2012. The complex interactions of retinal, optical and environmental factors in myopia aetiology. Prog. Retin. Eye Res. 31, 622–660.

Fricke, T.R., Holden, B.A., Wilson, D.A., Schlenther, G., Naidoo, K.S., Resnikoff, S., Frick, K.D., 2012. Global cost of correcting vision impairment from uncorrected refractive error. Bull. World Health Organ. 90, 728-38.

Frost, M.R., Norton, T.T., 2007. Differential protein expression in tree shrew sclera during development of lens-induced myopia and recovery. Mol. Vis.13, 1580-8.

Fujikado, T., Kawasaki, Y., Suzuki, A., Ohmi, G., Tano, Y., 1997. Retinal function with lens-induced myopia compared with form-deprivation myopia in chicks. Graefe's Arch. Clin. Exp. Ophthalmol. 235, 320–324.

Gao, H., Frost, M.R., Siegwart, J.T., Norton, T.T., 2011. Patterns of mRNA and protein expression during minus-lens compensation and recovery in tree shrew sclera. Mol. Vis. 17, 903–19.

Gaton, D.D., Sagara, T., Lindsey, J.D., Gabelt, B.T., Kaufman, P.L., Weinreb, R.N., 2001. Increased matrix metalloproteinases 1, 2, and 3 in the monkey uveoscleral outflow pathway after topical prostaglandin F2α-isopropyl ester treatment. Arch. Ophthalmol. 119, 1165-70.

Genest, R., Chandrashekar, N., Irving, E., 2012. The effect of intraocular pressure on chick eye geometry and its application to myopia. Acta Bioeng. Biomech. 14, 3–8.

Gentle, A., McBrien, N.A., 2002. Retinoscleral control of scleral remodelling in refractive development: a role for endogenous FGF-2? Cytokine 18, 344–8.

Giannetto, C., Piccione, G., Giudice, E., 2009. Daytime profile of the intraocular pressure and tear production in normal dog. Vet. Ophthalmol. 12, 302-5.

Glasser, A., Murphy, C.J., Troilo, D., Howland, H.C., 1995. The mechanism of lenticular accommodation in chicks. Vision Res. 35, 1813-24.

Glasser, A., Troilo, D., Howland, H.C., 1994. The mechanism of corneal accommodation in chicks. Vision Res. 34, 1549-66.

Goel, M., Picciani, R.G., Lee, R.K., Bhattacharya, S.K., 2010. Aqueous humor dynamics: a review. Open Ophthalmol. J. 4, 52-59.

Goldmann H, 1950. Minute volume of the aqueous in the anterior chamber of the human eye in normal state and in primary glaucoma. Ophthalmologica 120, 19–21.

Goldschmidt, E., Jensen, H., Marushak, D., 1985. Can timolol maleate reduce the progression of myopia? Acta Ophthalmol 63, 173.

Graham, B., Judge, S.J., 1999. The effects of spectacle wear in infancy on eye growth and refractive error in the marmoset (Callithrix jacchus). Vision Res. 39, 189-206.

Guggenheim, J.A., McBrien, N.A., 1996. Form-deprivation myopia induces activation of scleral matrix metalloproteinase-2 in tree shrew. Invest. Ophthalmol. Vis. Sci. 37, 1380–95.

Guo, S.S., Sivak, J.G., Callender, M.G., Diehl-Jones, B., 1995. Retinal dopamine and Lens-induced refractive errors in chicks. Curr. Eye Res. 14, 385-9.

Harper, A.R., Summers, J.A., 2015. The dynamic sclera: Extracellular matrix remodeling in normal ocular growth and myopia development. Exp. Eye Res. 133, 100-11.

Hodos, W., Kuenzel, W.J., 1984. Retinal-image degradation produces ocular enlargement in chicks. Investig. Ophthalmol. Vis. Sci. 25, 652-9.

Hoh, S.-T., Lim, M.C.C., Seah, S.K.L., Lim, A.T.H., Chew, S.-J., Foster, P.J., Aung, T., 2006. Peripapillary retinal nerve fiber layer thickness variations with myopia. Ophthalmology 113, 773–7.

Holden, B.A., Fricke, T.R., Wilson, D.A., Jong, M., Naidoo, K.S., Sankaridurg, P., Wong, T.Y., Naduvilath, T.J., Resnikoff, S., 2016. Global Prevalence of Myopia and High Myopia and Temporal Trends from 2000 through 2050. Ophthalmology 123, 1036–42.

Hosaka, A., 1988. The growth of the eye and its components: Japanese studies. Acta Ophthalmol. 66, 65–68.

Howlett, M.H.C., McFadden, S.A., 2009. Spectacle lens compensation in the pigmented guinea pig. Vision Res. 49, 219–227.

Howlett, M.H.C., McFadden, S.A., 2007. Emmetropization and schematic eye models in developing pigmented guinea pigs. Vision Res. 47, 1178-90.

Howlett, M.H.C., McFadden, S.A., 2006. Form-deprivation myopia in the guinea pig (Cavia porcellus). Vision Res. 46, 267–283.

Hoyng PF, van B.L., 2000. Pharmacological therapy for glaucoma: a review. Drugs 59, 411–34.

Huang, J., Hung, L.F., Smith, E.L., 2012. Recovery of peripheral refractive errors and ocular shape in rhesus monkeys (Macaca mulatta) with experimentally induced myopia. Vision Res.15, 30-9.

Huang, J., Hung, L.F., Smith, E.L., 2011. Effects of foveal ablation on the pattern of peripheral refractive errors in normal and form-deprived infant rhesus monkeys (Macaca mulatta). Investig. Ophthalmol. Vis. Sci. 52, 6428-34.

Hung, L.-F., Crawford, M.L.J., Smith, E.L., 1995. Spectacle lenses alter eye growth and the refractive status of young monkeys. Nat. Med. 1, 761–765.

Hung, L.F., Wallman, J., Smith, E.L., 2000. Vision-dependent changes in the choroidal thickness of macaque monkeys. Investig. Ophthalmol. Vis. Sci. 41, 1259–69.

I. Papastergiou, G., F. Schmid, G., M. Laties, A., Pendrak, K., Lin, T., A. Stone, R., 1998a. Induction of axial eye elongation and myopic refractive shift in one-year-old chickens. Vision Res. 38, 1883–1888.

I. Papastergiou, G., F. Schmid, G., M. Laties, A., Pendrak, K., Lin, T., A. Stone, R., 1998b. Induction of axial eye elongation and myopic refractive shift in one-year-old chickens. Vision Res. 38, 1883–1888.

Irving, E.L., Sivak, J.G., Callender, M.G., 1992. Refractive plasticity of the developing chick eye. Ophthalmic Physiol. Opt. 35, 600-6.

Jantzen, J.P.A.H., 1988. Anesthesia and intraocular pressure. Anaesthesist. 37, 458-69.

Jensen, H., 1992a. Myopia progression in young school children and intraocular pressure. Doc. Ophthalmol. 82, 249–255.

Jensen, H., 1992b. Myopia progression in young school children and intraocular pressure. Doc. Ophthalmol. 82, 249–255.

Jensen, H., 1991. Myopia progression in young school children. A prospective study of the myopia progression and the effect of a trial with bifocal lenses and beta blocker eye drops. Acta Ophthalmol 185, 65–8.

Jeong, D.W., Kook, M.S., Lee, K.S., Lee, J.R., Han, S., 2014. Circadian pattern of intraocular pressure fluctuations in young myopic eyes with open-angle glaucoma. Investig. Ophthalmol. Vis. Sci.55, 2148-56.

Jia, Xu, Yu, Juan, Liao, Sheng-Hui, Duan, X.-C., 2016. Biomechanics of the sclera and effects on intraocular pressure. Int J Ophthalmol 9, 1824–1831.

Jiang, L., Garcia M., Hammond D., Dahanayake, D., Wildsoet, C., 2019. Strain-dependent Differences in Sensitivity to Myopia-inducing Stimuli in Guinea Pigs and Role of Choroid. Invest Ophthalmol Vis Sci. 60, 1226-1233.

Jiang, L., Zhang, S., Schaeffel, F., Xiong, S., Zheng, Y., Zhou, X., Lu, F., Qu, J., 2014. Interactions of chromatic and lens-induced defocus during visual control of eye growth in guinea pigs (Cavia porcellus). Vision Res. 94, 24–32.

Jin, N., Stjernschantz, J., 2000. Effects of prostaglandins on form deprivation myopia in the chick. Acta Ophthalmol. Scand 78, 495–500.

Jnawali, A., Beach, K.M., Ostrin, L.A., 2018. In Vivo Imaging of the Retina, Choroid, and Optic Nerve Head in Guinea Pigs. Curr. Eye Res. 43, 1006–1018.

Jobling, A.I., Gentle, A., Metlapally, R., McGowan, B.J., McBrien, N.A., 2009. Regulation of scleral cell contraction by transforming growth factor-β and stress: Competing roles in myopic eye growth. J. Biol. Chem. 284, 2072-9.

Jobling, A.I., Nguyen, M., Gentle, A., McBrien, N.A., 2004. Isoform-specific Changes in Scleral Transforming Growth Factor-β Expression and the Regulation of Collagen Synthesis during Myopia Progression. J. Biol. Chem. 279, 18121-6.

Jonas, J.B., 2005. Optic disk size correlated with refractive error. Am. J. Ophthalmol. 139, 346-8.

Jonas, J.B., Berenshtein, E., Holbach, L., 2004. Lamina cribrosa thickness and spatial relationships between intraocular space and cerebrospinal fluid space in highly myopic eyes. Investig. Ophthalmol. Vis. Sci. 45, 2660-5.

Jonas, J.B., Jonas, R.A., Jonas, S.B., Panda-Jonas, S., 2012. Lamina cribrosa thickness correlated with peripapillary sclera thickness. Acta Ophthalmol. 90, e248–e250.

Jonas, J.B., Jonas, S.B., Jonas, R.A., Holbach, L., Panda-Jonas, S., 2011. Histology of the parapapillary region in high myopia. Am. J. Ophthalmol. 152, 1021–9.

Jonas, J.B., Kutscher, J.N., Panda-Jonas, S., Hayreh, S.S., 2016. Lamina cribrosa thickness correlated with posterior scleral thickness and axial length in monkeys. Acta Ophthalmol. 94, e693–e696.

Jonas, J.B., Mardin, C.Y., Schlotzer-Schrehardt, U., Naumann, G.O.H., 1991. Morphometry of the human lamina cribrosa surface. Investig. Ophthalmol. Vis. Sci. 32, 401–405.

JT., W., 1991. Diurnal variations in intraocular pressure. Trans Am Ophthalmol Soc. 89, 757–90.

Jung, S.K., Lee, J.H., Kakizaki, H., Jee, D., 2012. Prevalence of myopia and its association with body stature and educational level in 19-year-old male conscripts in Seoul, South Korea. Invest Ophthalmol Vis Sci 53, 5579–5583.

Kahane, N., Bdolah-Abram, T., Raskansky, H., Ofri, R., 2016. The effects of 1%

prednisolone acetate on pupil diameter and intraocular pressure in healthy dogs treated with 0.005% latanoprost. Vet. Ophthalmol. 19, 473–479.

Katz, L.J., 1999. Brimonidine tartrate 0.2% Twice daily vs timolol 0.5% Twice daily: 1-year results in glaucoma patients. Am. J. Ophthalmol. 127, 20-6.

Kaufman, P.L., 2017. Latanoprostene bunod ophthalmic solution 0.024% for IOP lowering in glaucoma and ocular hypertension. Expert Opin. Pharmacother. 18, 433–444.

Kee, C.S., Marzani, D., Wallman, J., 2001. Differences in time course and visual requirements of ocular responses to lenses and diffusers. Invest. Ophthalmol. Vis. Sci. 42, 575–83.

Kennedy, R.H., Dyer, J.A., Kennedy, M.A., Parulkar, S., Kurland, L.T., Herman, D.C., McIntire, D., Jacobs, D., Luepker, R. V, 2000. Reducing the progression of myopia with atropine: a long term cohort study of Olmsted County students. Binocul. Vis. Strabismus Q. 15, 281–304.

Kim, J.W., Lindsey, J.D., Wang, N., Weinreb, R.N., 2001. Increased human scleral permeability with prostaglandin exposure. Invest Ophthalmol Vis Sci 42, 1514–1521.

Kim, Y.W., Kim, D.W., Jeoung, J.W., Kim, D.M., Park, K.H., 2015. Peripheral lamina cribrosa depth in primary open-angle glaucoma: A swept-source optical coherence tomography study of lamina cribrosa. Eye. 29, 1368-74.

Kimura, T., Yoshida, Y., Toda, N., 1992. Mechanisms of relaxation induced by prostaglandins in isolated canine uterine arteries. Am. J. Obstet. Gynecol. 167, 1409–1416.

Kinoshita, N., Konno, Y., Hamada, N., Kanda, Y., Shimmura-Tomita, M., Kakehashi, A., 2018. Additive effects of orthokeratology and atropine 0.01% ophthalmic solution in slowing axial elongation in children with myopia: first year results. Jpn. J. Ophthalmol. 62, 544-553.

Koina, M.E., Baxter, L., Adamson, S.J., Arfuso, F., Hu, P., Madigan, M.C., Chan-Ling, T., 2015. Evidence for Lymphatics in the Developing and Adult Human Choroid. Invest. Ophthalmol. Vis. Sci. 56, 1310–1327.

Konstas, A., Karabatsas, C., Lallos, N., Georgiadis, N., Kotsimpou, A., Stewart, J., Stewart, W., 2005. 24-Hour Intraocular Pressures with Brimonidine Purite versus Dorzolamide Added to Latanoprost in Primary Open-Angle Glaucoma Subjects. Ophthalmology 112, 603–608.

Konstas, A.G.P., Mikropoulos, D., Kaltsos, K., Jenkins, J.N., Stewart, W.C., 2006. 24-Hour Intraocular Pressure Control Obtained with Evening- versus Morning-Dosed Travoprost in Primary Open-Angle Glaucoma. Ophthalmology 113, 446–450.

Krishna, R., Mermoud, A., Baerveldt, G., Minckler, D.S., 1995. Circadian rhythm of intraocular pressure: a rat model. Ophthalmic Res 27, 163–7.

Lauber, J.K., Boyd, J.E., Boyd, T.A.S., 1972. Aqueous humor inflow in normal and glaucomatous avian eyes. Exp. Eye Res. 20, 147-52.

Lee, A.J., Saw, S.M., Gazzard, G., Cheng, A., Tan, D.T.H., 2004. Intraocular pressure associations with refractive error and axial length in children. Br. J. Ophthalmol. 88, 5–7.

Leung, C.K.-S., Mohamed, S., Leung, K.S., Cheung, C.Y.-L., Chan, S.L., Cheng, D.K., Lee, A.K., Leung, G.Y., Rao, S.K., Lam, D.S.C., 2006. Retinal Nerve Fiber Layer Measurements in Myopia: An Optical Coherence Tomography Study. Investig. Opthalmology Vis. Sci. 47, 5171.

Li, R., Liu, J.H.K., 2008. Telemetric monitoring of 24 h intraocular pressure in conscious and freely moving C57BL/6J and CBA/CaJ mice. Mol. Vis. 14, 745–9.

Li, T., Howland, H.C., 2003. The Effects of Constant and Diurnal Illumination of the Pineal Gland and the Eyes on Ocular Growth in Chicks. Investig. Opthalmology Vis. Sci. 44, 3692.

Li, T., Lindsley, K., Rouse, B., Hong, H., Shi, Q., Friedman, D.S., Wormald, R., Dickersin, K., 2016. Comparative Effectiveness of First-Line Medications for Primary Open-Angle Glaucoma. Ophthalmology 123, 129–140.

Li, X., He, F., Gabelt, B.T., Wang, Y., Cai, S., Cao, J., Fan, N., Kaufman, P.L., Liu, X., 2016. Effects of latanoprost and bimatoprost on the expression of molecules relevant to ocular inflow and outflow pathways. PLoS One. 11:e0151644.

Lindén, C., Alm, A., 2007. Latanoprost twice daily is less effective than once daily: indication of receptor subsensitivity? Curr. Eye Res. 17, 567-72.

Lindsey, J.D., Kashiwagi, K., Kashiwagi, F., Weinreb, R.N., 1997. Prostaglandins alter extracellular matrix adjacent to human ciliary muscle cells in vitro. Invest Ophthalmol Vis Sci 38, 2214–2223.

Lindsey, J.D., Weinreb, R.N., 2002. Identification of the mouse uveoscleral outflow pathway using fluorescent dextran. Investig. Ophthalmol. Vis. Sci. 43, 2201-5.

Liu, G., Zeng, T., Yu, W., Yan, N., Wang, H., Cai, S., Pang, I.-H., Liu, X., 2011. Characterization of intraocular pressure responses of the Tibetan monkey (Macaca thibetana). Mol. Vis. 17, 1405–13.

Liu, G.J., Mizukawa, A., Okisaka, S., 1994. Mechanism of intraocular pressure decrease after contact transscleral continuous-wave Nd:YAG laser cyclophotocoagulation. Ophthalmic Res. 26, 65-79.

Liu, J.H., Dacus, A.C., Bartels, S.P., 1991. Adrenergic mechanism in circadian elevation of intraocular pressure in rabbits. Invest. Ophthalmol. Vis. Sci. 32, 2178–83.

Liu, J.H.K., Dacus, A.C., 1991. Endogenous hormonal changes and circadian elevation of intraocular pressure. Investig. Ophthalmol. Vis. Sci. 32, 496-500.

Liu, J.H.K., Dacus, A.C., 1991. Aqueous humor cyclic AMP and circadian elevation of

intraocular pressure in rabbits. Curr. Eye Res. 10, 1175–1177.

Liu, J.H.K., Kripke, D.F., Hoffman, R.E., Twa, M.D., Loving, R.T., Rex, K.M., Lee, B.L., Mansberger, S.L., Weinreb, R.N., 1999. Elevation of human intraocular pressure at night under moderate illumination. Investig. Ophthalmol. Vis. Sci. 40, 2439-42.

Liu, J.H.K., Kripke, D.F., Weinreb, R.N., 2004. Comparison of the nocturnal effects of once-daily timolol and latanoprost on intraocular pressure. Am. J. Ophthalmol. 138, 389–395.

Liu, J.H.K., Medeiros, F.A., Slight, J.R., Weinreb, R.N., 2010. Diurnal and nocturnal effects of brimonidine monotherapy on intraocular pressure. Ophthalmology. 117, 2075-9.

Liu, J.H.K., Slight, J.R., Vittitow, J.L., Scassellati Sforzolini, B., Weinreb, R.N., 2016. Efficacy of Latanoprostene Bunod 0.024% Compared With Timolol 0.5% in Lowering Intraocular Pressure Over 24 Hours. Am. J. Ophthalmol. 169, 249–257.

Liu, J.H.K., Zhang, X., Kripke, D.F., Weinreb, R.N., 2003. Twenty-four-hour intraocular pressure pattern associated with early glaucomatous changes. Investig. Ophthalmol. Vis. Sci. 44, 1586–1590.

Liu, Y., Wang, Y., Lv, H., Jiang, X., Zhang, M., Li, X., 2017. α-adrenergic agonist brimonidine control of experimentally induced myopia in guinea pigs: A pilot study. Mol. Vis. 23, 785–798.

Liu, Y., Wildsoet, C., 2012. The Effective Add Inherent in 2-Zone Negative Lenses Inhibits Eye Growth in Myopic Young Chicks. Investig. Opthalmology Vis. Sci. 53, 5085.

Liu, Y., Wildsoet, C., 2011. The Effect of Two-Zone Concentric Bifocal Spectacle Lenses on Refractive Error Development and Eye Growth in Young Chicks. Investig. Opthalmology Vis. Sci. 52, 1078.

Loewen, N.A., Liu, J.H.K., Weinreb, R.N., 2010. Increased 24-hour variation of human intraocular pressure with short axial length. Invest. Ophthalmol. Vis. Sci. 51, 933–7.

Lopes-Ferreira, D., Ribeiro, C., Maia, R., García-Porta, N., Queirós, A., Villa-Collar, C., González-Méijome, J.M., 2011. Peripheral myopization using a dominant design multifocal contact lens. J. Optom. 4, 14–21.

Lozano, D.C., Hartwick, A.T.E., Twa, M.D., 2015. Circadian rhythm of intraocular pressure in the adult rat. Chronobiol. Int. 32, 513-23.

Lu, F., Zhou, X., Zhao, H., Wang, R., Jia, D., Jiang, L., Xie, R., Qu, J., 2006. Axial myopia induced by a monocularly-deprived facemask in guinea pigs: A non-invasive and effective model. Exp. Eye Res. 82, 628–636.

Lu, P.C., Chen, J.C., 2010. Retarding progression of myopia with seasonal modification of topical atropine. J. Ophthalmic Vis. Res. 5, 75–81.

Maeda, A., Tsujiya, S., Higashide, T., Toida, K., Todo, T., Ueyama, T., Okamura, H., Sugiyama, K., 2006. Circadian intraocular pressure rhythm is generated by clock genes. Investig. Ophthalmol. Vis. Sci. 47, 4050-2.

MAIGAARD, S., FORMAN, A., ANDERSSON, K.-E., 1986. Relaxant and contractile effects of some amines and prostanoids in myometrial and vascular smooth muscle within the human uteroplacental unit. Acta Physiol. Scand. 128, 33–40.

MANNY, R.E., DENG, L., CROSSNOE, C., GWIAZDA, J., 2008. IOP, Myopic Progression and Axial Length in a COMET Subgroup. Optom. Vis. Sci. 85, 97–105.

Martín-Suárez, E., Molleda, C., Tardón, R., Galán, A., Gallardo, J., Molleda, J., 2014a. Diurnal variations of central corneal thickness and intraocular pressure in dogs from 8:00 am to 8:00 pm. Can. Vet. J. = La Rev. Vet. Can. 55, 361–5.

May, C.A., Lütjen-Drecoll, E., 2002. Morphology of the murine optic nerve. Investig. Ophthalmol. Vis. Sci. 43, 2206-12.

Mcbrien, N.A., Arumugam, B., Gentle, A., Chow, A., Sahebjada, S., 2011. The M4 muscarinic antagonist MT-3 inhibits myopia in chick: Evidence for site of action. Ophthalmic Physiol. Opt. 31, 529-39.

McBrien, N.A., Cornell, L.M., Gentle, A., 2001. Structural and ultrastructural changes to the sclera in a mammalian model of high myopia. Investig. Ophthalmol. Vis. Sci. 42, 2179-87.

McBrien, N.A., Gentle, A., 2003. Role of the sclera in the development and pathological complications of myopia. Prog. Retin. Eye Res. 22, 307–38.

McBrien, N.A., Jobling, A.I., Gentle, A., 2009. Biomechanics of the Sclera in Myopia: Extracellular and Cellular Factors. Optom. Vis. Sci. 86, E23–E30.

McBrien, N.A., Lawlor, P., Gentle, A., 2000. Scleral remodeling during the development of and recovery from axial myopia in the tree shrew. Investig. Ophthalmol. Vis. Sci. 41, 3713–3719.

McBrien, N.A., Metlapally, R., Jobling, A.I., Gentle, A., 2006. Expression of collagen-binding integrin receptors in the mammalian sclera and their regulation during the development of myopia. Invest. Ophthalmol. Vis. Sci. 47, 4674–82.

McLaren, J.W., Brubaker, R.F., Fitzsimon, J.S., 1996. Continuous measurement of intraocular pressure in rabbits by telemetry. Invest Ophthalmol Vis Sci 37, 966–975.

Metlapally, R., Wildsoet, C.F., 2015. Scleral Mechanisms Underlying Ocular Growth and Myopia, in: Progress in Molecular Biology and Translational Science. pp. 241–248.

Metlapally, S., McBrien, N.A., 2008. The effect of positive lens defocus on ocular growth and emmetropization in the tree shrew. J. Vis. 8, 1.1-12.

Miki, A., Ikuno, Y., Asai, T., Usui, S., Nishida, K., 2015. Defects of the Lamina Cribrosa in High Myopia and Glaucoma. PLoS One 10, e0137909.

Mishima, H.K., Kiuchi, Y., Takamatsu, M., Rácz, P., Bito, L.Z., 1997. Circadian intraocular pressure management with Latanoprost: Diurnal and nocturnal intraocular pressure reduction and increased uveoscleral outflow. Surv. Ophthalmol. 41, S139–S144.

Moore, C.G., Johnson, E.C., Morrison, J.C., 1996. Circadian rhythm of intraocular pressure in the rat. Curr. Eye Res. 15, 185–191.

Morales, J., Shihab, Z.M., Brown, S.M., Hodges, M.R., 2001. Herpes simplex virus dermatitis in patients using latanoprost. Am. J. Ophthalmol. 132, 114-6.

Morgan-Davies, J., 2004. Three dimensional analysis of the lamina cribrosa in glaucoma. Br. J. Ophthalmol. 88, 1299–1304.

Moring, A.G., Baker, J.R., Norton, T.T., 2007. Modulation of Glycosaminoglycan Levels in Tree Shrew Sclera during Lens-Induced Myopia Development and Recovery. Investig. Opthalmology Vis. Sci. 48, 2947.

Naidoo, K.S., Fricke, T.R., Frick, K.D., Jong, M., Naduvilath, T.J., Resnikoff, S., Sankaridurg, P., 2019. Potential Lost Productivity Resulting from the Global Burden of Myopia. Ophthalmology 126, 338–346.

Nickla, D.L., 2013. Ocular diurnal rhythms and eye growth regulation: Where we are 50 years after Lauber. Exp. Eye Res. 114, 25–34.

Nickla, D.L., Damyanova, P., Lytle, G., 2009. Inhibiting the neuronal isoform of nitric oxide synthase has similar effects on the compensatory choroidal and axial responses to myopic defocus in chicks as does the non-specific inhibitor l-NAME. Exp. Eye Res. 88, 1092-9.

Nickla, D.L., WILDSOET, C., WALLMAN, J., 1998. Visual Influences on Diurnal Rhythms in Ocular Length and Choroidal Thickness in Chick Eyes. Exp. Eye Res. 66, 163–181.

Nickla, D.L., Wildsoet, C.F., 2004. The Effect of the Nonspecific Nitric Oxide Synthase Inhibitor N G-Nitro-L-Arginine Methyl Ester on the Choroidial Compensatory Response to Myopic Defocus in Chickens. Optom. Vis. Sci. 81, 111-8.

Nickla, D.L., Wildsoet, C.F., Troilo, D., 2002. Diurnal rhythms in intraocular pressure, axial length, and choroidal thickness in a primate model of eye growth, the common marmoset. Investig. Ophthalmol. Vis. Sci. 43, 2519-28.

Nickla, D.L., Wilken, E., Lytle, G., Yom, S., Mertz, J., 2006. Inhibiting the transient choroidal thickening response using the nitric oxide synthase inhibitor l-NAME prevents the ameliorative effects of visual experience on ocular growth in two different visual paradigms. Exp. Eye Res. 83, 456-64.

Norman, R.E., Flanagan, J.G., Sigal, I.A., Rausch, S.M.K., Tertinegg, I., Ethier, C.R., 2011. Finite element modeling of the human sclera: Influence on optic nerve head biomechanics and connections with glaucoma. Exp. Eye Res. 93, 4–12.

Norton, T.T., 1999. Animal models of myopia: Learning how vision controls the size of the eye. ILAR J. 40, 59-77.

Norton, T.T., Kang, R.N., 1996. Morphology of tree shrew sclera and choroid during normal development, induced myopia, and recovery. Investig. Ophthalmol. Vis. Sci. 37, S324.

Norton, T.T., McBrien, N.A., 1992. Normal development of refractive state and ocular component dimensions in the tree shrew (Tupaia belangeri). Vision Res. 32, 833-42.

Ocklind, A., 1998. Effect of Latanoprost on the Extracellular Matrix of the Ciliary Muscle. A Study on Cultured Cells and Tissue Sections. Exp. Eye Res. 67, 179–191.

Oh, D.-J., Martin, J.L., Williams, A.J., Russell, P., Birk, D.E., Rhee, D.J., 2006. Effect of Latanoprost on the Expression of Matrix Metalloproteinases and Their Tissue Inhibitors in Human Trabecular Meshwork Cells. Investig. Opthalmology Vis. Sci. 47, 3887.

Ooi, Y.H., Oh, D.-J., Rhee, D.J., 2009. Effect of Bimatoprost, Latanoprost, and Unoprostone on Matrix Metalloproteinases and Their Inhibitors in Human Ciliary Body Smooth Muscle Cells. Investig. Opthalmology Vis. Sci. 50, 5259.

Orzalesi, N., Rossetti, L., Invernizzi, T., Bottoli, A., Autelitano, A., 2000a. Effect of timolol, latanoprost, and dorzolamide on circadian IOP in glaucoma or ocular hypertension11Edited by Thomas J. Liesegang, MD. Am. J. Ophthalmol. 130, 686.

Ostrin L, Mok-Yee J, W.C., 2011. Behavioral Measures of Spatial Vision during Early Development in Pigmented and Albino Guinea Pigs. Assoc. Res. Vis. Ophthalmol. 52, 6296.

Ostrin, L.A., Wildsoet, C.F., 2016. Optic nerve head and intraocular pressure in the guinea pig eye. Exp. Eye Res. 146, 7–16.

Pan, C.-W., Dirani, M., Cheng, C.-Y., Wong, T.-Y., Saw, S.-M., 2015. The age-specific prevalence of myopia in Asia: a meta-analysis. Optom. Vis. Sci. 92, 258–66.

Pardue, M.T., Stone, R.A., Iuvone, P.M., 2013. Investigating mechanisms of myopia in mice. Exp. Eye Res. 114, 96-105.

Park, H.N., Qazi, Y., Tan, C., Jabbar, S.B., Cao, Y., Schmid, G., Pardue, M.T., 2012. Assessment of axial length measurements in mouse eyes. Optom. Vis. Sci. 89, 296-303.

Pärssinen, O., 1990. Intraocular pressure in school myopia. Acta Ophthalmol. 68, 559-63.

Phillips, J., 1995. Form deprivation myopia: elastic properties of sclera. Ophthalmic Physiol. Opt. 15, 357–362.

Piccione, G., Giannetto, C., Fazio, F., Giudice, E., 2010. Influence of different artificial lighting regimes on intraocular pressure circadian profile in the dog (Canis

familiaris). Exp. Anim. 59, 215-23.

Polska, E., Simader, C., Weigert, G., Doelemeyer, A., Kolodjaschna, J., Scharmann, O., Schmetterer, L., 2007. Regulation of Choroidal Blood Flow during Combined Changes in Intraocular Pressure and Arterial Blood Pressure. Investig. Opthalmology Vis. Sci. 48, 3768.

Prema O'Brien, 2010. Scleral bioreactor: Design and use for evaluation of myopia therapiese. PhD dissertation.

Prusky, G.T., Alam, N.M., Beekman, S., Douglas, R.M., 2004. Rapid Quantification of Adult and Developing Mouse Spatial Vision Using a Virtual Optomotor System. Investig. Opthalmology Vis. Sci. 45, 4611.

Qiao-Grider, Y., Hung, L.F., Kee, C.S., Ramamirtham, R., Smith, E.L., 2004. Recovery from form-deprivation myopia in rhesus monkeys. Investig. Ophthalmol. Vis. Sci.45, 3361-72.

Quaranta, L., Gandolfo, F., Turano, R., Rovida, F., Pizzolante, T., Musig, A., Gandolfo, E., 2006. Effects of Topical Hypotensive Drugs on Circadian IOP, Blood Pressure, and Calculated Diastolic Ocular Perfusion Pressure in Patients with Glaucoma. Investig. Opthalmology Vis. Sci. 47, 2917.

Quaranta, L., Pizzolante, T., Riva, I., Haidich, A.B., Konstas, A.G.P., Stewart, W.C., 2008. Twenty-four-hour intraocular pressure and blood pressure levels with bimatoprost versus latanoprost in patients with normal-tension glaucoma. Br. J. Ophthalmol. 92, 1227-31.

Quigley, H., Arora, K., Idrees, S., Solano, F., Bedrood, S., Lee, C., Jefferys, J., Nguyen, T.D., 2017. Biomechanical responses of lamina cribrosa to intraocular pressure change assessed by optical coherence tomography in glaucoma eyes. Investig. Ophthalmol. Vis. Sci. 58, 3377.

Quinn, G.E., Berlin, J.A., Young, T.L., Ziylan, S., Stone, R.A., 1995. Association of Intraocular Pressure and Myopia in Children. Ophthalmology 102, 180–185.

Rada, J.A., Nickla, D.L., Troilo, D., 2000. Decreased proteoglycan synthesis associated with form deprivation myopia in mature primate eyes. Investig. Ophthalmol. Vis. Sci. 41, 2050-8.

Rada, J.A., Perry, C.A., Slover, M.L., Achen, V.R., 1999. Gelatinase A and TIMP-2 expression in the fibrous sclera of myopic and recovering chick eyes. Invest. Ophthalmol. Vis. Sci. 40, 3091–9.

Rada, J.A., Thoft, R.A., Hassell, J.R., 1991. Increased aggrecan (cartilage proteoglycan) production in the sclera of myopic chicks. Dev. Biol. 147, 303–312.

Rajaei, S.M., Mood, M.A., Sadjadi, R., Azizi, F., 2016. Intraocular Pressure, Tear Production, and Ocular Echobiometry in Guinea Pigs (Cavia porcellus). J. Am. Assoc. Lab. Anim. Sci. 55, 475-9.

Ramrattan, R.S., Wolfs, R.C.W., Jonas, J.B., Hofman, A., De Jong, P.T.V.M., 1999. Determinants of optic disc characteristics in a general population: The Rotterdam study. Ophthalmology. 106, 1588-96.

Resnikoff, S., Pascolini, D., Mariotti, S.P., Pokharel, G.P., 2008. Global magnitude of visual impairment caused by uncorrected refractive errors in 2004. Bull. World Health Organ. 86, 63-70.

Russo, A., Riva, I., Pizzolante, T., Noto, F., Quaranta, L., 2008. Latanoprost ophthalmic solution in the treatment of open angle glaucoma or raised intraocular pressure: a review. Clin. Ophthalmol. 2, 897–905.

Read, SA., Collins MJ., Vincent SJ., Alonso-Caneiro D., 2013. Choroidal thickness in myopic and nonmyopic children assessed with enhanced depth imaging optical coherence tomography. Investig. Ophthalmol. Vis. Sci. 54, 7578-86.

Sall, K., 2000. The efficacy and safety of brinzolamide 1% ophthalmic suspension (Azopt) as a primary therapy in patients with open-angle glaucoma or ocular hypertension. Brinzolamide Primary Therapy Study Group. Surv. Ophthalmol. 44, S155-62.

Sankaridurg, P., Holden, B., Smith, E., Naduvilath, T., Chen, X., de la Jara, P.L., Martinez, A., Kwan, J., Ho, A., Frick, K., Ge, J., 2011. Decrease in rate of myopia progression with a contact lens designed to reduce relative peripheral hyperopia: One-year results. Investig. Ophthalmol. Vis. Sci. 52, 9362–9367.

Savini, G., Barboni, P., Parisi, V., Carbonelli, M., 2012. The influence of axial length on retinal nerve fibre layer thickness and optic-disc size measurements by spectral-domain OCT. Br. J. Ophthalmol. 96, 57-61.

Saw, S.M., 2006. How blinding is pathological myopia? Br. J. Ophthalmol. 90, 525–526.

Sawada, Y., Araie, M., Ishikawa, M., Yoshitomi, T., 2017. Multiple Temporal Lamina Cribrosa Defects in Myopic Eyes with Glaucoma and Their Association with Visual Field Defects. Ophthalmology 124, 1600–1611.

SCHAEFFEL, F., BURKHARDT, E., HOWLAND, H.C., WILLIAMS, R.W., 2004. Measurement of Refractive State and Deprivation Myopia in Two Strains of Mice. Optom. Vis. Sci. 81, 99–110.

Schaeffel, F., Glasser, A., Howland, H.C., 1988. Accommodation, refractive error and eye growth in chickens. Vision Res. 28, 639–657.

SCHERER, R., VIGFUSSON, G., LAWIN, P., 1986. Pulmonary blood flow reduction by prostaglandin F 2α and pulmonary artery balloon manipulation during one-lung ventilation in dogs. Acta Anaesthesiol. Scand. 30, 2–6.

Schmid, G.F., Papastergiou, G.I., Nickla, D.L., Riva, C.E., Lin, T., Stone, R.A., Laties, A.M., 1996. Validation of laser Doppler interferometric measurements in vivo of axial eye length and thickness of fundus layers in chicks. Curr. Eye Res. 15, 691–696.

Schmid, K., Wildsoet, C., 1996. Breed- and gender-dependent differences in eye growth and form deprivation responses in chick. J. Comp. Physiol. A 178, 551-61.

Schmid, K.L., Abbott, M., Humphries, M., Pyne, K., Wildsoet, C.F., 2000. Timolol lowers intraocular pressure but does not inhibit the development of experimental myopia in chick. Exp. Eye Res. 70, 659–66.

Schmid, K.L., Wildsoet, C.F., 2004. Inhibitory Effects of Apomorphine and Atropine and Their Combination on Myopia in Chicks. Optom. Vis. Sci. 81, 137-47.

Schmucker, C., Schaeffel, F., 2004a. A paraxial schematic eye model for the growing C57BL/6 mouse. Vision Res. 44, 1857-67.

Schmucker, C., Schaeffel, F., 2004b. In vivo biometry in the mouse eye with low coherence interferometry. Vision Res. 44, 2445–2456.

Schroedl, F., Brehmer, A., Neuhuber, W.L., Kruse, F.E., May, C.A., Cursiefen, C., 2008. The normal human choroid is endowed with a significant number of lymphatic vessel endothelial hyaluronate receptor 1 (LYVE-1) - Positive macrophages. Investig. Ophthalmol. Vis. Sci. 49, 5222-9.

Schroedl, F., Kaser-Eichberger, A., Schlereth, S.L., Bock, F., Regenfuss, B., Reitsamer, H.A., Lutty, G.A., Maruyama, K., Chen, L., Lütjen-Drecoll, E., Dana, R., Kerjaschki, D., Alitalo, K., De Stefano, M.E., Junghans, B.M., Heindl, L.M., Cursiefen, C., 2014. Consensus Statement on the Immunohistochemical Detection of Ocular Lymphatic Vessels. Investig. Opthalmology Vis. Sci. 55, 6440.

Serle, J.B., Katz, L.J., McLaurin, E., Heah, T., Ramirez-Davis, N., Usner, D.W., Novack, G.D., Kopczynski, C.C., 2018. Two Phase 3 Clinical Trials Comparing the Safety and Efficacy of Netarsudil to Timolol in Patients With Elevated Intraocular Pressure: Rho Kinase Elevated IOP Treatment Trial 1 and 2 (ROCKET-1 and ROCKET-2). Am. J. Ophthalmol. 186, 116-127.

Shih, Y.-F., Chen, C.-H., Chou, A.-C., Ho, T.-C., Lin, L.L.-K., Hung, P.-T., 2009. Effects of Different Concentrations of Atropine on Controlling Myopia in Myopic Children. J. Ocul. Pharmacol. Ther. 15, 85-90.

Siegwart, J., Norton, T.T., 2001. Steady state mRNA levels in tree shrew sclera with form-deprivation myopia and during recovery. Investig. Ophthalmol. Vis. Sci. 42, 1153-9.

Siegwart, J.T., Norton, T.T., 2005. Selective regulation of MMP and TIMP mRNA levels in tree shrew sclera during minus lens compensation and recovery. Investig. Ophthalmol. Vis. Sci. 46, 3484-92.

Siegwart, J.T., Norton, T.T., 2001. Steady state mRNA levels in tree shrew sclera with form-deprivation myopia and during recovery. Invest. Ophthalmol. Vis. Sci. 42, 1153–9.

Siegwart, J.T., Norton, T.T., 1999. Regulation of the mechanical properties of tree shrew sclera by the visual environment. Vision Res. 39, 387–407.

Silver, L.H., 1998. Clinical efficacy and safety of brinzolamide (Azopt™), a new topical carbonic anhydrase inhibitor for primary open-angle glaucoma and ocular hypertension. Am. J. Ophthalmol. 126, 400–408.

Sjöquist, B., Stjernschantz, J., 2002. Ocular and systemic pharmacokinetics of latanoprost in humans. Surv. Ophthalmol. 47, S6-12.

Smith, E.L., Huang, J., Hung, L.F., Blasdel, T.L., Humbird, T.L., Bockhorst, K.H., 2009. Hemiretinal form deprivation: Evidence for local control of eye growth and refractive development in infant monkeys. Invest Ophthalmol Vis Sci 50, 5057–5069.

Smith, E.L., Hung, L.-F., Huang, J., 2012. Protective Effects of High Ambient Lighting on the Development of Form-Deprivation Myopia in Rhesus Monkeys. Investig. Opthalmology Vis. Sci. 53, 421.

Smith, E.L., Hung, L.F., Arumugam, B., Huang, J., 2013a. Negative lens-induced myopia in infant monkeys: Effects of high ambient lighting. Investig. Ophthalmol. Vis. Sci. 54, 2959-69.

Smith, E.L., Hung, L.F., Huang, J., Arumugam, B., 2013b. Effects of local myopic defocus on refractive development in monkeys. Optom. Vis. Sci. 90, 1176-86.

Smith, E.L., Ramamirtham, R., Qiao-Grider, Y., Hung, L.F., Huang, J., Kee, C.S., Coats, D., Paysse, E., 2007. Effects of foveal ablation on emmetropization and form-deprivation myopia. Investig. Ophthalmol. Vis. Sci. 48, 3914–3922.

Smith, R.S., Zabaleta, A., Savinova, O. V., John, S.W.M., 2001. The mouse anterior chamber angle and trabecular meshwork develop without cell death. BMC Dev.1:3.

Song, Y., Zhang, F., Zhao, Y., Sun, M., Tao, J., Liang, Y., Ma, L., Yu, Y., Wang, J., Hao, J., 2016. Enlargement of the Axial Length and Altered Ultrastructural Features of the Sclera in a Mutant Lumican Transgenic Mouse Model. PLoS One 11, e0163165.

Stewart, W.C., Castelli, W.P., 1996. Systemic side effects of topical beta-adrenergic blockers. Clin. Cardiol. 19, 691–697.

Stjernschantz, J., 1999. Effect of Latanoprost on Regional Blood Flow and Capillary Permeability in the Monkey Eye. Arch. Ophthalmol. 117, 1363.

Stone, R.A., Lin, T., Laties, A.M., Iuvone, P.M., 1989. Retinal dopamine and form-deprivation myopia. Proc. Natl. Acad. Sci. 86, 704–706.

Summers Rada, J.A., Shelton, S., Norton, T.T., 2006. The sclera and myopia. Exp. Eye Res. 82, 185–200.

Swarbrick, H.A., Alharbi, A., Lum, E., Watt, K., 2011a. Overnight orthokeratology for myopia control: short-term effects on axial length and refractive error. Contact Lens Anterior Eye 34, S3.

Takagi, Y., Nakajima, T., Shimazaki, A., Kageyama, M., Matsugi, T., Matsumura, Y., Gabelt, BT., Kaufman, PL., Hara, H., 2004. Pharmacological characteristics of AFP-168 (tafluprost), a new prostanoid FP receptor agonist, as an ocular hypotensive drug. Exp. Eye Res. 78, 767–76.

Tao, Y., Pan, M., Liu, S., Fang, F., Lu, R., Lu, C., Zheng, M., An, J., Xu, H., Zhao, F., Chen, J., Qu, J., Zhou, X., 2013. cAMP Level Modulates Scleral Collagen Remodeling, a Critical Step in the Development of Myopia. PLoS One 8, e71441.

Tejedor, J., De la Villa, P., 2003. Refractive changes induced by form deprivation in the mouse eye. Investig. Ophthalmol. Vis. Sci.44, 32-36.

Ticak, A., Walline, J.J., 2013. Peripheral Optics with Bifocal Soft and Corneal Reshaping Contact Lenses. Optom. Vis. Sci. 90, 3–8.

Tigges, M., Tigges, J., Fernandes, A., Eggers, H.M., Gammon, J.A., 1990. Postnatal axial eye elongation in normal and visually deprived rhesus monkeys. Investig. Ophthalmol. Vis. Sci. 31, 1035-46.

Tkatchenko, T. V., Shen, Y., Tkatchenko, A. V., 2010. Analysis of postnatal eye development in the mouse with high-resolution small animal magnetic resonance imaging. Investig. Ophthalmol. Vis. Sci. 51, 1297-303.

Tomlinson, A., Phillips, C.I., 1970. Applanation tension and axial length of the eyeball. Br. J. Ophthalmol. 54, 548-553.

Tong, L., Huang, X.L., Koh, A.L.T., Zhang, X., Tan, D.T.H., Chua, W.-H., 2009. Atropine for the Treatment of Childhood Myopia: Effect on Myopia Progression after Cessation of Atropine. Ophthalmology 116, 572–579.

Toris, C., 2007. Brimonidine, in: XPharm: The Comprehensive Pharmacology Reference. Elsevier, pp. 1–6.

Toris, C.B., Camras, C.B., Yablonski, M.E., 1993. Effects of PhXA41, A New Prostaglandin F2α Analog, on Aqueous Humor Dynamics in Human Eyes. Ophthalmology 100, 1297–1304.

Toris, C.B., Zhan, G.-L., Zhao, J., Camras, C.B., Yablonski, M.E., 2001. Potential mechanism for the additivity of pilocarpine and latanoprost. Am. J. Ophthalmol. 131, 722–728.

Tran, H.D.M., Tran, Y.H., Tran, T.D., Jong, M., Coroneo, M., Sankaridurg, P., 2018. A Review of Myopia Control with Atropine. J. Ocul. Pharmacol. Ther. 34.

Troilo, D., Li, T., Glasser, A., Howland, H.C., 1995. Differences in eye growth and the response to visual deprivation in different strains of chicken. Vision Res.35, 1211-6.

Troilo, D., Nickla, D.L., Mertz, J.R., Rada, J.A.S., 2006. Change in the Synthesis Rates of Ocular Retinoic Acid and Scleral Glycosaminoglycan during Experimentally Altered Eye Growth in Marmosets. Investig. Opthalmology Vis. Sci. 47, 1768.

Troilo, D., Nickla, D.L., Wildsoet, C.F., 2000. Choroidal thickness changes during altered eye growth and refractive state a primate. Investig. Ophthalmol. Vis. Sci. 41, 1249–58.

Troilo, D., Quinn, N., Baker, K., 2007. Accommodation and induced myopia in marmosets. Vision Res. 47, 1228-44.

Troilo, D., Totonelly, K., Harb, E., 2009. Imposed anisometropia, accommodation, and regulation of refractive state. Optom. Vis. Sci. 86, E31-9.

Tsukamoto, H., Noma, H., Mukai, S., Ikeda, H., Mishima, H.K., 2005. The Efficacy and Ocular Discomfort of Substituting Brinzolamide for Dorzolamide in Combination Therapy with Latanoprost, Timolol, and Dorzolamide. J. Ocul. Pharmacol. Ther. 21, 395–399.

Uski, T.K., Andersson, K.-E., 1984. Effects of prostanoids on isolated feline cerebral arteries. Acta Physiol. Scand. 120, 197–205.

Uski, T.K., Andersson, K.-E., Brand T, L., Ljunggren, B., 1984. Characterization of the prostanoid receptors and of the contractile effects of prostaglandin F 2a in human pial arteries. Acta Physiol. Scand. 121, 369–378.

Van de Velde, S., De Groef, L., Stalmans, I., Moons, L., Van Hove, I., 2015. Towards axonal regeneration and neuroprotection in glaucoma: Rho kinase inhibitors as promising therapeutics. Prog. Neurobiol. 131, 105–119.

Van Der Valk, R., Webers, C.A.B., Schouten, J.S.A.G., Zeegers, M.P., Hendrikse, F., Prins, M.H., 2005. Intraocular pressure-lowering effects of all commonly used glaucoma drugs: A Meta-analysis of randomized clinical trials. Ophthalmology. 112, 1177-85.

Vetrugno, M., Cantatore, F., Gigante, G., Cardia, L., 1998. Latanoprost 0.005% in POAG: effects on IOP and ocular blood flow., Acta ophthalmologica Scandinavica. Supplement. 227, 40-1.

Vitale, S., Cotch, M.F., Sperduto, R., Ellwein, L., 2006. Costs of Refractive Correction of Distance Vision Impairment in the United States, 1999-2002. Ophthalmology. 113, 2163-70.

Vitale, S., Sperduto, R.D., Ferris, F.L., 2009. Increased prevalence of myopia in the United States between 1971-1972 and 1999-2004. Arch. Ophthalmol. 127, 1632–1639.

Wahl, C., Li, T., Howland, H.C., 2016. Intraocular pressure fluctuations of growing chick eyes are suppressed in constant light conditions. Exp. Eye Res. 148, 52-54.

Walline, J.J., 2012. Myopia Control with Corneal Reshaping Contact Lenses. Investig. Opthalmology Vis. Sci. 53, 7086.

Walline, J.J., Jones, L.A., Sinnott, L.T., 2009. Corneal reshaping and myopia progression. Br. J. Ophthalmol. 93, 1181–1185.

Wallman, J., Turkel, J., Trachtman, J., 1978. Extreme myopia produced by modest change in early visual experience. Science (80-.). 201, 1249–1251.

Wallman, J., Wildsoet, C., Xu, A., Gottlieb, M.D., Nickla, D.L., Marran, L., Krebs, W., Christensen, A.M., 1995. Moving the retina: Choroidal modulation of refractive state. Vision Res. 35, 37-50.

Wand, M., Gaudio, A.R., Shields, M.B., 2001. Latanoprost and cystoid macular edema in high-risk aphakic or pseudophakic eyes. J. Cataract Refract. Surg. 27, 1397-401.

Wang, N., Lindsey, J.D., Angert, M., Weinreb, R.N., 2001. Latanoprost and matrix metalloproteinase-1 in human choroid organ cultures. Curr Eye Res. 22, 198-207.

Wang, S., Wang, Y., Gao, X., Qian, N., Zhuo, Y., 2015. Choroidal thickness and high myopia: a cross-sectional study and meta-analysis. BMC Ophthalmol. 15, 70.

Wang, X., Dong, J., Wu, Q., 2013. Twenty-four-hour measurement of IOP in rabbits using rebound tonometer. Vet. Ophthalmol. 16, 423–428.

Wang, Y., 2006. Optic disc size in a population based study in northern China: the Beijing Eye Study. Br. J. Ophthalmol. 90, 353–356.

Warwar, R.E., Bullock, J.D., Ballal, D., 1998. Cystoid macular edema and anterior uveitis associated with latanoprost use: Experience and incidence in a retrospective review of 94 patients. Ophthalmology.105, 263-8.

Wayman, L.L., Larsson, L.I., Maus, T.L., Brubaker, R.F., 1998. Additive effect of dorzolamide on aqueous humor flow in patients receiving long-term treatment with timolol. Arch. Ophthalmol. (Chicago, Ill. 1960) 116, 1438–40.

Weinreb, R.N., 2001. Enhancement of scleral macromolecular permeability with prostaglandins. Trans. Am. Ophthalmol. Soc. 99, 319-43.

Weinreb, R.N., Lindsey, J.D., 2002. Metalloproteinase gene transcription in human ciliary muscle cells with latanoprost. Invest. Ophthalmol. Vis. Sci. 43, 716–22.

Weiss, A.H., 2003. Unilateral high myopia: optical components, associated factors, and visual outcomes. Br. J. Ophthalmol. 87, 1025–31.

Wendling, W.W., Harakal, C., 1991. Effects of prostaglandin F2 alpha and thromboxane A2 analogue on bovine cerebral arterial tone and calcium fluxes. Stroke 22, 66–72.

Wiesel, T.N., Raviola, E., 1977. Myopia and eye enlargement after neonatal lid fusion in monkeys. Nature. 266, 66-8.

Wildsoet, C., Wallman, J., 1995. Choroidal and scleral mechanisms of compensation for spectacle lenses in chicks. Vision Res. 35, 1175–1194.

Wisard, J., Chrenek, M.A., Wright, C., Dalal, N., Pardue, M.T., Boatright, J.H., Nickerson, J.M., 2010. Non-contact measurement of linear external dimensions of the mouse eye. J. Neurosci. Methods. 187, 156-66.

Wong, T.Y., Klein, B.E.K., Klein, R., Knudtson, M., Lee, K.E., 2003. Refractive errors, intraocular pressure, and glaucoma in a white population. Ophthalmology 110, 211–217.

Xu, L., Wang, Y., Wang, S., Wang, Y., Jonas, J.B., 2007. High Myopia and Glaucoma Susceptibility. Ophthalmology 114, 216–220.

Yan, L., Huibin, L., Xuemin, L., 2014. Accommodation-induced intraocular pressure changes in progressing myopes and emmetropes. Eye. 28, 1334-40.

Yang, H., Downs, J.C., Girkin, C., Sakata, L., Bellezza, A., Thompson, H., Burgoyne, C.F., 2007a. 3-D Histomorphometry of the Normal and Early Glaucomatous Monkey Optic Nerve Head: Lamina Cribrosa and Peripapillary Scleral Position and Thickness. Investig. Opthalmology Vis. Sci. 48, 4597.

Yang, H., Downs, J.C., Sigal, I.A., Roberts, M.D., Thompson, H., Burgoyne, C.F., 2009. Deformation of the normal monkey optic nerve head connective tissue after acute IOP elevation within 3-D histomorphometric reconstructions. Investig. Ophthalmol. Vis. Sci. 52, 345-63.

Young, F.A., 1965. The effect of atropine on the development of myopia in monkeys. Optom. Vis. Sci. 42, 439-49.

Yousufzai, S.Y.K., YE, Z., Abdel-latif, A.A., 1996. Prostaglandin F2αand its Analogs Induce Release of Endogenous Prostaglandins in Iris and Ciliary Muscles Isolated from Cat and Other Mammalian Species. Exp. Eye Res. 63, 305–310.

Yu, W., Cao, G., Qiu, J., Liu, X., Ma, J., Li, N., Yu, M., Yan, N., Chen, L., 2009. Evaluation of monkey intraocular pressure by rebound tonometer. Mol. Vis. 15, 2196-2201.

Zhang, Y., Liu, Y., Wildsoet, C.F., 2012. Bidirectional, optical sign-dependent regulation of BMP2 gene expression in chick retinal pigment epithelium. Invest Ophthalmol Vis Sci 53, 6072–6080.

Zhang, Y., Wildsoet, C.F., 2015. RPE and Choroid Mechanisms Underlying Ocular Growth and Myopia, in: Progress in Molecular Biology and Translational Science. pp. 221–240.

Zhou, X., Qu, J., Xie, R., Wang, R., Jiang, L., Zhao, H., Wen, J., Lu, F., 2006. Normal development of refractive state and ocular dimensions in guinea pigs. Vision Res. 46, 2815-23.

Zimmerman, T.J., 1993. Topical Ophthalmic Beta Blockers: A Comparative Review. J. Ocul. Pharmacol. Ther. 9, 373-84.